# Dynamic Stability Analysis on a DC Powered Propulsion System

## A Power System With Uncontrolled Rectifiers

J. C . Boone

Technische Universiteit Delft


TU Delft Delft University of Technology

Challenge the future

# Dynamic Stability Analysis on a DC Powered Propulsion System

## A Power System With Uncontrolled Rectifiers

by

**J. C . Boone**

in partial fulfillment of the requirements for the degree of

**Master of Science**

at the Delft University of Technology,
to be defended publicly on Friday July 9, 2021 at 9:00 AM.

| | | |
|---|---|---|
| Supervisor: | Dr. ir. L. R. Elizondo | |
| Thesis committee: | Dr. ir. J. R. Torres, | TU Delft |
| | Dr. L. Mazzarella, | TU Delft |
| | Dr. ir. A. Haseltalab, | TU Delft |
| | Ir. P. Vos, | Royal IHC |

*This thesis is confidential and cannot be made public until July 01, 2023.*



TU Delft Delft University of Technology

# PREFACE

Before you lies my master thesis. I started working on this thesis at the beginning of February 2019, quite some time has passed. I have followed the Master Electrical Power Engineering part-time and worked as a part-time lecturer at the Hogeschool Rotterdam and the study Elektrotechniek (Electrical Engineering). There I tried to inspire young engineers and tried to incorporate the new things I learned into practice. Due to COVID-19 a lot changed, everything became digital and a lot of work came upon each and every one. Nevertheless, I have enjoyed working on my thesis. I can look back on interesting discussions, lessons learned and a beautiful experience at the TU-Delft.

I have always had a soft spot for the Maritime and Offshore industry. I chose to complete my internship at Royal IHC and wanted to complete my master project there as well. During my courses, I found big inspiration in the course Power System Dynamics. The power of calculation tools and the possibility to prototype, test and validate something using linear algebra interested me. However, I knew from experience that within many of the companies these software packages are not often used. Whilst they have to make micro-grids for every ship over and over. I wanted to change that and put the effort into design tools to keep the power grids onboard vessels stable, safe and most of all sustainable.

Researching this topic revealed that research is done in this area, however, practical implementations were rare. After some interviews, I learned that the control parameters of vessels were not really investigated or simulated and with the growth of fast-acting power electronics, these grids could become unstable. I enjoyed my time researching what kind of tools are available to determine stability and explored the mathematics behind it. I quickly learned that mathematics is not my strong point but making models and simulations which are robust was.

In this project, two simulation software packages are used to validate each other of a DC power propulsion system. In addition, a prony analysis tool is developed to analyse the simulation and is used to get information on the oscillatory modes. This can be used to tweak the power propulsion system and can be used to gain knowledge in the intricate relation of different controllers. The results show the importance of a DC input in the AVR which increased the voltage stability. It also showed the ability of the prony analysis to investigate undamped oscillations and the type of oscillation it consists out of.

I would like to thank Hogeschool Rotterdam for being flexible and giving me all the space, even in COVID times, to work on my thesis project. I would also like to thank Royal IHC for giving me the chance to prove myself and allow me to research this topic. I would like to thank Pieter Vos for all the discussions during the project about grid stability and about grilling on the barbeque. I would also thank the thesis committee: Dr. Ir. Jose Rueda Torres, Dr. L. Mazzarella, Dr. ir. L. R. Elizondo and Dr. ir. A. Haseltalab for taking the time to evaluate my work.

Finally, a word of thanks to Jetske for supporting me throughout the thesis.

*J. C . Boone*
*Delft, June 2021*

# ABBREVIATIONS

| | |
|---|---|
| DC-PPS | Direct Current - Power Propulsion System |
| SFC | Specific Fuel Consuption |
| AVR | Automatic Voltage Regulator |
| CIG | Converter Integrated Generation |
| CPL | Constant Power Load |
| LC | Local Control |
| CC | Centralized Control |
| MPC | Model Predictive Control |
| RES | Renewable Energy Resources |
| RTDS | Real Time Digital Simulation |
| IMF | Intrinsic Mode Function |
| NCF | Node Contritubtion Factor |
| LSE | Least Square Error |
| PS | Portside |
| SB | Sideboard |
| PSS | Power System Stabilizer |

# CONTENTS

# 1

# INTRODUCTION

Power systems grow, evolve and adapt. This is noticed in the consumption side, distribution side and load side. The changes are noticeable on land but also in offshore power systems. Our generation got the challenge to improve the power network, make it more sustainable but still maintain stability. This chapter introduces the subject of this master thesis project. Section 1.1, describes the background which gives insight into the context and urgency of this master thesis. Section 1.2 describes the motivation of why this topic is chosen and its importance. The third section 1.4 describes the research objectives followed by the research questions in section 1.3. Section 1.5 describes the methodology followed during the master thesis. The outline of this master thesis is described in the last section, section 1.6.

## 1.1. BACKGROUND

The background consists of three parts to properly explain the main areas of research for this thesis. The first area is the background behind the architecture of the researched ship layout, the DC power propulsion system. Within this section, the reasoning behind the layout, benefits and challenges are described. The second area is based on the control of the power system. It describes the background, possible opportunities and the requirements to implement these kinds of novel control strategies. The third area describes the stability analysis tool. To properly analyse the system a method should be applied. The third part describes this method and how it helps with the analysis.

### SHIPBOARD POWER GENERATION

The context of this thesis is confined to problems in the offshore market, specifically the dredging market. Dredging vessels come in various sizes and types. Their main function is to collect soil, such as sand, gravel, silt, clay and rock from different depths under the water. Large electric motors are used to loosen the soil with ratings up to several MWs. The soil is mostly pumped from the bottom of the water to land or holding tanks. Large pumps are required which can also go up to several MWs of power. The propulsion of such a vessel is quite important since the vessel has to collect soil from a specific location. Therefore the ship has to remain in position, this is called dynamic positioning. To remain in position, large thrusters are used with power ratings of up to several MWs. It is clear that the power generation, distribution and quality needs to be designed with care to allow the ship to function.

The conventional ship power propulsion system is an AC common bus network. Large generators are coupled via a transformer to a main AC common bus. The loads are connected to this main bus with for example inverters to power and control the machines. An example of this type of network is shown in figure 1.1. In the figure, a **G** denotes a synchronous generator and a **M** denotes a motor. The discussion between AC or DC powered networks is also applicable for ships. Previous research supports the potential of a DC shipboard power propulsion systems [1–3]. An example of a DC common bus network is shown in figure 1.1. It shows that the generators are connected by uncontrolled rectifiers to a common DC bus. Comparison with the AC network, it becomes evident that fewer converters are required. The loads are connected to the DC-bus employing inverters.

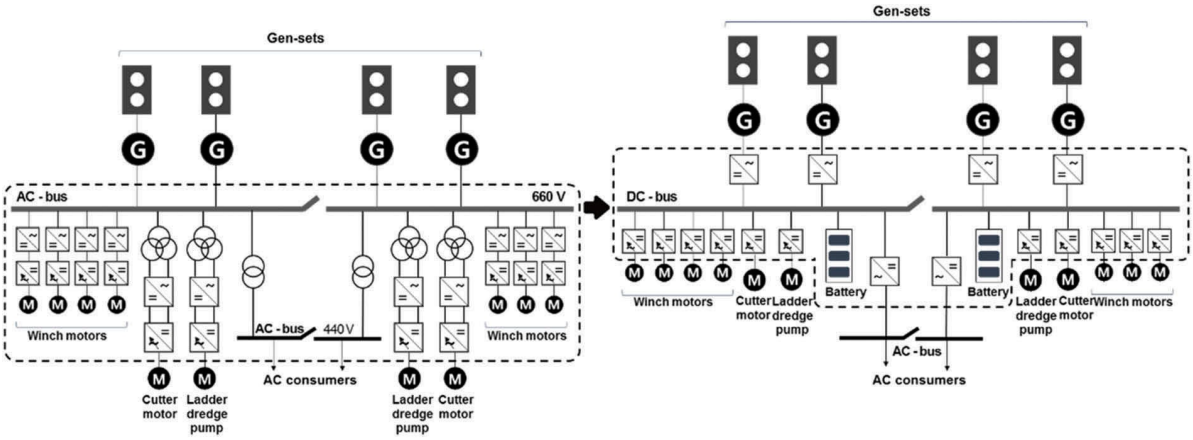


Figure 1.1: A SPS of a dredger: Left a typical AC network, Right a DC network [2]

Kim et al. [2] states that the benefit of a DC-grid can be categorized into two categories. The first category is power stability and power quality the other category are the economical and environmental aspects. Within an AC grid, the voltage and frequency need to remain within a certain bandwidth to maintain the stability of the grid. All generators need to maintain synchronism to maintain the frequency. This is not required for a DC grid, and thus a big benefit. A DC grid only requires the voltage to remain within the limits, reducing the complexity of the control. It also allows different speed operation points between diesel engines within the grid.

When comparing the two network types from figure 1.1 it is evident that the AC network needs rectifiers before the inverter for each load while the DC-grid topology only requires one inverter for the load. This reduces the number of required components of the grid. Another aspect to this difference is the power quality, the AC-grid is objected to harmonics due to the rectifiers. Filters are required to maintain a clean AC grid whereas the DC grid does not require filters. The harmonics are not imposed on the DC voltage and do not influence the quality. The benefits of a DC-grid over an AC-grid regarding the power stability and quality aspects can be summarized as:

- No rotor angle stability criteria
- Freedom of the frequency of the generators (no need for synchronisation)
- DC-grid power distribution (reducing harmonic distortions and increasing power quality)

The benefits of a DC-grid over an AC-grid regarding economic and environmental aspects are:

- Variable speed/frequency operation of gensets (reducing fuel consumptions, emissions)
- Removing a rectifier in a VFD for motor controls (reducing weight and volume)
- Eliminating harmonic mitigation equipment (reducing weight and volume)
- Easy integration of DC power sources to a DC-bus (improving energy efficiency)

The decoupled synchronous machines allow variable speed between the generators which may result in a better operation point for the diesel engine allowing a lower Specific Fuel Consumption (SFC). Figure 1.2 depicts an example of a SFC graph. The engine load corresponds to the power or torque it produces, the colour shows the fuel consumption rate of which red requires the largest amount of fuel and blue the least amount of fuel. The horizontal line of constant speed shows that the speed limits the engine to move to a more efficient operation point. The variable curve shows the amount of freedom the engine has. For example at an engine load of 75% at a constant speed, the fuel consumption is at 204, while if the speed would be variable it could be moved to 198. This enables optimization control on different parameters, for example, economic dispatch. The benefit of a variable frequency of the generators can also be implemented for AC but

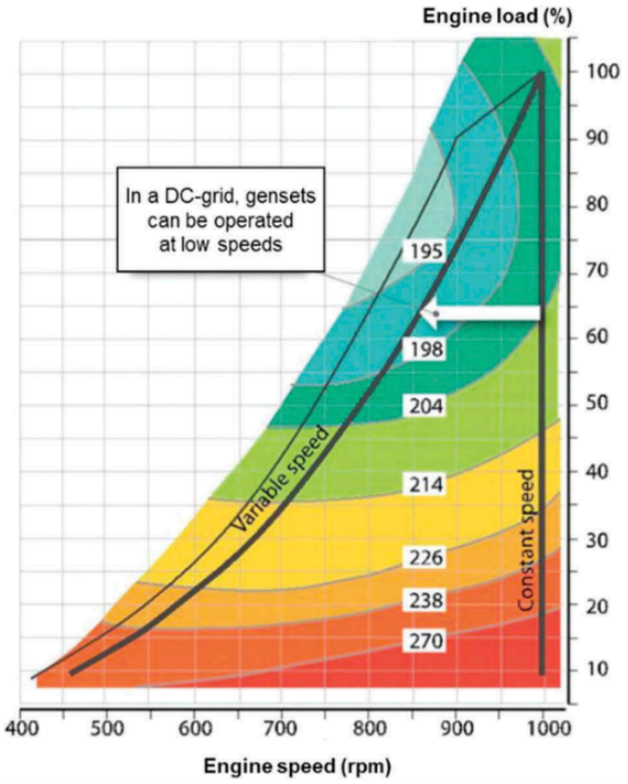


Figure 1.2: Example of a diesel engine fuel consumption curve [4]

is less flexible and is limited in the frequency control.

A DC grid has advantages but is not perfect. Some of the disadvantages are limiting the use of a DC grid such as fault detection and isolation. Short circuits in a DC grid are challenging since there are no natural zero crossings of the current. Therefore, the interruption of it becomes difficult which is a big disadvantage compared to the AC-grid.

Royal IHC is interested in the advantages of a DC grid when using only passive rectifiers to convert the AC voltage to DC. The effect of these rectifiers on the stability of the power grid is to be analyzed since uncontrolled rectifiers cannot control the power flow. This requires the AVR and Governor to maintain the stability of the DC-PPS. The AVR and Governor are relatively slow controllers compared to power electronic-based converters.

The definition for power system stability has been determined by a task force consisting of IEEE and Cigre. They established a definition of power system stability. The definition given the task force [5] is:

*Power system stability is the ability of an electric power system, for a given initial operating condition, to regain a state of operating equilibrium after being subjected to a physical disturbance, with most system variables bounded so that practically the entire system remains intact.*

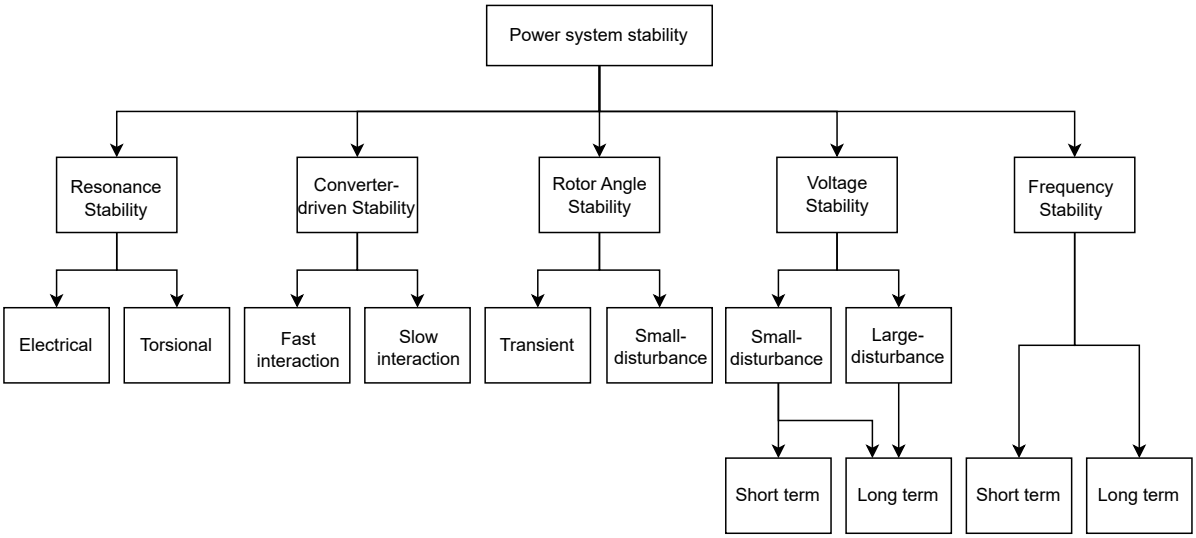


Figure 1.3: Overview of stability clasifications [6]

The initial works of the taskforce [5] has been expanded and new stability criteria have been added [6]. Figure 1.3 gives an overview of the defined stability classes. Resonance stability and converter driven stability are two of the added criteria by [6] this results in the following five stability classes:

1. Rotor Angle stability
2. Frequency stability
3. Voltage stability.
4. Resonance stability
5. Converter-driven stability

Rotor Angle stability is the ability of generators to operate in synchronism in an interconnected system. This is applicable for systems that are interconnected and have to operate in synchronism which is not the case in the DC-PPS. Frequency stability is described as the ability of the power system to operate at a steady frequency with minor deviations. Frequency stability is also not of interest since the frequency does not have to operate at one value. Voltage stability is defined as the ability to maintain a safe steady voltage at all buses in the system after being subjected to a disturbance. This is a stability class that is of interest in a DC-PPS. Resonance stability is the ability to damp out oscillatory energy exchange in which the exchanges occur periodically. Converter-driven stability refers to converter integrated generation (CIG) which behaves differently than conventional synchronous generators. These CIGs are mostly tightly controlled by multiple control loops. In the network under analysis, this type of generation is not applicable. It could be argued that the generator-rectifier combination is a CIG however since we use a passive rectifier it no longer fall under that description.

A well-known voltage stability issue in DC and AC microgrids is that of tightly controlled loads, commonly known as constant power loads (CPL) [7–9]. Most DC-microgrids incorporate a high level of power electronic-based loads. An example of a constant power load is an inverter which is tightly controlling the speed of a motor. CPLs are known for destabilizing the power grid. This effect is seen in smaller microgrids such as full electric automotive systems [10]. The effect of CPLs is also seen in large microgrids [11, 12]. A DC-PPS predominantly consist of tightly controlled induction motors (e.g. motors, winches, thrusters etc.) and passive loads (e.g. heaters, lights, transformers etc.) [2]. The destabilizing effect of a CPL is therefore applicable on a DC-PPS.

The characteristic of a CPL is described as a negative incremental resistance ($dV/dI < 0$). Let us consider a typical voltage source and a CPL, the v-i curve is shown in figure 1.4. The equilibrium point is achieved when the voltage of the source equals that of the load shown by point A. Let's consider a small disturbance

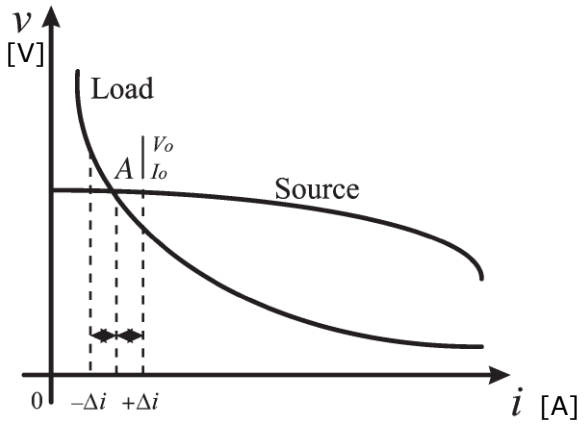


Figure 1.4: v-i charactersistic of typical voltage sources and constant power loads [10]

that results in a small reduction of the current denoted as $\Delta i$. When the new current is achieved, the voltage is lower than the load voltage. This results in a further decrease of the current, therefore the operation point moves further away from A. This effect acts as positive feedback [10, 13] and destabilizes the DC microgrid. Control is required to maintain a stable grid and to cope with the negative incremental resistance.

In this thesis, the voltage stability of a DC-PPS utilizing a passive rectifier is to be studied. Previous research showed the destabilizing effect of a CPL is produced by tightly controlled inverters [9, 10, 13]. Analysis regarding voltage stability [8] used new state of the art control strategies but used limited detail of the generator. The dynamics between generators is therefore not analysed. New topologies regarding DC-PPS [11, 12] showcase multiple generators and different energy storage systems. What will the effect of parallel generators be on a DC bus voltage? This together with the dynamic response of using multiple generators in parallel need to be investigated.

### POWER CONTROL STRATEGY

The control of a power system is of great interest due to the energy transition and the new types of energy sources. New types of converter based sources but also energy storage systems play an important role in the operation of a DC-microgrid [9, 11, 14]. Different topologies of control have been classified, the topology of the control allows a different type of control. Let us first consider the classification of three control topologies given by Dragicevic et al [9]:

1. Decentralized control: digital control links do not exist and power lines are used as the only channel of communication.

2. Distributed control: Data from distributed units are collected in a centralized aggregator, processed and feedback commands are sent back to them via digital control links.

3. Centralized control: Digital control links exist, but are implemented between units and coordinated control strategies are processed locally.

Figure 1.5 gives an illustration of the different control topologies. LC denotes the local control in figure 1.5 and DG a distributed generators. The last abbreviation used is CC which means centralized communication.

Royal IHCs power system control strategy is predominantly decentralized. It uses an Automatic Voltage Regulator (AVR) and Governor to control the power system. An overall power monitoring system is available but is used to only limit power output to reserve enough power for propulsion or critical tasks. Decentralized control is a proven strategy that works and is the conventional way of controlling the power grid within the company. However, the grid is changing on a vessel such as different fuel sources and large energy storage systems. This changes the dynamic behaviour of the grid and different control strategies may be required for safe operation. Centralized control may allow allocation of resources on a system-level optimizing the power production on fuel consumption for example. The lack of a power system simulation limits the company to

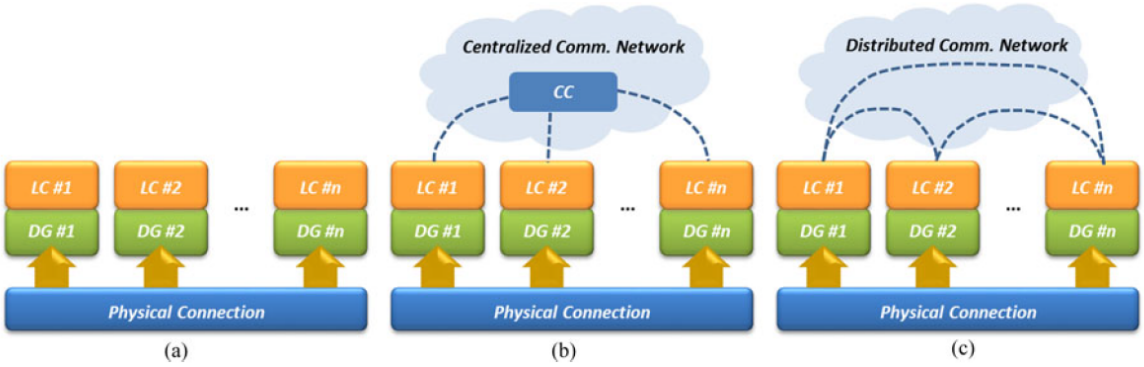


Figure 1.5: control strategies. (a) Decentralized control. (b) Centralized control. (c) Distributed control. [9]

experiment with these kinds of strategies, which further increases the need for a power system simulation. With a base simulation, more sophisticated forms of control such as Predictive control or Adaptive Droop control can be explored.

Predictive control is a novel control strategy applied in many areas. Microgrids apply Model Predictive Control (MPC) to improve performance based on a ruleset. MPC is popular within electrical systems for it allows to implement constraints such as active and reactive power on components. Some of the controllers focus on energy management of distributed energy resources [15][16]. Others try to implement MPC to improve dynamic response [17]. Renewable Energy Resources (RES) are using predictive models to optimize the generation of energy out of the RES such as photovoltaic [18] and wind [19]. While offshore networks do not incorporate RES at such a large scale and have a predictable amount of available energy, they mostly have an unpredictable load profile. For example, when manoeuvring a vessel waves and wind result in unpredictable load for the vessel requires more power to manoeuvre or stay in position. Optimization of power flow control is one of the main challenge [20]. This shows that another way to increase the sustainability of a vessel is to enhance the control strategy. Such that it can optimise control on the most optimal SFC operation point for example. A model of a DC-PPS is required to test or implement new types of controllers which again shows the need for a model.

Studies regarding the stability and control of a DC-PPS have been performed such as [21, 22]. In [21] a full state-space model of a DC-PPS has been developed. In this model, a passive rectifier was used and conventional control for the system such as an AVR and a Governor to maintain the DC grid stable. A battery system is used which is used in a tertiary control level. The paper uses all the components under investigation for this thesis and build a good performing model. The developed system acts as a platform to showcase the possibility of experimenting with different control strategies. For Royal IHC such a model would be very useful if this is built in Matlab Simulink. The analysis has been conducted for a shipboard power system of several tens of kilo Watts. In this thesis, a system of several Mega Watts is under investigation. The results and differences in the model are to be investigated.

The model from [21] has been expanded by replacing the passive rectifier with an active front end [22]. This showcases the possibilities when having a base model, it is expanded such that new control topologies and devices are tested and experimented with. It showcases the predictive model control of a ship using the active front-end.

A passive rectifier limits the controllability in comparison with a fully controlled rectifier. When used to supply energy to a tightly controlled power converter this can cause problems. Mitigation solutions are available such as proposed in [23]. An extra switch on the DC-bus is proposed which stabilizes the DC voltage when supplying CPLs. However, this switch is an extra component and it is a questionable solution. The paper however showcased the problem of a CPL in a network where passive rectifiers are used. This shows the problem which is to be solved for large DC-PPSs when utilizing passive rectifiers.

The effect of a passive rectifier in larger power systems is investigated in [24, 25]. The premise of both theses is similar to this one. The system under investigation is a singular generator with a passive rectifier. For this thesis, the model is expanded to two parallel generator sets and two areas with loads. Their research is limited in investigating the dynamic behaviour between two generator sets which may further decrease stability under certain loads.

The above-described literature shows the use of a DC-PPS model. It allows to investigate new controllers but also get insight into the unstable operation points. Some of the literature used state-space representations of the system, this allows analysing the eigenvalues of the system but also participation factors. Other literature reviews the time-domain data with a comparative analysis. A tool to get more detailed insight into the acquired dynamic behaviour of time-domain simulations may be beneficial here. It could allow increasing the detail of the comparative analysis of different control strategies.

### STABILITY ANALYSIS TOOL

The stability of a system can be determined in multiple ways. In general, there is a model-based approach and a measurement-based approach. A model-based approach uses the mathematical representation of a system, for example, a state-space model. State changes are objected to the set of equations and from it, the change of state is calculated. This mathematical approach in which the eigenvalues of the system are visualized for different operation points is a strong method. Changes in the states can alter the operating point which is visible in the place of the eigenvalues of some of the states such as in [23].

A data-based approach uses the data from for example field tests or a simulation of a model. A data-based approach tries to approximate the received data with a set of equations. The approximated equations parameters give insight into the parameters of the analysed system. However some of the dynamics are visible in the data while others may not be apparent, therefore limits the analysis in its accuracy.

For this thesis, a measurement-based approach is adapted. The reasoning behind it is the useability for analysing field data. Currently, the received data in case of a problem in the power network is analysed by hand. The data is analysed and figures are made in excel to try to seek the root of the problem. If necessary a Fourier transform is made to see the frequency decomposition of a dataset. It requires experience and a good understanding of the complete system to be able to find the problem. With the growth in complexity and the coupled dynamic behaviour of all-electric components, this becomes very difficult and time-consuming. New tooling is required to give new insight into the data which may lead to faster problem identification and better solutions.

Different measurement-based approaches are available such as Koopmans analysis and Prony analysis. Prony analysis is a widely used method for analysing transient and oscillatory behaviour in power systems [26–28]. It can directly estimate the frequency, damping, strength and relative phase of modal components present in a given data-set without the requirement of a fundamental frequency needed in Fourier analysis. Its strength is the ease of use and the direct approximation of different parameters. However, the downside is that it performs poorly when non-linear behaviour and noise are introduced in the signal.

Koopmans method continues on the measurement-based analysis and shows that even non-linear signals can be approximated and give similar results as the prony analysis [29]. This method is used to study the global dynamics of non-linear systems. The difficulty however is that direct application may result in a large number of modes. The system analysed in this thesis is non-linear however, the voltage stability analysis will test with only small disturbances. The non-linear behaviour is expected to be minimal and thus the system may be assumed to be linear. Prony analysis has been selected as the method for two reasons. First the reduction in mathematical complexity and second the fact that the system can be linearized and will be linearized in the Matlab-Simulink simulation.

Prony analysis is particularly valuable for transient stability analysis. Giving insight into modal interaction (modal analysis) [26]. The downsides of the prony method are that it is heavily influenced by noise. Due to the approximating nature, the larger the data set, the less accurate the approximation. The analysis is also lacking in analysing discontinues behaviour, selecting different time scopes still allows the prony analysis to

give a good approximation.

## 1.2. MOTIVATION

The motivation of this master thesis has two aspects one practical of nature, the other with an academic nature. Both aspects form the motivation for this thesis.

### PRACTICAL ASPECTS

Royal IHC builds many vessels installs power propulsion systems on many of those. However, the initialisation and parameterisation of the controllers such as AVR and Governor are mostly done by either the company of the products or experienced commissioners. There are no models available for thorough parametric analysis during the design. This limits experimenting with different ship layouts or controller types. It also limits the implementation of different level of controllers. Different fuel types and the upcoming need for energy storage systems further increases the need for a model. Those components behave differently and the long time experience of commissioning engineers may be insufficient. It is required to model these changes into a base simulation. To accomplish that a base reference simulation is needed of a DC-PPS.

Royal IHC has years of experience building vessels. The complete vessel is built by Royal IHC including the power system. Power systems of vessels grow in complexity and size, moreover, they become more advanced due to required mission equipment which means a general increase in power electronic devices and loads. The growth in complexity also results in more complex problems during commissioning, requiring in-depth knowledge and more advanced tooling to properly analyse data. A data-based analysis tool would help in perceiving the received data such that the right conclusions regarding the data can be made. Models, as well as data analysis tooling, should be developed such that these power system stability problems can be properly analyzed.

The current market expectation is that DC powered vessels will become more prominent. This requires insight into the dynamic behaviour of such a system. Passive rectifiers are a common product to use in vessels and therefore the question arises whether a DC-PPS would work if only passive rectifiers are used to convert the AC voltage to a DC voltage. The voltage stability is of interest but also the behaviour of the generators when they are operating in parallel. This further increases the need for a base model of a DC-PPS allowing further research in different areas such as new control strategies and different energy sources.

### ACADEMIC ASPECTS

The challenge and academic gap within this thesis lie within the limitation of only using passive rectification to convert the AC to DC. Previous work on DC-PPS often includes an active rectifier which allows the DC common bus voltage to be controlled [22]. The analysis, in this case, is mostly in investigating novel control strategies such as model predictive control. Where the fuel consumption is mostly optimized whilst stable operation points are maintained. Other works do analyse the passive rectifier [20, 21] however the dynamics of the generators are not analysed. Examples of these dynamics are local area oscillations or inter-area oscillations.

Research regarding shipboard power systems with uncontrolled rectifiers has been conducted. For example, Sopapirm et al. [23] investigated the effect of uncontrolled rectifiers and a tightly controlled CPL. A low power, low voltage hardware in the loop system was the result. An adaptive stabilization cancellation loop is implementing in which an active element (switch) is placed behind the diode rectifier. It showcased unstable behaviour when load steps were conducted. The question remains whether for high-power systems this remains the case and what the effect of a parallel set of generators is.

Two Norse master theses are investigating the effect of an uncontrolled rectifier in a DC-PPS [24, 25]. Torunn [24] investigated the relationship between the impedance of the system and its stability. The analysis limits itself to a single Generator-rectifier-load set-up in the Matlab Simulink simulations. However, it shows that the problems of stability are evident. Jarle [25] investigated the problems related to a synchronous generator connected to a passive rectifier. Here a modal analysis is introduced and the effect of the type of generator is analysed with parametric analysis. However, it did not elaborate on the modal analysis in de-

tail and was also investigating a single Generator-rectifier-load setup. They both advise in further work to investigate the implementation of the power system stabiliser, dynamic interaction between two generators working in parallel and the impact of tuning the AVR parameters.

This thesis investigates the voltage stability of a DC-PPS using only uncontrolled rectifiers. The DC-PPS consists of multiple generator-rectifier-load sets connected by a common DC bus. Voltage stability is investigated using modal analysis. The Control of the DC-PPS has been limited to a conventional controller and investigates the possible effect of a power system stabilizer. It enables future research to investigate novel control strategies and may extend the model with batteries.

## 1.3. RESEARCH QUESTIONS

Based on the previously described aspects and background, the following research question is formulated:

*"How to ensure robust dynamic voltage performance of a DC shipboard power system whilst using passive rectification of the DC voltage?"*

- What is the necessary detail of the DC-PPS model for voltage stability analysis?
  - Which components or parameters influence the voltage stability?
  - What is the critical scenario's in which a standard control method may be ineffective?
  - What kind of control is required to enhance the stability of the DC-PPS?
- What method can be used to analyse the stability of a DC-PPS?
  - How can unstable operations points of a DC-PPS be identified?
  - How can unstable operations points categorized or linked to a source?

## 1.4. RESEARCH OBJECTIVES

The main idea of this project presented by this thesis is the ability to analyse the voltage stability of DC-PPS implementing only passive rectifiers. The DC-PPS uses conventional decentralized control employing the AVR and Governor. The model will consist of a diesel-generator set, a passive rectifier, a common DC bus and the load. An energy storage system will be omitted in this thesis but may be implemented in further research. The model and the tests performed should be analysed by a tool that allows finding unstable modes. This tool needs to be able to allocate dominant modes and which area contributes the most to that mode.

Regarding the modelling of the DC-PPS and the ability to simulate relevant tests for the analysis of voltage stability, the following research objectives are defined:

- The first objective is to build a model of a DC-PPS with passive rectifiers for a generic ship lay-out and implement decentralized control.
- The second objective is to identify unstable operation points and implement a mitigation solution to further improve the stability.

Regarding the analysis of the results from the simulation, the following research objectives are defined:

- First a method for oscillation mode analysis is to be selected based on data from either the field or simulation results.
- The second objective is to develop a tool that allows to analyse of synthetic signals and validate the method.
- The third objective is to expand the tool such that it can analyse multiple signals from the DC-PPS simulation.

The analysis tool would allow the analysis of both simulated data as the data acquired from the field. This further allows validation and identification of possible undamped oscillations. The analysis tool would further allow stability analysis of the signal and may give insight into small undamped signals.

## 1.5. METHODOLOGY

The need for a model of a DC-PPS has been described in previous chapters. The choice regarding the simulation software is based on the preference of the company. Royal IHC builds its controllers and system in Matlab or Matlab Simulink, therefore it is suggested to keep the same software. To test and verify whether this software is capable of simulating this dynamic behaviour a different package is used to verify. This package is RScad. This software package has been selected since it can be operated on a Real-Time Digital Simulator (RTDS). The software RScad is highly specialised in the area of stability analysis for power systems. Therefore Matlab Simulink has been selected to build the simulation in and RScad has been selected to verify the Matlab Simulink model.

Matlab and Matlab Simulink have a good interface. This allows the stability analysis model to be built in the same environment allowing ease of use of both products. The tool however should be able to handle different input forms such that it can be used for data from the field. The prony tool is therefore built in Matlab.

There are three distinct products for this master thesis: Matlab-Simulink model, RScad model for verification and the prony analysis tool. Figure 1.6 shows the workflow of this project with per workflow the related chapter in this thesis. First, the Matlab-Simulink and RScad models have been build in steps. Then they were validated and after that, the case study Matlab-Simulink model was finalized. The analysis tool has been developed parallel to the verification. The method and the tool have been validated before used for the case study analysis.

## 1.6. DOCUMENT OUTLINE

The model of the DC-PPS is described in chapter 2. It describes the overview of the model used for the case study. It showcases the verification through RScad and describes the performance of the Matlab-Simulink model. Chapter 3 describes the analysis tool. Within the chapter, the tool is tested with multiple signals to validate its functionality. A case study is performed testing the DC-PPS under different circumstances and applying the analysis tool in chapter 4. Power steps and parameter changes are conducted to see the performance of the DC-PPS. Finally, in chapter 5 the conclusion of this thesis report is given. This answers the research questions and reflects on the goals.

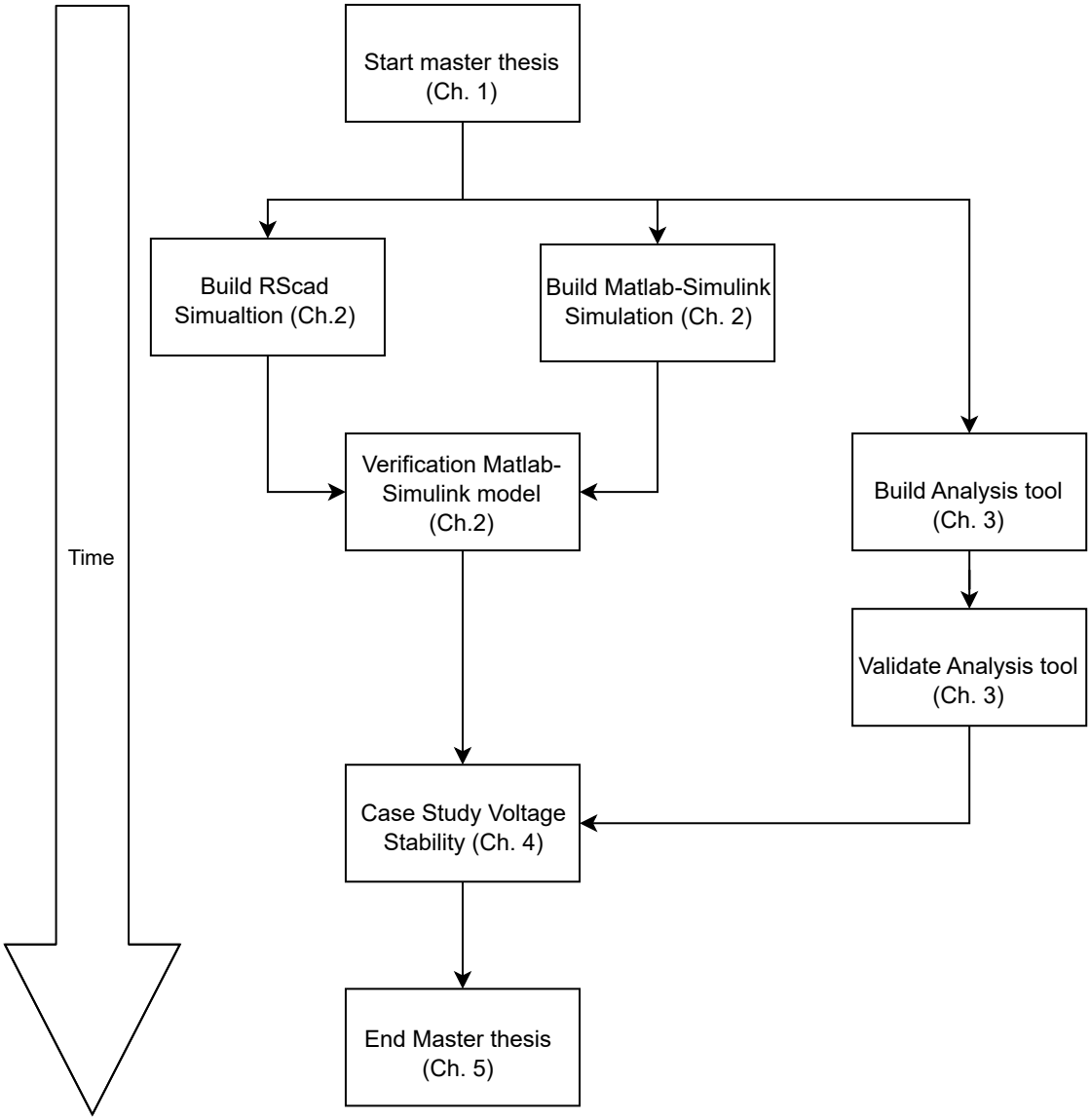


Figure 1.6: Workflow of the Thesis Project

# 2

# Modelling a Shipboard Power Distribution System

In the previous chapter, the background, motivation and research objectives have been described. In this chapter, the first research questions regarding the modelling of the DC-PPS will be described. A DC-PPS model is proposed and the decentralized controllers are parameterized.

This chapter describes the design of the DC-PPS model and its verification. First, a general overview is given of the complete system in section 2.1. As described two software packages are used RScad v5.011.1 and Matlab 2020b. A general overview of the programs is given in section 2.2. After the software packages, each model is described in more detail in section 2.3. The controllers of the DC-PPS require to be parameterized and a set of tests describe the procedure and results of the parameterisation in section 2.4. Section 2.5 describes the qualitative comparison of the Matlab-Simulink model with the RScad model and compares the results. The last section 2.6 describe some of the conclusions made within this chapter.

## 2.1. General overview of a DC-PPS

The simulation is built in Matlab Simulink 2020b with the specialized power system toolbox. The complete system is based on a conceptual design from Royal IHC for a DC-PPS. The concept consists of general power ratings of the machines and a single line of the power system layout of the vessel. The single-line is depicted in figure 2.1 and shows multiple loads, batteries and generators connected to a common DC bus. Two transformers connected to inverters feed an AC common bus for other smaller appliances.

The architecture of the DC-PPS is an all-electric vessel. This means that the propulsion and all the loads are powered by electricity. This type of vessel has a high demand on the availability, stability and quality of the electric power grid for all loads are connected to it. A hybrid vessel has a lower demand on the power system. In the case of a hybrid vessel, the propulsion is powered by both a diesel and an electric motor, hence hybrid. Therefore, the demand on the electric system is lower since the diesel engine could take over the load of the electric motor. Therefore an all-electric vessel has been selected as a case model for it has the largest demand on the availability, stability and quality of the electric power grid.

To model an all-electric vessel, a generic layout is required. As described in the section the batteries are omitted for this analysis. This allows us to investigate the effect of two parallel sets of generators without the effect of a battery. An energy storage system, such as a battery, affects the performance of the grid. The control system of the energy storage system and the role it has changes the stability performance. The energy storage system can be used to replace one generator discharging slowly and supplying the power. This allows a reduction of running hours of generators and allows maintenance time slots on the generators. Another implementation could be to enhance the stability of the DC voltage. In this case, the battery will supply power whenever the voltage drops below a certain level. The control of the energy storage system could also destabilize the grid by supplying or absorbing power at the wrong instance. In this thesis the performance of the generator and diesel is under investigation, therefore the battery is omitted.

As visible in the single-line given in figure 2.1, the bus is split into two areas and is interfaced via a DC switch. This switch will be modelled as an ideal switch, the performance of this DC-switch is not within the scope. The loads are also generalized, in practice, they each have a distinct function but are of no interest to model in detail. Hence, they will be seen as power consumers and therefore will be modelled as one load for each bus area. This allows us to model the power flow between two bus areas but enables us to control the load on each area with one parameter.

The result of the generalisation of the model is depicted at the bottom of figure 2.2. The architecture of the DC-PPS under study in this thesis consists of two parallel synchronous generators powered by diesel engines. It is assumed that the vessel is all-electric power. The generated electric power by the synchronous machines is converted to DC via a passive rectifier. The DC bus can be coupled by connecting the two generators to the same DC bus. This enables power-sharing and enables to shut down one generator set in case of maintenance. The loads are connected to the DC bus via inverters. The inverters control the loads, large consumers are mostly motors or pumps. The propulsion system is a set of thrusters and is modelled as power consumers. In that case, the inverter follows a certain speed set-point or power set-point.

With a defined model layout, each component needs to be defined as well. The detail for each model will be investigated such that it allows to analyse voltage stability. The following components and controllers have to be designed for the DC-PPS:

1. Diesel engine and governor
2. Synchronous generator
3. automatic voltage regulator
4. DC bus and DC coupler
5. Passive rectifier
6. Electric load

This section showed the DC-PPS under study and in it, the energy battery system has been omitted. This allows the investigation of the voltage stability of only the generators. This simplification also has a practical aspect since the vessels have a relatively small energy storage system, the ability to improve voltage stability would be very limited.

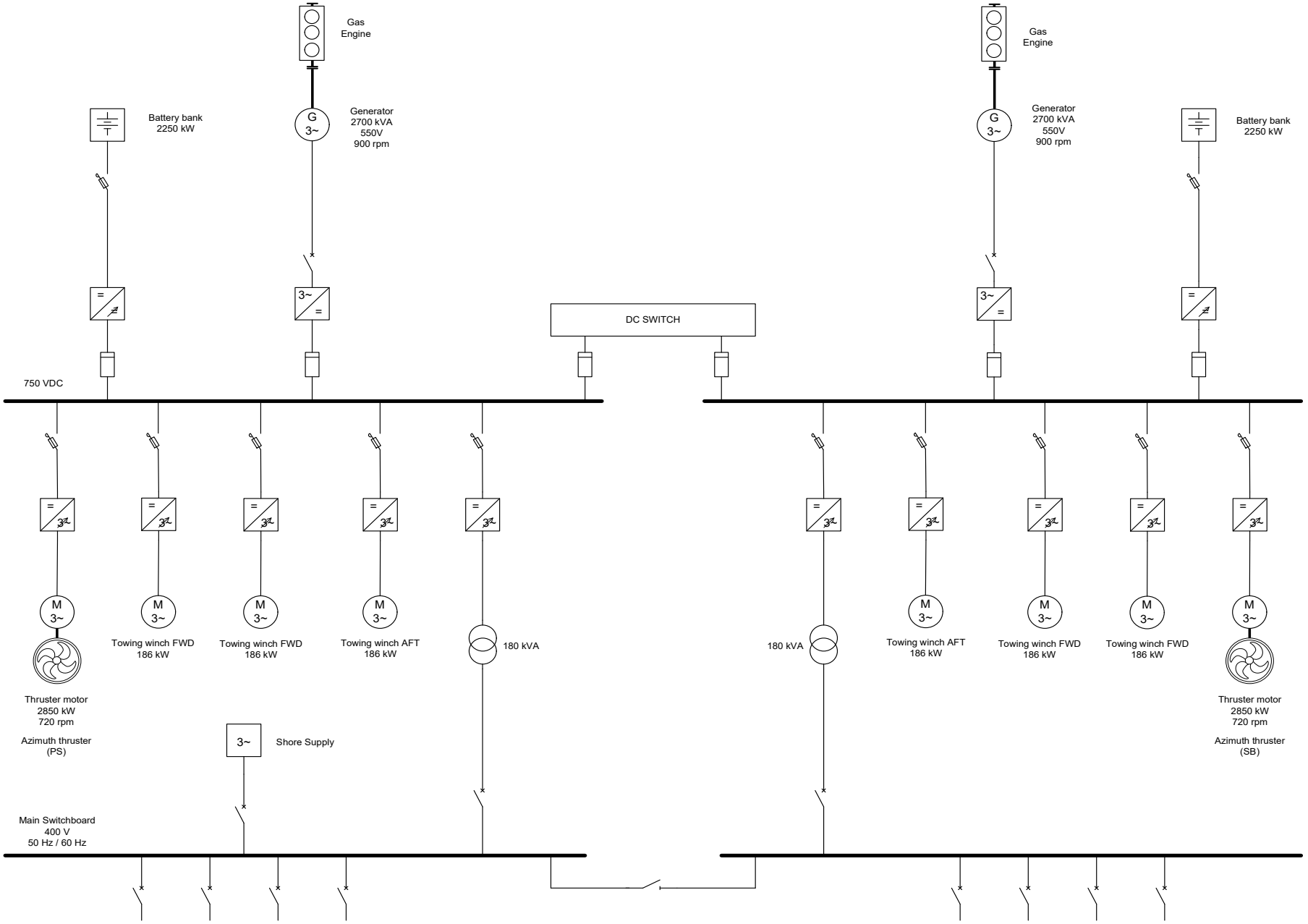


Figure 2.1: Overview of a conceptual DC-PPS

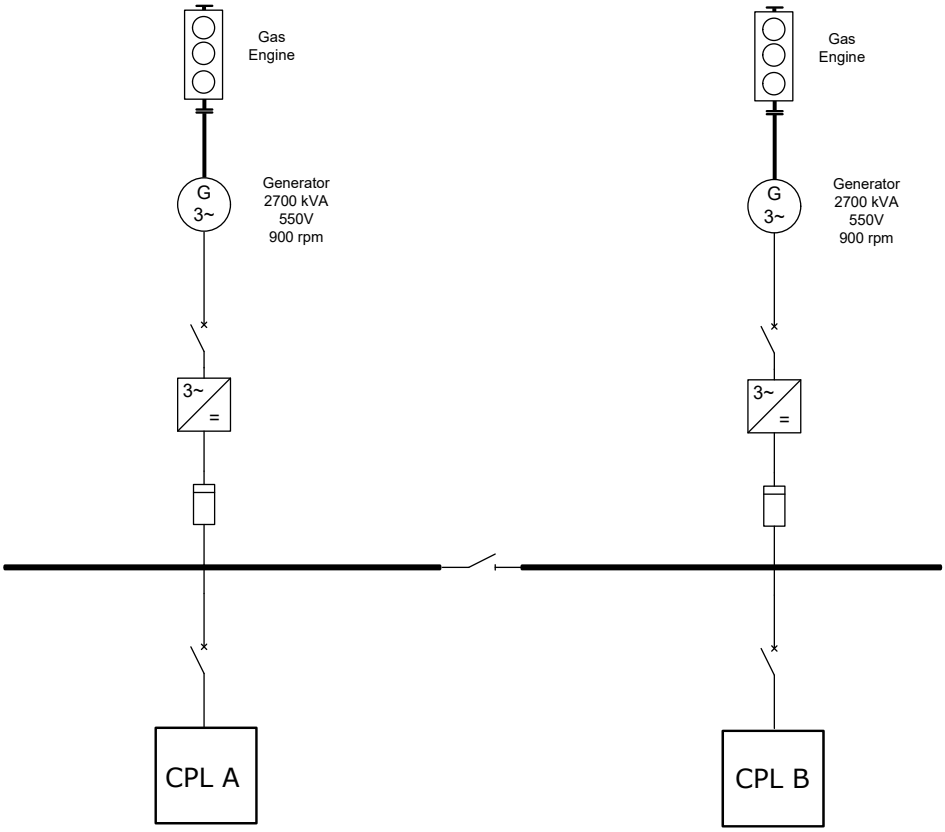


Figure 2.2: Overview of a generalized model of a DC-PPS

## 2.2. MATLAB SIMULINK AND RSCAD

As shown in figure 1.6, the model in Matlab-Simulink will be verified by the use of an RScad simulation. Therefore it is required to build both models in Matlab-Simulink and RScad. This section briefly describes the simulation programs. It describes the functionality within the build model, how they are implemented and the reasoning behind it.

### 2.2.1. MATLAB SIMULATION MODEL

Matlab and Matlab-Simulink are user-friendly programs, the documentation of the program is detailed and thorough and many examples exist to help with some of the general problems. Figure 2.3 shows the overview of the simulation. The load can change according to an array of time and power setpoints as well as the voltage setpoint. Two different measurement points for the AVR can be used, either measuring the voltage on the AC side of the generator or the DC voltage side of the rectifier. The bus tie can be opened and closed to simulate a network split. The data from the measured signals are saved in the workspace such that they can be analysed later or be used in an analysis tool. The parameters of the equipment are determined via datasheets from Royal IHC.

A general observation during the design of the simulation was the importance of the simulation time and sample rate. Selecting a large sample rate results in an increase in computational power and the generated simulation data. In some cases, it even results in unstable behaviour and high-frequency oscillations. On the other hand, choosing a small sample rate results in problems for the controllers and the accuracy of the results. It shows the importance of highly specialized technology for simulating large multi-machine systems and the need to think the model through. Configuring a robust and most of all fast but accurate simulation requires going into the details of solver types, data types, data allocation and simplifying the system.

The model is built in Matlab 2020b. It is important to mention that to use the data for prony analysis it has to be sampled at a constant rate. Thus only fixed-step solvers can be used to enable us of prony analysis

in a later stage. A variable step solver can be used however it requires that the data has to be resampled before being usable for the analysis tool. The effects which are to be analysed are slow oscillatory effects in the range of $0.1Hz$ to $3Hz$ and the simulation times are long in the range of $40to120s$. Therefore a sample rate of $0.5ms$ has been selected to be sufficient.

The model is completely parameterized via script and can be altered when required. The data from the model is saved in the workspace and can be saved for further analysis. It is also possible to run the simulation multiple times with different controller settings which allow fast parametric comparison.

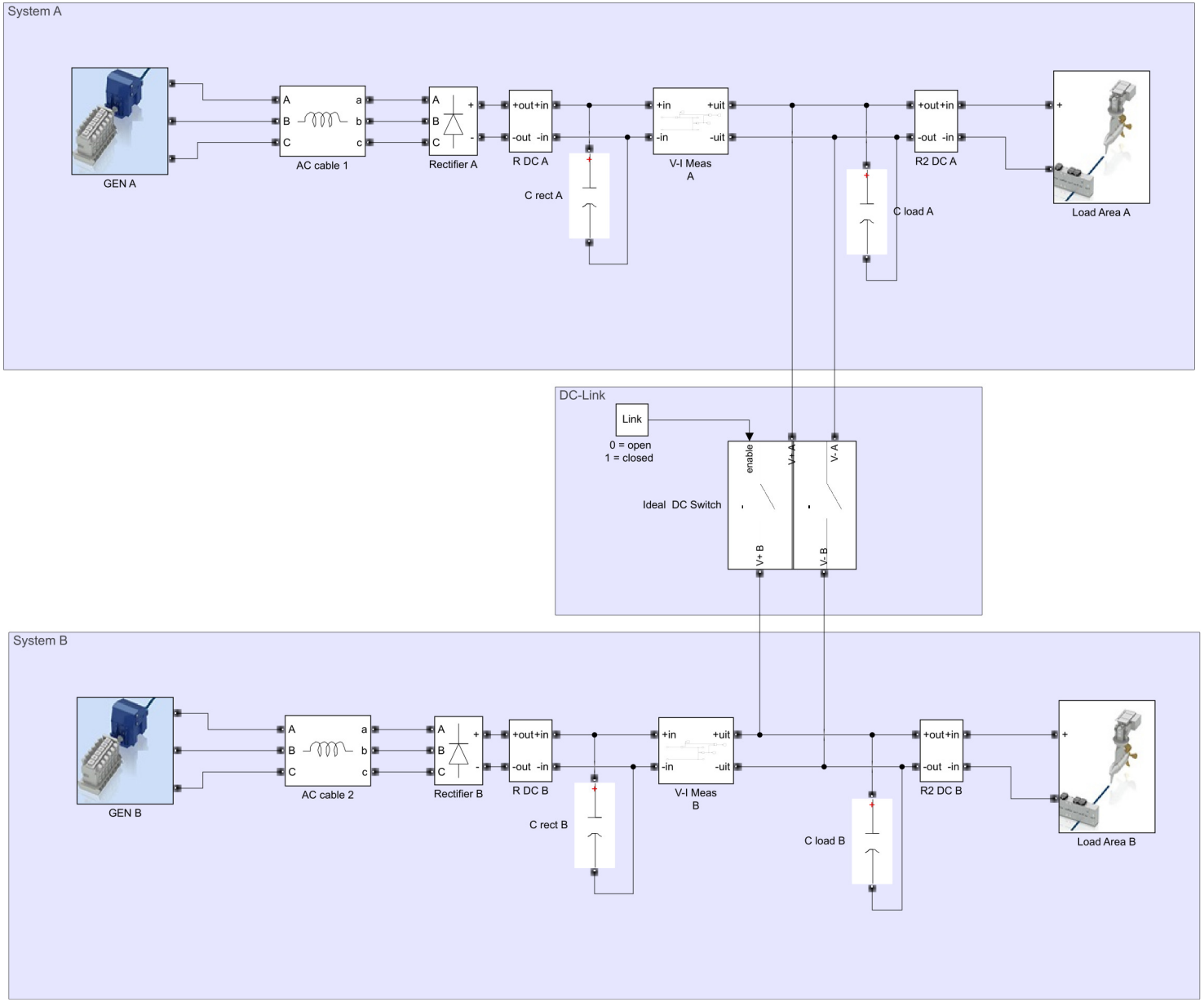


Figure 2.3: Overview Matlab Simulink Simulation

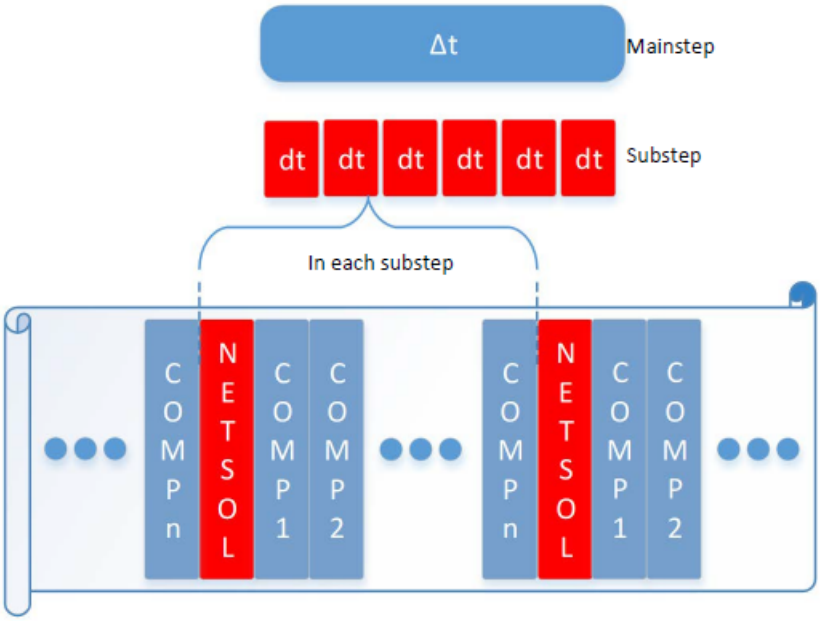


Figure 2.4: Relation between substep and mainstep [30]

### 2.2.2. RSCAD SIMULATION MODEL

RScad is a specialized power system tool enabling the power system to be used in real-time digital simulations (RTDS). This program has been selected because of personal interest and the ability for future hardware in the loop solutions. At the beginning of the thesis project, the idea was to couple an AVR to the simulation to find the performance of a real AVR in a DC-PPS. Due to Covid-19, it has been decided to change the approach.

For this thesis RScad version, 5.011.1 is used. In RScad the mainstep determines the step interval or sample time. With the help of the substep feature, the model can be updated with a smaller time interval shown in figure 2.4. This allows to include detailed models and the ability to study higher frequency electromagnetic transient phenomena accurately. Another feature is superstep, this allows a larger time-step compared to the main time-step. The models are simplified and larger architectures can be modelled.

As described the frequencies under investigation are in the range of $0.1Hz$ to $3Hz$ which would suggest mainstep or even superstep would be sufficient. However, the model needs to accurately model the behaviour of the passive rectifier. This means that the rectified signal of $360Hz$ needs to be simulated. To do so substep is required also because the model lies within the substep library.

The parameterisation and running of simulations of RScad can be automated with the use of a python script. However, for this thesis, the simulation will be used one time to validate the model of Matlab Simulink. Therefore flexibility in parameterisation is not within the scope. In RScad there are two environments to work in. The first environment is the base model called Draft and the second is the Runtime. In the draft, the model can be drafted by coupling the required components and inputs. The measurements and controls are made within the draft. The used draft model in Rscad is shown in figure 2.5.

To run the model and acquire the requested data a runtime application needs to be made. In this environment, the user can select which data is plotted and can make programmable switches that interface in real-time in the simulation. This allows simulating a system split for example. The runtime file allows making graphs, controlling parameters and exporting some of the data. Running a simulation is done according to the following order:

1. Build Draft model (simulation)

2. Build Runtime model (data acquisition)

3. connect to a real-time device (via VPN)
4. Compile the draft model
5. Run model from runtime model
6. save data

### 2.2.3. MODEL OVERVIEW

Table 2.1 gives an overview of the selected models out of the library of Matlab-Simulink and RScad. Both AVR and Governor need to be properly initialized to let the model work.

Table 2.1: Overview of used models for the equipment

| Equipment | Matlab Simulink | RScad | Notes |
|---|---|---|---|
| Diesel Engine and Governor | Degov1 | Degov1 | n.a. |
| Synchronous machine | Synchronous machine fundamental | Synchronous machine model with transformer and loads | Transformer & loads are disabled |
| Automatic Voltage regulator | IEEE type 1 DC voltage regulator | IEEE type 1 DC voltage regulator | n.a |
| DC-Bus | R-C network | R-C network | Impedance is critical |
| Rectifier model | Universal bridge | *rtds_ss_LEV2_V3.def* | n.a |
| Inverter Model | CPL | CPL | n.a |

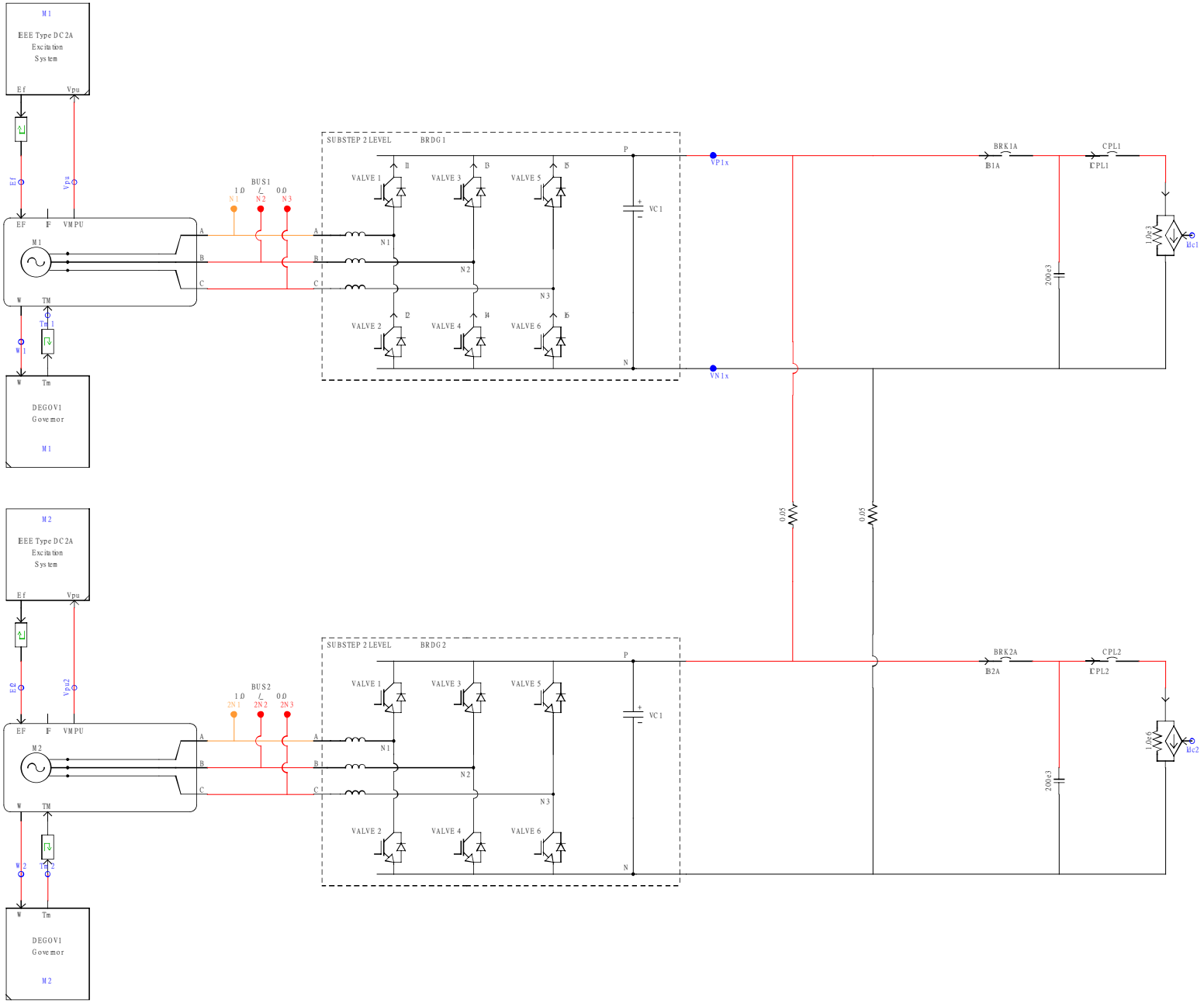


Figure 2.5: Overview RScad simulation

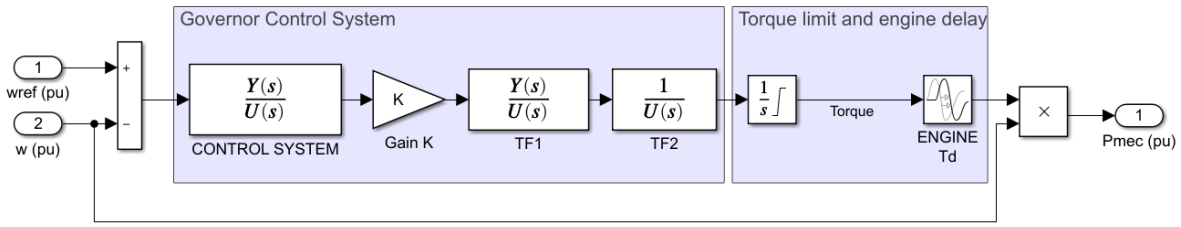


Figure 2.6: Control Schematic Diesel Engine and Governor

## 2.3. MODELS OF THE COMPONENTS

Two simulation software programs are used (Matlab-Simulink and RScad). For both packages, the DC-PPS is built by the required components listed in 2.1. Due to the different software programs, differences between the models may influence the performance and comparison. This section explores what the required detail, necessary for voltage stability analysis, is for the components. This contributes to the answer to the first research question.

The selection criteria for each model is first and foremost determined by the ability to analyse voltage stability. The second selection criteria is that of available data of components through data sheets or comparable examples. The models are predominantly based on standard models and are not build around used products by Royal IHC. The main reason for this is the lack of information about the control loops, parameters and implementation of some of these components. Companies are not always willing to give these freely. Therefore it has been decided to keep to the standardized components.

### 2.3.1. DIESEL ENGINE AND GOVERNOR

The diesel engine provides mechanical energy to the synchronous generator such that it produces the required amount of power. This process is controlled by a governor controller. For the simulation, we are interested in the performance of the power network when objected to large and small disturbances. Thus we need to model the reaction time and torque limits of the diesel engine. The diesel engine is therefore represented by a torque limiter and a delay which represents the time the diesel requires to accelerate and provide the power.

The engine speed is controlled by the governor. Royal IHC uses PID based controllers for both governor and AVR. For this thesis, a standardized control topology is used which is presented in the RTDS manual [30] and is also found in [31].

The design of the diesel engine and the governor is depicted in figure 2.6. The same model is used in both RScad and Matlab Simulink. The model is split into two parts the Governor Control System and the torque limit and engine delay.

The component name in RSCAD is *"rtds_DEGOV"*. DEGOV1 is a model of a governor for a diesel engine. The model is based on the Woodward diesel engine. For that model, droop control is used with either throttle or electric power feedback. The Control system is given by the following transfer function

$$\mathrm{CS} = \frac{(T_{r3}s+1)}{(T_{r1}T_{r2}s^2+T_{r1}s+1)} \tag{2.1}$$

in which $T_{r3}, T_{r2}$ and $T_{r1}$ are the regulator time constants in seconds. TF1 and TF2 are the actuator transfer functions given by:

$$\begin{aligned} \mathrm{TF1} &= \frac{(T_{a1}s+1)}{(T_{a2}s+1)} \\ \mathrm{TF2} &= \frac{1}{(T_{a3}s+1)} \end{aligned} \tag{2.2}$$

here the parameters $T_{a3}, T_{a2}$ and $T_{a1}$ are the actuator time constants in seconds. The gain of the system is represented by the parameter $K$ and the engine delay $T_d$ is in seconds. There are no noticeable differences

between the RScad model and the Matlab model. It should be noted that the droop control is only used in the verification of the model.

### 2.3.2. SYNCHRONOUS GENERATOR MODEL

The model of the synchronous machine is determined by two criteria. First, the detail of the model should be sufficient such that voltage stability analysis can be conducted. Second, there should be sufficient data from datasheets such that it can be parameterized properly.

Both [32] and [31] describe the requirements of the model regarding the type of analysis. For this thesis, rotor angle stability is not an issue since the generators are decoupled and are not required to operate in synchronism. According to [32]:

"*For voltage stability studies, the voltage control and reactive power supply capabilities of generators are of prime importance. During conditions of low system voltages, the reactive power demand on generators may exceed their field-current limits. In such situations, usually, the generator field currents are automatically limited by overexcitation limiters, further aggravating the situation and possibly leading to voltage instability ([31]). Therefore, the generator models should be capable of accurately determining the transient field currents and accounting for the actions of field-current limiters.*"

Thus the excitation and the limits should be modelled and the generator should be detailed enough to incorporate transient behaviour of the field.

The model used in Matlab Simulink is the *"Synchronous Machine Fundamental"* block. The model takes the dynamics of the stator, field and damper windings into account and is represented in the rotor reference dq-frame. The obtained model is described in detail in [32]. It consists of two equivalent damper circuits on the Q-axis, one on the D-axis, the Field circuit + one equivalent damper circuit. Another name for the model is a Synchronous machine Model 2.2. Appendix A shows the parameters of the synchronous machine used. The model used in RScad is the *"Synchronous Machine model with transformer and loads"*, which allows saturation factors. The model uses flux linkages as state variables. The transformer can be omitted from the model. By doing so there are no further differences between the models of Matlab-Simulink and RScad.

The parameterisation of the models is similar to the datasheet supplied by Royal IHC. And thus both models are made according to the two main criteria.

### 2.3.3. AUTOMATIC VOLTAGE REGULATOR

The output voltage of the generator is controlled by the AVR. AVR's are standardized in [33] and readily available blocks can be used in both Matlab Simulink and RScad. Royal IHC uses a PID-based AVR controller. When looking at the datasheets of these AVR's it appeared that the standardization is mostly in academic fields. For the used AVR's at Royal IHC does not mention any of the standardized controller types. However, the documentation lacks to supply the actual control loop. Therefore instead of using the companies used AVR control topology, a standardized model for the AVR is selected based on the direct current commutator rotating exciter.

It should be noted that to obtain a representative model, more effort is required to make the models more comparable to the in the field used components. The underlying schemes of control of the AVR are mostly hidden for the buyer, therefore the standard model is used as a reference. In the future, this could be expanded to a more detailed model of the AVR.

Figure 2.7 shows the basis of the control scheme of the implemented AVR which is the *"IEEE type 1 synchronous machine voltage regulator combined to an exciter*. It consists of a terminal voltage transducer which is represented by a low pass filter with a time constant of $T_r$ in seconds. It is followed by a transient gain reducer with time constants $T_b$ and $T_c$ in seconds which represents a lead-lag compensator. The main regulator is behind the lead-lag compensator with a time constant $T_a$ in seconds and gain $K_a$. The time delay and gain of the exciter are implemented by the parameters $K_e$ and $T_e$ in seconds. Last, the damping is implemented with a feedback loop consisting of a gain $K_F$ and time constant $T_F$ in second.

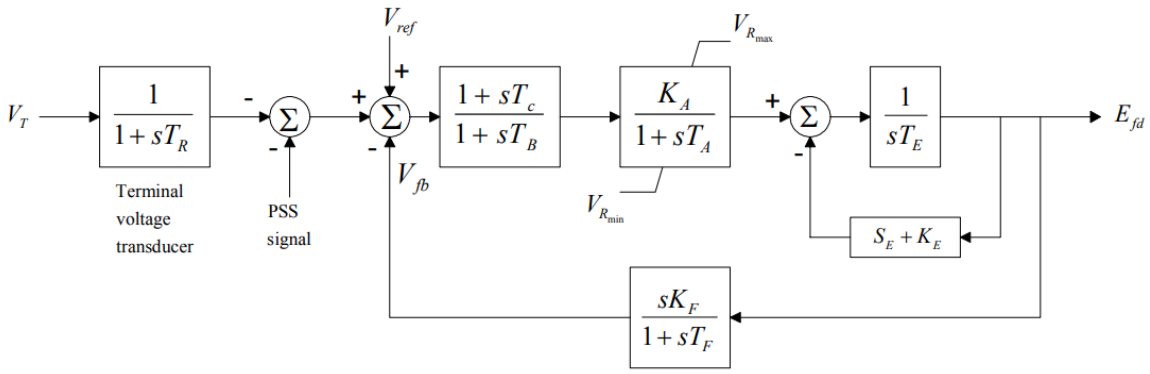


Figure 2.7: Control Scheme of the AVR [31]

### 2.3.4. DC-BUS

A ships power network, compared to land has a higher impedance. This results in a weaker power network. Small changes in load have a larger impact in terms of voltage fluctuations. The impedance of the DC-bus is simulated by a series resistance with a parallel capacitance.

In previous work, during the internship, a DC-busbar was modelled for the calculation of Solid State Breakers. The model of DC-busbar is a small resistance of $0.1 m\Omega$ and a capacitance of $7.89 pF$ per section. The inductance is also very low and can be neglected in this case. When studying transient behaviour during short circuits, these values have a big influence and should be modelled. The load consists of a large capacitance as well as a rectifier. Thus the capacitance of the DC bus is neglected.

### 2.3.5. RECTIFIER MODEL

The AC voltage is rectified to a DC voltage by a passive rectifier. This is conventionally done by a 3 legs diode rectifier. The effects of snubbers and dynamics within the rectifier are out of the scope, thus an average model or simplified model can be used [34]. The DC-side of the rectifier consists of a capacitor that helps stabilize the DC voltage. However, it results in large current spikes on the AC side and requires to be filtered.

The rectifier model used in Matlab-Simulink is the *"Universal bridge"* block with diodes selected as power electronic device. For RScad a 2 level converter is used where the gates are disabled and only the bypass diodes are used. In this way, it acts as a passive rectifier. The model used in RScad is the *"rtds_ss_LEV2_V3.def"*.

The rectifier introduces complexity to this problem due to its non-linear behaviour. The analysis tool is mostly used on linearized or assumed to be linear measurements.

### 2.3.6. INVERTER MODEL AND LOAD

The loads for this network are large inverter modules powering the thrusters of the vessel. These tightly controlled inverters ensure that thrusters, pumps and motors are powered accordingly. In practice, this could be a speed set-point at which the thrusters should turn. The machine is often a large induction machine sometimes up to several MW of power.

The detail of the model is kept to a minimum to keep the complexity of the system as low as possible. The goal of the simulation is to determine the voltage stability of this vessel lay-out. The load can be seen as an energy absorption component based on the voltage of the DC bus. It should act as fast as the induction motor and inverter could act. This way the transient behaviour and complex control schemes for motor control can be simplified. This model is known as a constant power load (CPL). The CPL is used often to simplify the load of a power network [10] [35] [36] especially to investigate stability issues. Therefore the model used as inverter and load is a CPL.

The CPL is modeled as voltage controlled curent source. The current of the source is determined as follows:

$$I_{\text{CPL}} = \frac{P_{\text{setpoint}}}{V_{\text{bus}}} \tag{2.3}$$

the current $I_{\text{CPL}}$ given in ampere, power $P_{\text{setpoint}}$ in Watt and $V_{\text{bus}}$ in volts. A PID controller is used to maintain the power setpoint.

## 2.4. INITIALISATION OF THE MODEL

The previous section showed the selected models, they ought to be sufficiently detailed for voltage stability analysis. The controllers, the AVR and Governor, need to be parameterized. This section describes the tests performed to initialise the model such that it is ready to use for voltage stability analysis. This section contributes to answering the research question regarding the influence of the components on voltage stability.

The section is split into two parts. First, the system is parameterized using the Matlab-Simulink model. Then these values are copied to the RScad simulation and tested. The tests are compared to validate the simulation and the performance of Matlab-Simulink.

The Simulink model has been build in steps to allow analysis and performance of the controllers, the AVR and the governor. The tests are performed on a single generator - rectifier - load setup. This is done for two reasons. First, it simplifies the model and second it tests the hypothesis that simply copying controller parameters is not enough to maintain stability. The second reason is more practical of nature. During commissioning the generators are tested similarly. When the generator is performing well, the settings are often copied to the other generators. The question arises whether this is a viable working method or that more effort should be put into the initialisation process.

The following tests are executed:

1. Voltage step response
2. Load step response
3. AC measurement versus DC measurement
4. CPL performance
5. Parallel generator - rectifier - load setup

### 2.4.1. VOLTAGE STEP RESPONSE

The AVR is responsible for stabilizing the output voltage of the generator. In this case, a generator - rectifier - load setup is used and therefore there are two possible observation points. The voltage measurement on the AC side can be used as input for the AVR or on the DC side. The performance of both points will be investigated in section . This section focuses on the performance of the AVR in keeping the DC-side voltage stable.

The reference voltage of the AVR is given a step from 1 p.u. to 1.2 p.u. voltage reference. Normally this is a no-load test, in which the performance of the AVR is tested. In the simulation, a no-load test cannot be performed due to computational loops. A small load of $0.1 p.u.$ is used to allow the simulation to run.

The tests are performed using the voltage of the DC-bar as the input for the AVR. The DC voltage after rectification can be calculated as:

$$V_{\text{DC}} = \frac{3\sqrt{2}}{\pi} V_{\text{LL}} \tag{2.4}$$

where $V_{\text{LL}}$ is the line to line r.m.s. voltage. The resulting DC-bus voltage is 742 Volts. The regulator gain, exciter and damping filter need to be parameterized such that the voltage remains in stable operating points and has a fast enough response. The Exciter dynamics are set on $Ke = 1$ and $Te = 50ms$. The effect of the damping constant is shown in figure 2.8, the top part shows the field voltage and the bottom part of the figure

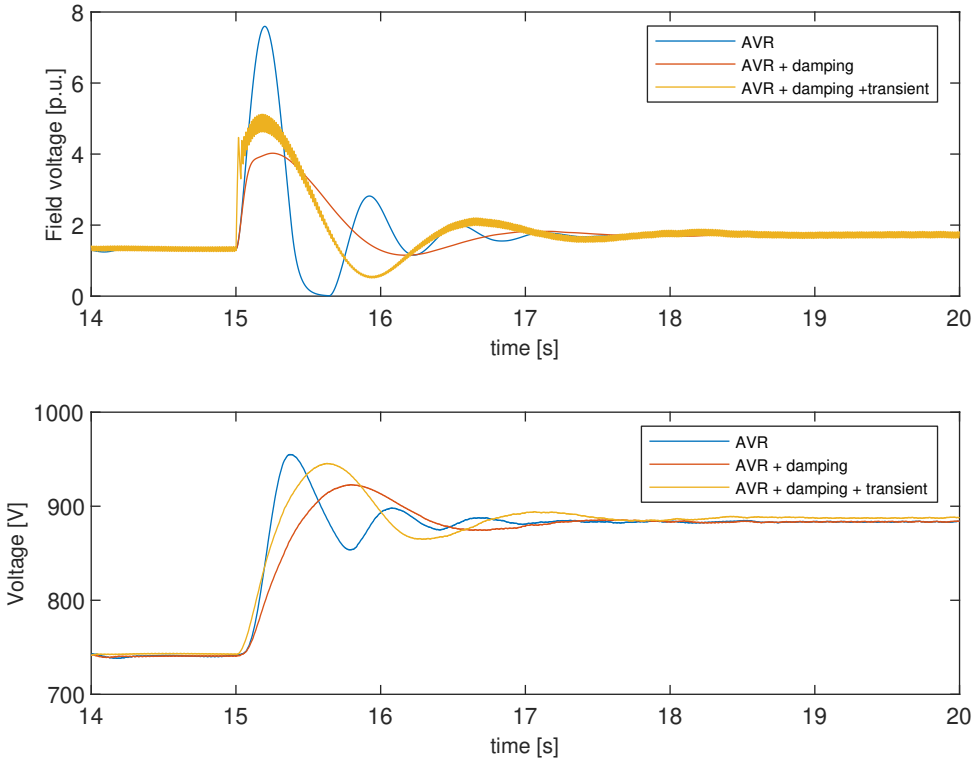


Figure 2.8: Results of the voltage step test; Top: Field voltage; Bottom: Voltage

depicts the AC voltage response. The damping reduces the oscillations.

The overshoot could be dangerous to the equipment on board and should be avoided. Therefore the transient limiter is implemented to adjust the control loop such that the overshoot is limited. Figure 2.8 shows the effect of the transient reduction in the form of a lead-lag compensator. The top part of figure 2.8 shows the torque response and the lower part depicts the speed response. The overshoot is limited but the settling time is a bit longer.

### 2.4.2. LOAD STEP RESPONSE

Conventionally, the governor controls the diesel engine such that the frequency of the power network is maintained. The relation of the frequency and power are therefore related. To test the performance of the governor load steps are performed. These load steps test whether the governor is fast enough to act and supply more power such that the frequency is maintained.

The frequency is a variable which in DC-PPS does not require to maintain at a stable point. Instead, the DC voltage becomes the only variable that is bound to limits. Both AVR and the governor control the DC voltage and influence it. The input for the governor in the model under study is the frequency. Still a conventional way of operating is used.

The test consists of a load step from $0.1 p.u.$ to $0.8 p.u.$. The load step is initiated at $t = 15s$. The test is performed with different gain settings $K$ of the controller. Figure 2.9 shows the result when the system is objected to a load step of $0.7 p.u.$ increase. The first 5 seconds are the system start-up oscillations. These are not of interest in this analysis. From figure 2.9 the effect of the gain is visible. Increasing the gain $K$ increases the settling time and reduces the oscillation. Minor deviations in speed are allowed therefore a $K = 40$ is sufficient for this controller.

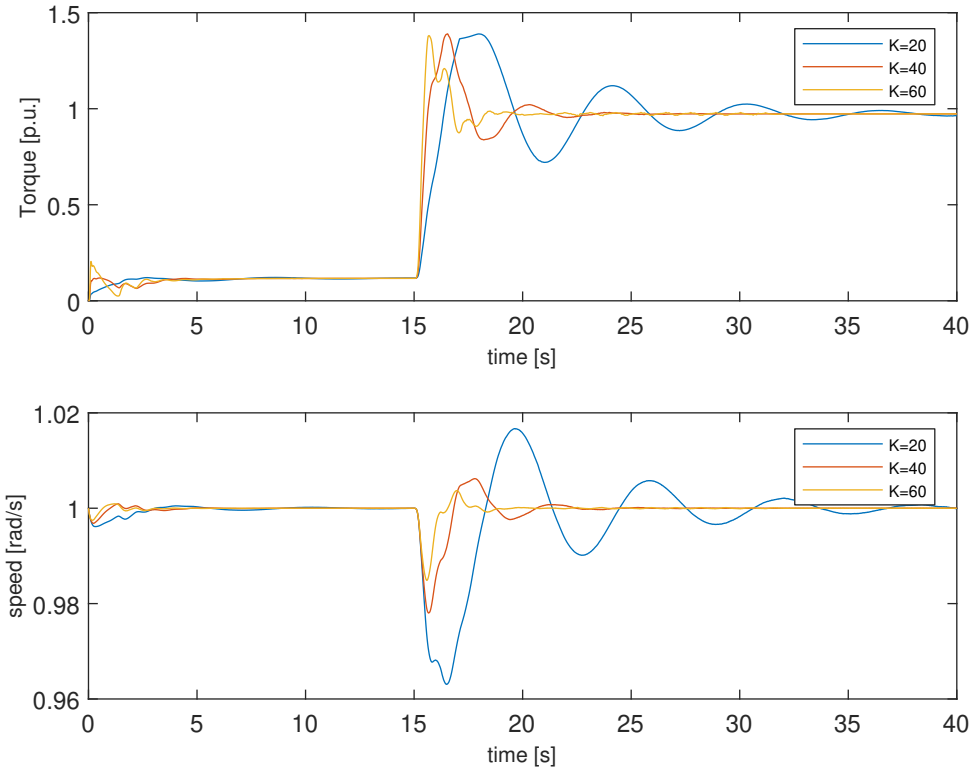


Figure 2.9: Result of a load step test with different Gain values, Top: Torque; Bottom: Speed

### 2.4.3. AC MEASUREMENT VERSUS DC MEASUREMENT

The system has limited controllability because a passive diode rectifier is used. The conventional input for the AVR is the output voltage of the generator terminals. However, DC voltage changes may not be noticed by the AC voltage measurement and can cause a lower or higher DC voltage than allowed.

The AVR could also use the DC voltage measurement as an input. The performance of using AC voltage as the input parameter or the DC voltage as an input control parameter is tested by two tests in this section. In these tests all the parameters of the controllers are similar. Thus only the actual controller input differs. The first test consists of a voltage step setpoint increase as shown in section 2.4.1. The second test is that of a load step shown in section 2.4.2. This contributes to testing what components influence the voltage stability of the DC-PPS.

#### AC VS DC VOLTAGE STEP

Figure 2.10 shows the result of a voltage step from $1.0 p.u.$ to $1.2 p.u.$ at $t = 15 s$. The upper figure depicts the DC bus voltage, the middle part shows the field voltage and the lower part depicts the response of the line voltage. The tracking of the setpoint when using the AC measurements has a steady-state error of around $20 V$ and is not compensated. The AC measurement line voltage is exactly on the $550 V$ and is perfectly maintained at $660 V$ at the $1.2 p.u.$ voltage reference point. It shows that the performance of maintaining a stable DC voltage using the AC input voltage requires compensation.

When using the DC voltage as input for the AVR the new voltage reference point is maintained. It shows that a slightly higher line voltage is required to obtain the new voltage level. This also shows the danger of this method. The AC voltage should not exceed the limits of the generator and should be implemented in the control to prevent damage to the machines.

The field voltage when using the DCvoltage as input for the AVR is slightly larger. This is a logical explanation for the large line voltage and the better tracking of the DC voltage. The type of measurement does not influence the behaviour of the controller, both settling time, damping and overshoot remain similar.

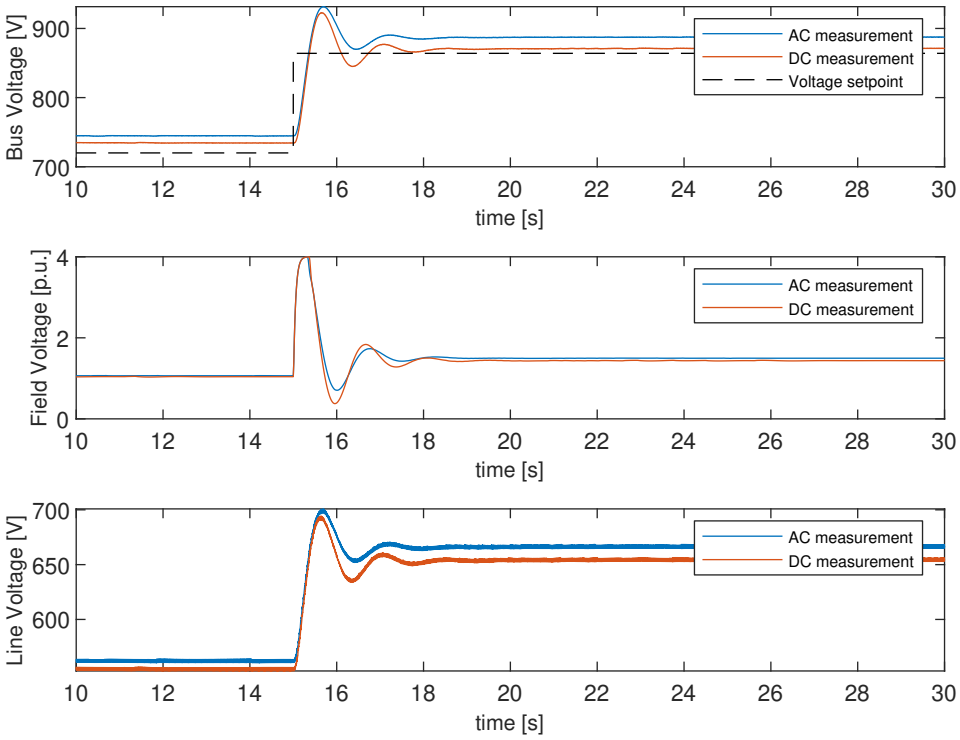


Figure 2.10: Comparison of AC and DC voltage as input of the AVR; Top: DC voltage; Middle: Field Voltage; Bottom: Line voltage

### AC VS DC LOAD STEP

Figure 2.11 shows the result of a load step. The top part of the figure shows the DC bus Voltage, the middle part shows the field voltage and the bottom part depicts the line voltage. Similar to the previous load-step test the power is increased from $0.1 p.u.$ to $0.8 p.u.$ at $t = 15 s$. There is a notable difference between the AC voltage and DC voltage as input reference.

When using the AC voltage as input for the AVR it is the tracking of the DC voltage bus is bad. The static error is large almost $100 V$. This because the AC side does not see the DC voltage drop, the rectifier seems to slow that process and the Field voltage is even slightly dropped initially.

The voltage stability is increased by using the DC bus voltage as input for the AVR. The effect of a load step is measured and the Field voltage is increased accordingly. The DC voltage drop is decreased due to the adequate response of the AVR. Both AVR and Governor influence the voltage stability when using a passive rectifier. The AC line voltage increases to around $600 V$ which is a 10% increase. It is important to limit the output of the line voltage such that this line voltage increase does not damage the generator. From both tests, it can be concluded that both the governor and AVR should be parameterized accordingly to maintain voltage stability.

Figure 2.11 also shows that both AC and DC measurement come to a similar Field voltage. This can be explained as follows, the generated power of simplified synchronous machine is as follows:

$$P = \frac{E_\mathrm{p} V_\mathrm{t}}{X_\mathrm{d}} sin(\delta) \tag{2.5}$$

It can be seen that when using the DC measurement the $V_t$ rises and therefore the $\delta$ is lower. This means that by using the DC - measurement the chance of suddenly overloading the generator ($\delta > 90$) is lower than when using AC measurement but at the risk of overvoltage if not limited.

Another observation for both tests is that the speed of the controller is not influenced by the type of measurement. Both AC and DC have similar settling times. The only difference is the static error which is different for both measurement inputs.

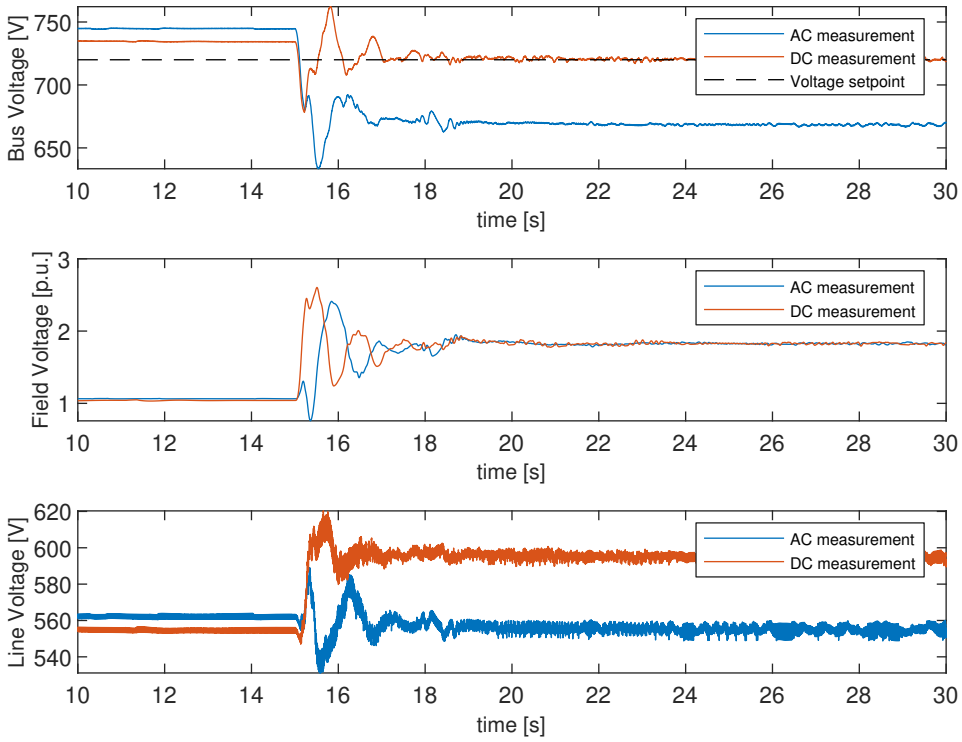


Figure 2.11: Load step comparison AC versus DC voltage input of the AVR; Top: DC voltage; Middle: Field Voltage; Bottom: Line voltage

### 2.4.4. CPL PERFORMANCE

As shown in 1.4 a CPL has the effect of a negative incremental resistance. When a sudden load increase occurs in a power system the voltage tends to drop. This results in an increase of the current from the CPL which is programmed to maintain a certain power level. This results in even further dropping the voltage and may lead to the collapse of the grid. This phenomenon is observable if the generator side is slow in restoring the voltage. For this test a load-step of 0.1 p.u. to 1.0 p.u. is made.

First, the performance of the CPL itself is tested. Figure 2.12 shows that at 15$s$ the load step is initiated. The top part of the figure depicts the DC voltage, the middle part shows the current on the bus and the lower part shows the power setpoint and DC power. The DC voltage decreases rapidly. The current rises quick such that the power matches the setpoint. The CPL can track the power accurately and can achieve the power fast.

It is evident that the CPL is quick, figure 2.13, the top part depicts the DC voltage and bottom part the DC current, shows that the voltage drops to almost 650$V$ and the current rises quickly to the nominal current. The current is controlled by the CPL and the voltage by the AVR, thus by comparing the DC bus voltage and the Field voltage we can conclude whether the AVR is too slow to cope with the quick voltage drop. Figure 2.14 shows the DC bus voltage and the Field voltage. The top part of the figure depicts the bus voltage and the bottom part shows the field voltage. It is evident that the field voltage reacts but is too slow to keep the voltage at the nominal voltage level.

The results indicate that a CPL can follow the power setpoint quickly and the destabilizing effect is observed on the DC bus. This is compensated only by the generator controls due to the lack of controllability from the passive rectifier. It limits the system in coping with fast load changes. A solution could be to restrict fast current rises such that the generator can cope with power fluctuations. However, those limitations mustn't interfere with the operation of the ship.

Vessels are equipped with safety systems such that severe damage is prevented. One of those systems on inverters is under-voltage protection. This protection device interrupts the operation when the voltage drops below the safety value. This is to prevent overcurrent inside the inverter. Overvoltage protection is not

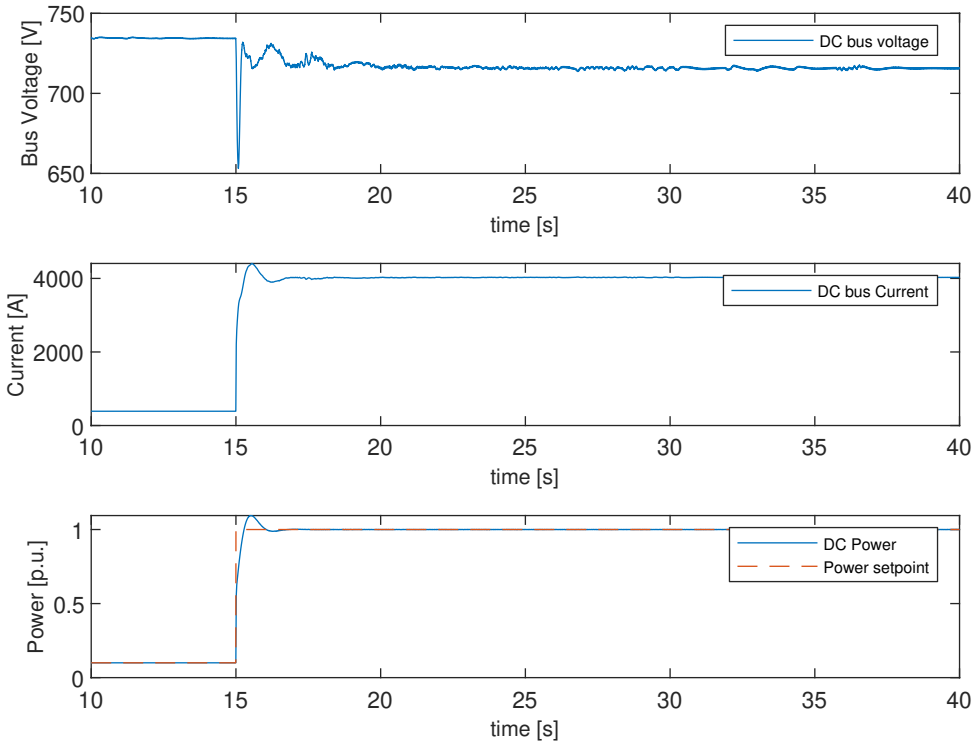


Figure 2.12: Load step CPL effect; Top: DC bus voltage; Middle: DC current; Bottom: DC power

installed however, overvoltage could damage the capacitors and IGBT's as well and should be limited to the rated values of the inverter.

### 2.4.5. PARALLEL GENERATOR - RECTIFIER - LOAD SETUP

The performance of one generator-rectifier-CPL has been tested and it has been shown that both the AVR and governor influence the voltage stability of the DC grid. The analysis is now extended to a case with two parallel generator-rectifier-CPLs. Both [24, 25] suggested looking into the dynamic behaviour and the relation between the generator-rectifiers when operated in parallel.

The DC bus is coupled via an ideal switch and a small resistance. For a first test, the parameters of both the AVRs and generators are kept the same, emulating the fact that they are duplicates in the vessel. The test consists of a load step in one of the loads. The expected effect of a sudden load switch is the reduction of the DC bus voltage. The negative incremental effect of the load should be compensated by the AVR quick enough to remain stable.

At $t = 15s$ a load step of 0.1 to $1.0p.u.$ of one of the loads is initiated the other load is kept at a load of $0.5p.u.$. At $t = 40s$ the power is reduced from $1p.u.$ to $0.1p.u.$ The results are shown in figure 2.15 in which the A and B denote the separate areas. The top part of the figure depicts the DC voltage, the middle part shows the Current of the system and the bottom part depicts the power setpoints in area A and B. In the figure, the current $I_{rectifier}$ represents the current supplied by the rectifier, $I_{\text{CPL}}$ represents the current absorbed by the load.

The following observations are made:

- heavy oscillations in supplied current from the rectifier during low load
- small oscillations in voltage during low load
- small voltage drop when the system is loaded
- Power of area A keeps stable without any reduction in load during load switch

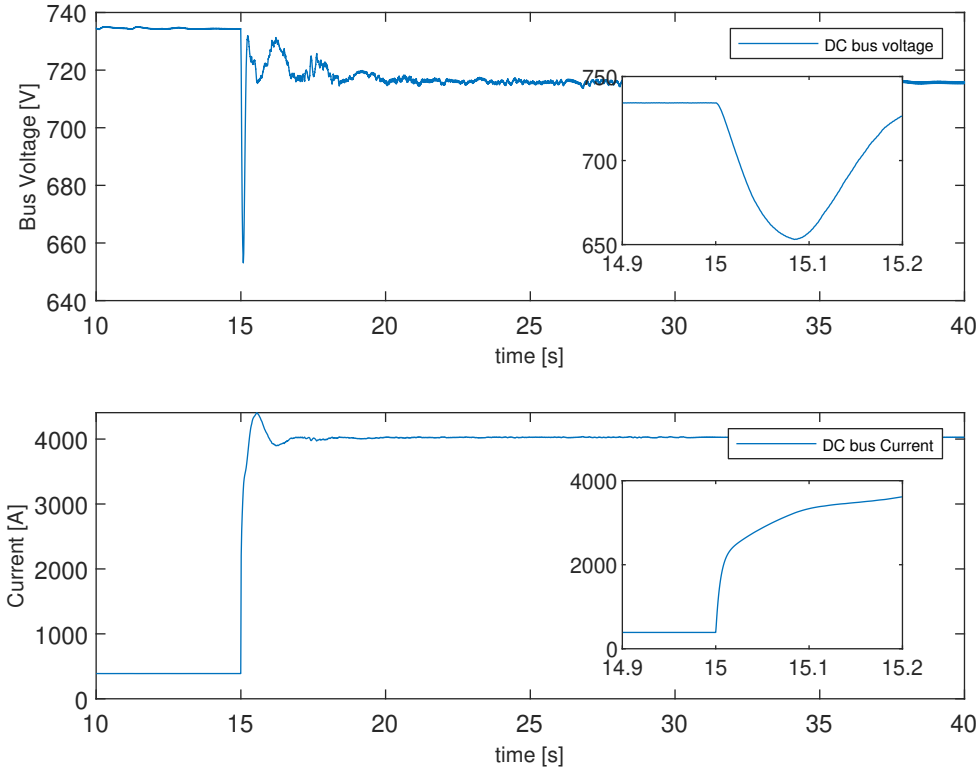


Figure 2.13: Load test zoom current and bus voltage; Top: DC bus Voltage; Bottom: DC current

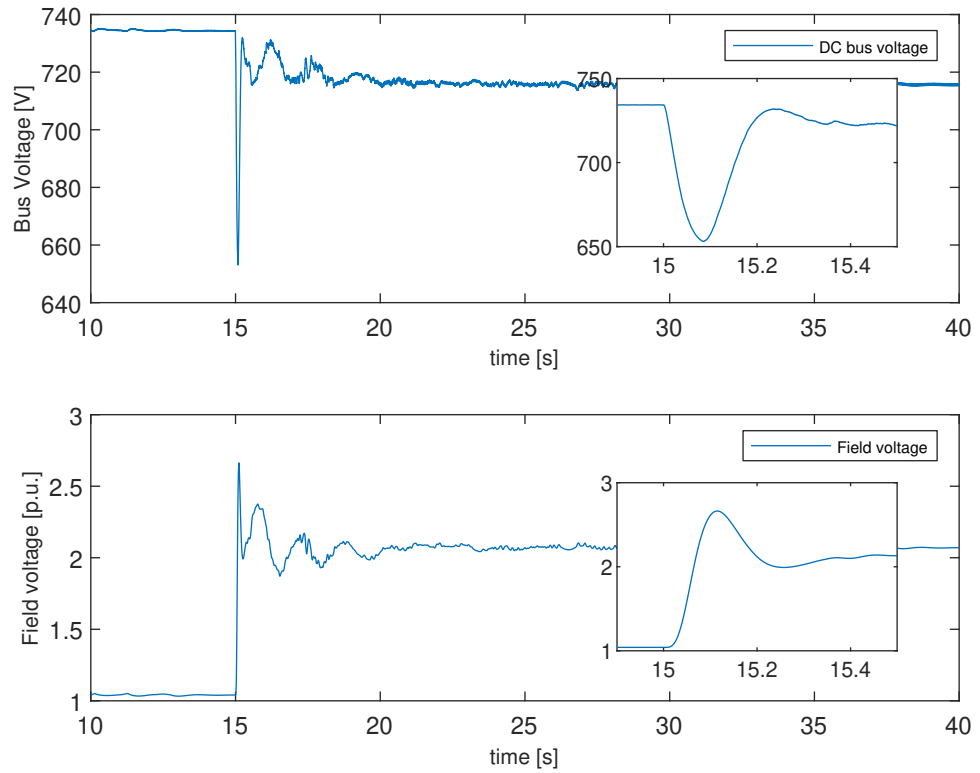


Figure 2.14: Field voltage and bus voltage CPL effect; Top: DC bus voltage; Bottom: Field Voltage

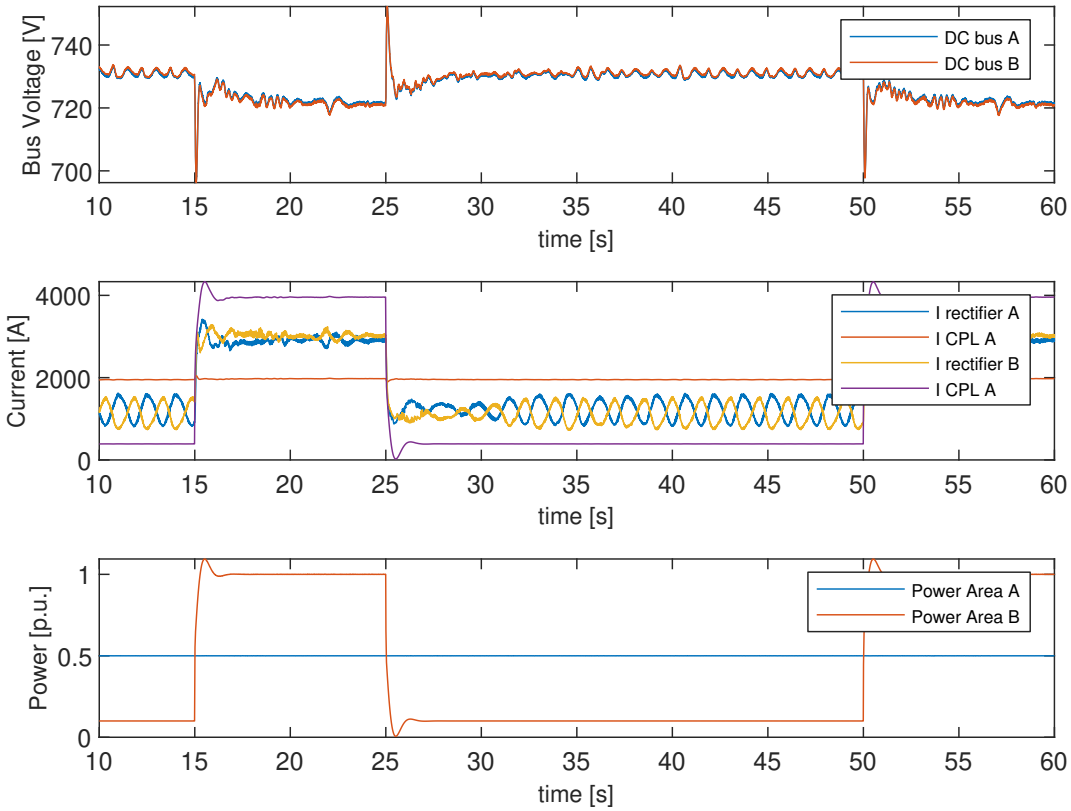


Figure 2.15: Load step test of two parallel generator sets with 2 loads; Top: DC bus voltages; Middle: DC currents; Bottom: Power

- Both generators supply the same amount of power

An important note to the observations is that the current from the rectifier is oscillating in anti-resonance. This could hint at a local oscillation mode between the two areas. This can not yet be concluded only by the figure, it shows that an analysis tool could enhance the analysis and is of good use here.

In conventional AC systems, the real power is related to the mechanical energy and speed of the generator. The reactive power is related to the AC voltage of the system. With the DC rectifier, there is no reactive power in the DC bus, the voltage is no longer controlled by reactive power but is controlled by the real power in the DC system. When there is a surplus of real power the voltage rises, and it drops when a shortage of real power is apparent. If this is true then the oscillations of the voltage should be dominant in the speed control (torque).

The frequency of the oscillation is around $0.5Hz$ which indicates an inter-area oscillation. Figure 2.16 depicts the DC voltage in the top of the figure, the torque setpoint in the middle part and the field setpoint in the bottom part of the figure during the period of the oscillation. It shows that the torque oscillates a-periodically and the field voltage setpoint are operating only with a small static difference. The difference between the field generators can be explained when looking at the path of the power. Generator set A towards the load in area B has a larger impedance. Therefore it has to produce a larger field voltage to maintain the voltage on the DC bus.

This test indicates that one well parameterized single generator-rectifier-load set will not guarantee that it will perform well when operated in parallel with an identical set. It shows that the problems are intricate and tests, simulations and analysis tools are required.

This model functions as a baseline for future DC-vessel analysis. For now, the model has to be validated to access whether Simulink can reproduce similar results as a dedicated software package used to access stability. All the parameters are available in the appendix A. The following functions are available within the baseline simulation:

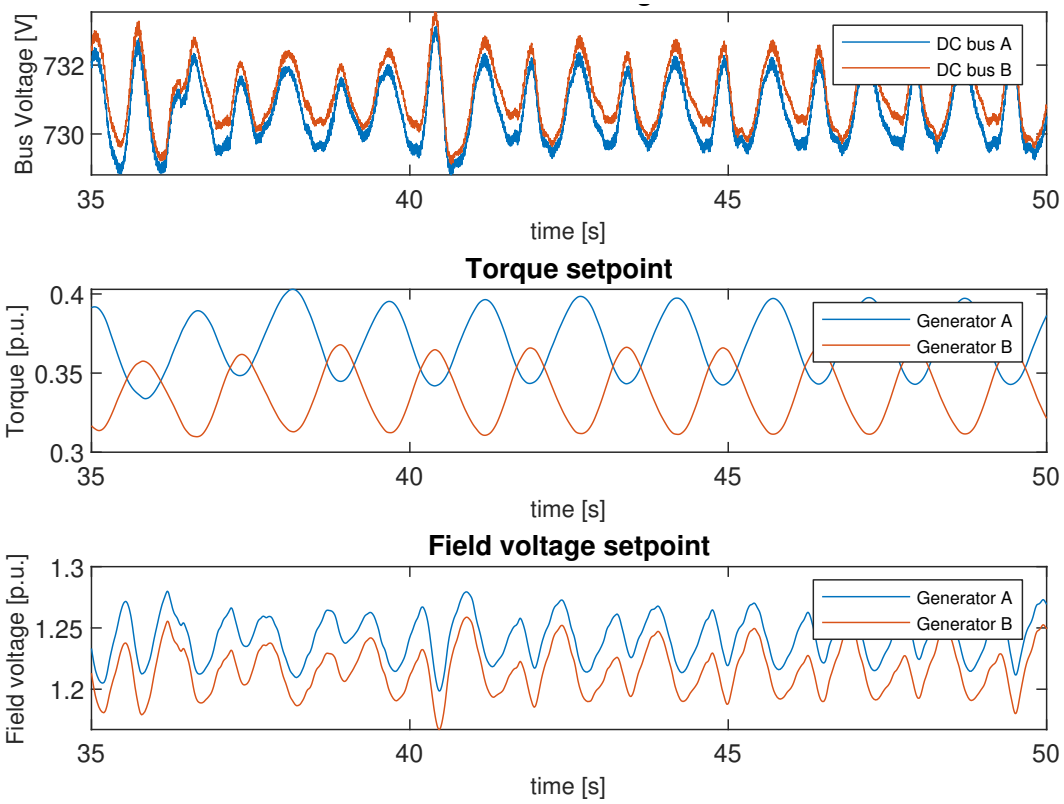


Figure 2.16: Oscillations during low loads; Top: DC bus voltages; Middle: Torque setpoint; Bottom: Field voltage

1. Simulate different load-profiles
2. Parametric freedom of controllers
3. Parametric freedom in load profiles (di/dt)
4. Availability of data and ease in running different simulations in parallel

## 2.5. MODEL VERIFICATION USING RSCAD RTDS

The simulation from Matlab-Simulink is verified by comparing it to the results of the RScad real-time simulation on a Novacor. The simulations are made as identical as possible therefore it is not a validation of the model. The function of this verification is to test whether Matlab-Simulink can compute the same phenomenon compared to a highly specialised environment such as RScad. The results of both tests should be similar to verify the model.

The voltage stability is tested by introducing load steps in the system. The dynamic behaviour of the system represents the response of the control system and the component parameters. The test of the verification consists of multiple sequential load steps starting from a load of 0.1 p.u. to 1.0 p.u. The intention is to see whether the response of the model in RScad behaves similar to that of the model in Matlab-Simulink. The test represents the limits within the model such as field limiters of the AVR and torque limiters from the governor.

The RScad simulation has been made in an early stage of this thesis project and it differs slightly from the tests done in previous sections. The differences between this test and the previous Matlab model are:

1. The control parameters (gains and time constants) of the AVR and Governor differ
2. The controller of the governor has a droop regulator

The complete list of parameters is given in appendix A. The droop constant has been set to 0.03.

Table 2.2: Deviations of RScad simulation and Matlab Simulation

| t [s] | 20 | 40 | 60 | 80 | 100 | 120 |
|---|---|---|---|---|---|---|
| $I_\Delta$ [kA] | 0.0617 | 0.1261 | 0.1598 | 0.2631 | 0.2868 | 0.3496 |
| $V_\Delta$ [kV] | 0.0035 | 0.0045 | 0.0045 | 0.0011 | 0.0004 | 0.0037 |
| $P_\Delta$ [MW] | 0.0475 | 0.0962 | 0.1205 | 0.1804 | 0.1908 | 0.2165 |
| $\omega_\Delta$ [rad/s] | 0.193 | 0.47 | 0.61 | 0.939 | 0.958 | 1.134 |

Both systems, shown in figure 2.3 and figure 2.5, are objected to load steps at the same interval and same change. The DC current, DC voltage, measured power, power setpoint and frequency are measured. The results of the simulation are shown in figure 2.17.

From visual inspection, it can be concluded that the dynamic behaviour in both simulations is comparable. Both simulations behave similarly and thus the dynamical behaviour of the models can be assumed to be similar. For example, the voltage of the DC bus shows similar behaviour. The start of the system shows bigger deviations. This is due to the initialisation of the Matlab-Simulink model. The initial voltage of the DC-bus bar has been set at $0.8kV$ whereas RScad is at $0.78kV$. This is the initialisation of the model and is not the area of interest thus these deviations are allowed. Another minor deviation is the time at which the timestep is initiated.

The results show that the droop control works in the simulation. The frequency of the generator drops for every load step and therefore also the voltage level on the DC bus. This shows that the variable frequency rate, given as an advantage for DC over AC, is limited when using only a passive rectifier.

The deviations between the two simulations are shown in table 2.2. The current $I_\Delta$, voltage $V_\Delta$, power $P_\Delta$ and frequency $\omega_\Delta$ deviations are shown. The deviation is determined by the average value of both simulations for 19 seconds. Thus for values of $t = 20$ s the average value has been taken between $t = 20$ until $t = 39$. From table 2.2 it is clear that the difference between RScad and Matlab increase when the power is increased. The voltage $V_\Delta$ seems to change slightly but the current and power have larger differences. At full power, the power difference is around 10% of the nominal power level. The power fluctuates due to the current form which is altered by the passive rectifier. Matlab Simulink has a smaller timestep and accurately reproduces the current form while RScads timestep is larger. The effect of a larger timestep is visible in figure 2.18, the average current of the simulation increases the average error.

From this simulation, it can be concluded that both Matlab Simulink and RScad incorporate the same dynamic behaviour. The same response is observed after each load step and a similar steady-state operation point is acquired. No large discrepancies are found other than the steady-state error due to small differences in the model. The Matlab-Simulink model has been chosen to continue to work on due to the ease in use of the model and the fact that Royal IHC prefers Matlab Simulink over a new software package.

## 2.6. CONCLUSIONS

In this chapter, the overall system under study has been modelled. The parameters of the controller have been determined and tested. The detail of the model has been determined allowing voltage stability studies. The occurring phenomena due to the components (CPL, passive rectification) have been checked and proved to be in the model. Eventually, the total system under study has been verified via a comparative analysis between the results of the Matlab-Simulink model and an RScad model. The results of this chapter contribute to answering the research questions presented in chapter 1 by proposing a model which will be used in chapter 4. This generic model allows the further study of parametric analysis of the controllers and enables the investigation of different control topologies and methods for future works.

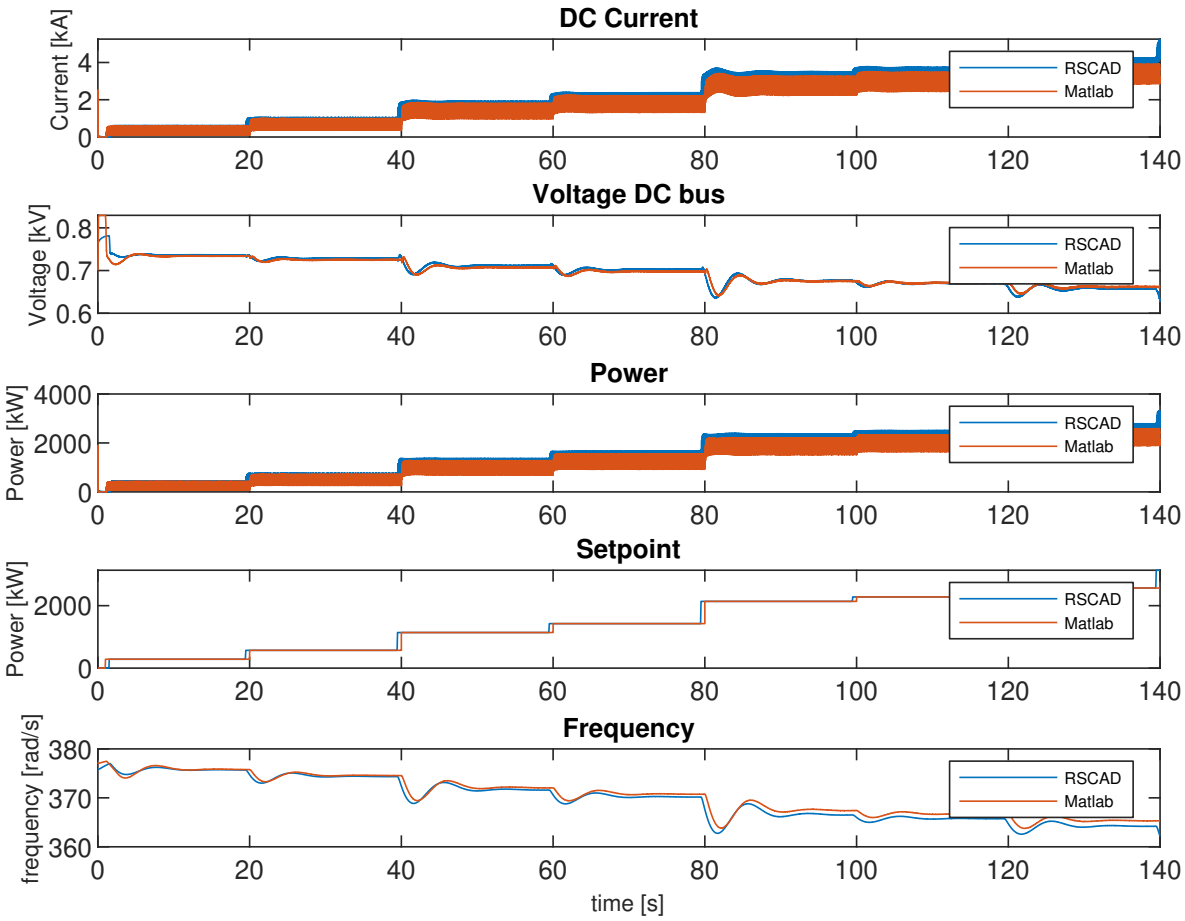


Figure 2.17: Verification results with matlab simulink and RScad

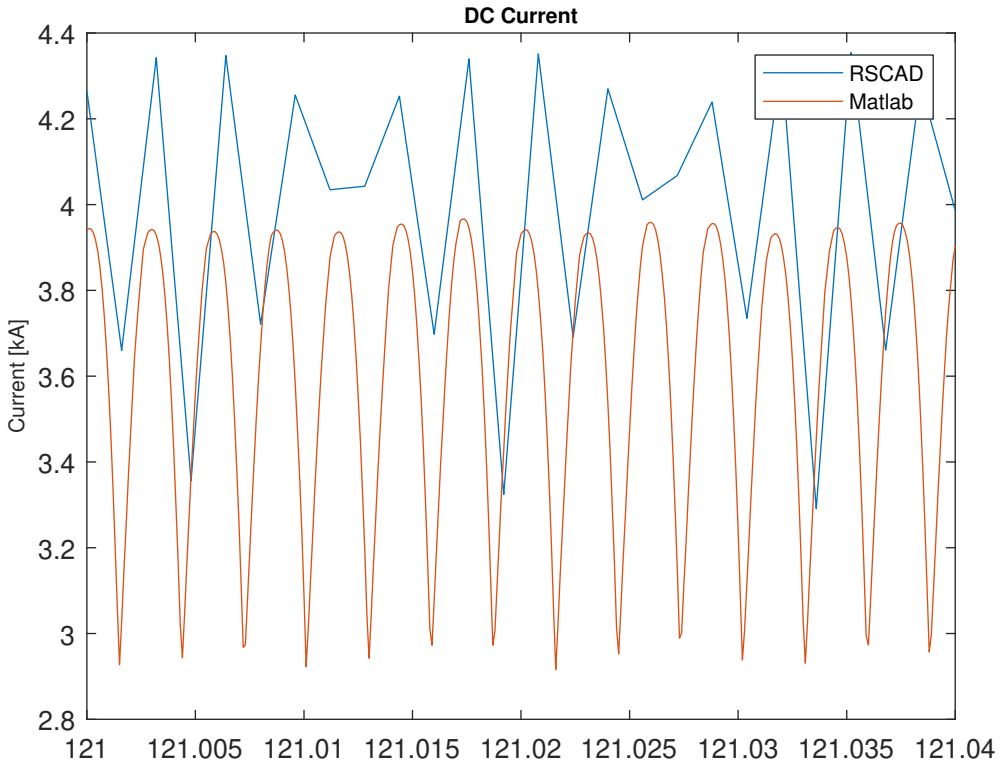


Figure 2.18: Current of RScad and Matlab simulation

# 3

# STABILITY ANALYSIS TOOL

The previous chapter showcased the development and validation of the model under study. It showed that an analysis tool could be beneficial in understanding the underlying oscillations within a signal. A tool is required such that both simulation data and field data can be analysed. This chapter describes the development of the stability analysis tool. With this tool different oscillatory modes can be extracted from a signal. The basic methodology of the selected method, prony analysis, is described in paragraph 3.1. It describes the base steps to calculate the intrinsic mode functions (IMFs). To implement the method such that it can be used on different signals or multiple signals some intermediate steps are required. Section 3.2 describes the code implementation of the prony analysis and explains some of the intermediate steps. The contribution of [37] is implemented in which a node contribution factor (NCF) is proposed, section 3.3 explains the NCF. The prony method allows self-validation, in section 3.4 these validation tests are described and the performance of the tool is tested. The last section 3.5 summarizes the conclusions and relates them to the research questions and objectives. This section contributes to the research questions by implementing a method to analyse the stability of a DC-PPS. It allows to locate unstable operation points and enables the categorisation of different oscillatory types.

## 3.1. BASIS OF PRONY ANALYSIS

Before implementing pronys method the basis is explained in this section. The basis of prony analysis is to assemble a set of functions that approximates the analysed signal. Prony analysis is a method for fitting a linear combination of exponential terms to a signal [38]. The prerequisite of the analysis is to have a data set sampled at a constant sample time. A comparison can be made with a fast Fourier transform. The main difference is that the latter requires information about the main frequency of the signal whilst prony is directly calculating the dominant frequencies. This section explains the basics of the prony analysis.

Consider a continues function signal described by $y(t)$. This is to be approximated by a combination of exponential terms like:

$$y(t) = \sum_{i=1}^{n} \gamma_i e^{\lambda_i t} \tag{3.1}$$

where $\lambda_i$ are the eigenvalues or modes of the approximated system and $n$ denotes the modes. Prony analysis approximated the unknown parameters from the exponential functions. In this case, the unknown parameters are $\gamma_i$ and $\lambda_i$ [37]. The approximation is executed so that the difference between the data and the approximation is minimum. The signal of $y(t)$ should be sampled with a constant sample time $T_s$ [38]. Measurements are in the discrete-time domain and therefore the equation in 3.1 becomes

$$y(kT) = \sum_{i=1}^{n} = \beta_i z_i^k, \qquad k = 1,2,3\ldots,N \tag{3.2}$$

$N$ is the length of the datasignal $y(t)$. The terms $z_i$ represent the time domain or z-domain eigenvalues of the approximated system. $\beta_i$ are the residues corresponting to $z_i$ and i are the number of modes to be determined

of which n is the total order of the system of approximation equations. Equation 3.2 in matrix form gives [38] [37]:

$$\begin{bmatrix} z_1^1 & z_2^1 & \cdots & z_n^1 \\ z_1^2 & z_2^2 & \cdots & z_n^2 \\ \vdots & \vdots & \ddots & \vdots \\ z_1^N & z_2^N & \cdots & z_n^N \end{bmatrix} \begin{bmatrix} \beta_1 \\ \beta_2 \\ \vdots \\ \beta_n \end{bmatrix} = \begin{bmatrix} y[1] \\ y[2] \\ \vdots \\ y[N] \end{bmatrix} \tag{3.3}$$

From this, the characteristic equation of $y(t)$ can be determined and has the form of

$$z^n - a_1 z^{n-1} - a_2 z^{n-2} - \cdots - a_{n-1} z - a_n = 0, \qquad a_0 = 1 \tag{3.4}$$

the coefficients from equation 3.4 are obtained by solving the linear predictive equation

$$\begin{bmatrix} y_{n+1} \\ y_{n+2} \\ \vdots \\ y_N \end{bmatrix} = \begin{bmatrix} y_n & y_{n-1} & \cdots & y_1 \\ y_{n+1} & y_n & \cdots & y_2 \\ \vdots & \vdots & \ddots & \vdots \\ y_{N-1} & y_{N-2} & \cdots & y_{N-n} \end{bmatrix} \begin{bmatrix} a_1 \\ a_2 \\ \vdots \\ a_n \end{bmatrix} \tag{3.5}$$

Which can be given in a matrix form [37]:

$$D\underline{a} = \underline{y} \tag{3.6}$$

Here D is a $[Nxi]$ matrix and $a$ a vector of length $i$, the output y is the length of the data $N$. Thus the matrix D grows in dimensions if the dataset is increased or if the number of modes increases. Equation 3.5 shows that the original data obtained from measurements need to be restructured. This restructuring is in the form of a Toeplitz matrix. The subscript $n$ gives the order of the approximation function which is built to approximate the original signal. It shows that the order $n$ and the amount of data points $N$ influence the size and therefore the required computational power of the problem. It also shows that the data can be pre-processed to reduce the complexity of the required terms $n$.

The original signal can be reconstructed with equation 3.2 by expanding the complex numbers give the following equation:

$$\begin{aligned} y[kT] &= \sum_{i=1}^{n} \beta_i z_i^k \qquad k = 1, \ldots, N \\ &= \sum_{i=1}^{n} A_i e^{j\theta_i} e^{(\alpha_i + j2\pi f_i)T(k)} \end{aligned} \tag{3.7}$$

Equation 3.7 is the general expression for the solution. This equation shows that the method is self-validating. The original data can be compared with the approximated signal to see whether the approximation is valid. Equation 3.7 allows to determine the parameters $A_i, \theta_i, \alpha_i, f_i$ within the equation. Where the amplitude is $A_i$ in the same units as the units in $y[kT]$, the damping factor $\alpha_i$ in seconds$^{-1}$, the frequency $f_i$ in Hertz and $\theta_i$ which is the relative phase angle. $T$ is the sampling period (in seconds) of signal $y[kT]$.

To acquire the solution for those parameters the following steps should be followed [28] [39]:

1. Construct the D matrix and $\underline{y}$ using data according to equation 3.4
2. Solve a linear least square error (LSE) problem and acquire teh solution to vector $\underline{a}$
3. Solve the polynomial characteristic in equation 3.4 to acquire the z-domain eigenvalues
4. Solve a LSE problem for equation 3.3 to obtain $\beta_i$ values
5. Reconstruct the main signal with 3.2

The above-described equations and algorithm describe the general approach to obtain an approximation function out of the prony analysis. Prony approximates the system response, when the approximation is accurate the functions give insight into the response. For example, the damping of a mode indicates if the signal is undamped at a certain frequency. The frequency gives information of the cause of the oscillation.

Multiple signals can be analysed which allows the comparison between modes of different sources, this also gives insight into the behaviour of the system. Possible use of this is given in section 3.4. It should also be stated that pre-processing of the data is an option. In some cases, this can improve the accuracy of the signal or allow to filter out frequencies that are of no interest. Prony analysis is self-validating since the original signal can be reconstructed and compared to the original signal. This property will be used in validating the implementation.

## 3.2. IMPLEMENTATION OF A PRONY ANALYSIS TOOL

The stability analysis tool will use prony analysis to approximate a signal. The approximated signal contains information of the system used to get an insight into the stability. The approximation consists of multiple modes with each a different frequency, phase, amplitude and damping. These modes can be linked to certain sources by their frequency. The tool can also investigate the interaction between components by the phase of modes with similar frequencies. The phase shows whether sources are acting in anti-phase which would indicate that the sources oscillate against each other. This is valuable information for the analysis of both simulation data as well as data from the field.

The implementation of the analysis is highly dependent on the signals it has to analyse. For this thesis, multiple signals need to be analysed. The results of damping, frequency, amplitude and phase can be compared. Prony is most commonly used to analyse certain phenomenon for example the behaviour of a system after a fault, load step or other disturbances. To analyse the effect it is required to include the data consisting only of the behaviour which is to be analysed.

Previous research developed online tools, implementing prony analysis. One of these tools is developed by Satnam Singh [40] and has a user-friendly interface to analyse individual signals. It allows to compare saved data and can select a certain subset of the data. However, it lacks the freedom to import multiple signals into the analysis simultaneously. The underlying code of the tool has been used as an inspiration source for the code written within the thesis.

Rodríguez et al. [39] published their code for the prony analysis. This method implements different algorithms of solving steps 2 and 4 out of the algorithm. It gives the possibility to use the classical, least-square or total least square method to solve the LSE problem. Both the works Satnam Singh [40] and Rodríguez et al. [39] have led to the implementation of the prony analysis tool in this thesis.

This thesis focuses on applying augmented prony analysis in which the participation of certain modes can be analysed. The implementation of this theory hides a lot of the complexity and thought required to make a proper tool, rigid and valid for multiple signal analysis. Figure 3.1 shows the flow diagram of the code which is implemented. First, the data needs to load into the workspace of the code. This could be either from a .csv file or from a .mat file. The initialisation of the tool requires the critical value of the maximum error of the approximation and the initial number of modes. If the maximum error is too strict the code will stop, for it is unable to find an approximation within the maximum error. Either the error criteria needs to be loosened or the number of modes needs to be increased. After initialisation, the tool will apply the prony analysis for each mode and will determine the minimum amount of modes required to keep within the maximum error. The answer will consist of many conjugate signals, one IMF of a sinusoid will consist of two complex value's which is one intrinsic mode function. To collect all intrinsic mode functions the conjugates have to be found. The next step will evaluate all conjugates and collect them. The result is a collection of IMFs both sinusoidal and DC-offsets. The last step is to calculate the phase, frequency, damping and amplitudes from the selected IMFs which approximate the signal. These are given in a table and are ready to be evaluated.

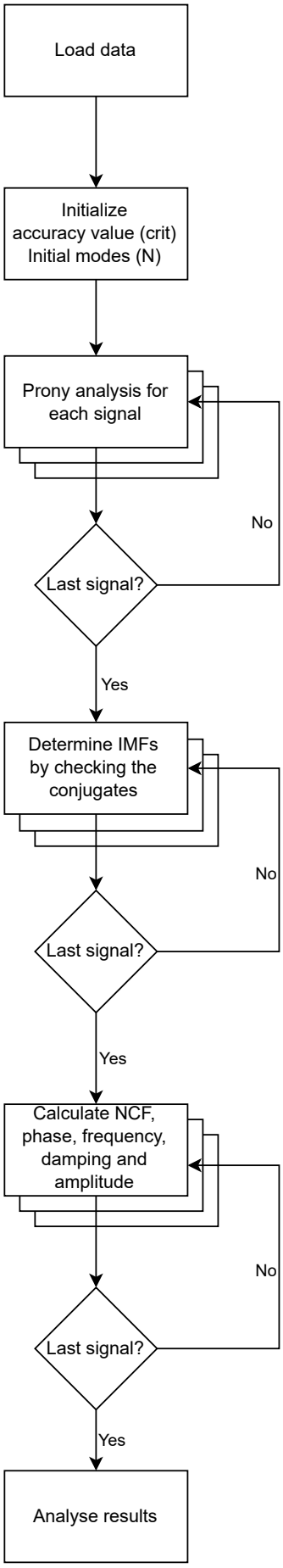


Figure 3.1: Overview of basic code flow

Another field using prony's method is filter design. The prescribed time-domain response is used to formulate a time-domain design of an IIR filter. The function *'prony'* in Matlab is based on the book [41]. The algorithm is described here to give a complete overview of how the formulae are used. Note that the formulation here is constructed to get the transfer function of the IIR filter. The transfer function of an IIR filter is given by:

$$H_{(z)} = \frac{B_{(z)}}{A_{(z)}} = \frac{b_0 + b_1 z^{-1} + \cdots + b_M z^{-M}}{1 + a_1 z^{-1} + \cdots + a_N z^{-N}} \tag{3.8}$$

the impulse response $h_{(n)}$ is related to the transfer function $H_{(z)}$ by the z transform.

$$H_{(z)} = \sum_{n=0}^{\infty} h_{(n)} z^{-n} \tag{3.9}$$

Equation 3.8 can be written as:

$$B_{(z)} = H_{(z)} A_{(z)} \tag{3.10}$$

which is the z transform version of convolution. This can be rewritten in a matrix multiplication form using the first $K+1$ terms of the impulse response such that it forms:

$$\begin{bmatrix} b_0 \\ b_1 \\ b_2 \\ \vdots \\ b_M \\ 0 \\ \vdots \\ 0 \end{bmatrix} = \begin{bmatrix} h_0 & 0 & 0 & \cdots & 0 \\ h_1 & h_0 & 0 & \cdots & 0 \\ h_2 & h_1 & h_0 & & \\ \vdots & \ddots & \ddots & \ddots & \vdots \\ h_M & & & & \\ & & & & \\ & & & & \\ h_k & & \cdots & & h_{K-N} \end{bmatrix} \begin{bmatrix} 1 \\ a_1 \\ a_2 \\ \vdots \\ a_N \end{bmatrix} \tag{3.11}$$

Next $a_n$ and $b_n$ need to be uncoupled by use of partitioning of the matrices:

$$\begin{bmatrix} \mathbf{b} \\ \cdots \\ 0 \end{bmatrix} = \left[\begin{array}{c|c} \mathbf{H_1} & \\ \hline \mathbf{h_1} & \mathbf{H_2} \end{array}\right] \begin{bmatrix} 1 \\ \mathbf{a}^* \end{bmatrix} \tag{3.12}$$

With this partitioning te terms for $\mathbf{a}$ and $\mathbf{b}$ are solved. The vector for the $M+1$ numerator coefficients is described as $\mathbf{b}$ and $\mathbf{a}^*$ is the vector of $N$ denominator coefficients where $a_0 = 1$. $\mathbf{h_1}$ is the vector of the last $K-M$ terms of the impulse response, or in our use the $K-M$ terms of the dataset. $H_1$ is the $M+1$ by $N+1$ partition of 3.11 and $H_2$ is the $K-M$ by $N$ remaining part. From 3.11 the lower parts can be solved and written as:

$$\mathbf{h_1} = -H_2 \mathbf{a}^* \tag{3.13}$$

and

$$\mathbf{b} = H_1 \mathbf{a} \tag{3.14}$$

note that $a^*$ stands for the polynomial without $a_0 = 1$ which is removed such that equations can be uncoupled. The roots of $\mathbf{a}$ contain the z-domain eigenvalues which are used to construct the matrix in equation 3.3. Equation 3.3 can be written as:

$$\mathbf{U}\beta = h_1 \qquad or \qquad \mathbf{U}\beta = y_1 \tag{3.15}$$

The matrix $\mathbf{U}$ can be constructed by:

$$U = \begin{bmatrix} z_1^{1_s} & z_2^{1_s} & \cdots & z_n^{1_s} \\ z_1^{2_s} & z_2^{2_s} & \cdots & z_n^{2_s} \\ \vdots & \vdots & \ddots & \vdots \\ z_1^{N} & z_2^{N} & \cdots & z_n^{N} \end{bmatrix} \tag{3.16}$$

Here the eigenvalues are denoted as $z_i$ where the subscript $n$ denotes the modes of the signal and the superscript $s$ denotes the time samples of which $N$ is the number of samples. Equation 3.16 can be solved employing the total least square algorithm to obtain $\beta$ from 3.15.

Based on the above described algorithm parameters of each mode $n$ can be obtained. The damping $\alpha_i$ and frequency $f_i$ can be obtained from the matrix $\mathbf{U}$ and the phase angle $\theta_i$ and amplitude $A_i$ can be obtained from $\beta_i$ as follows:

$$\alpha_i = \frac{\ln|z_i|}{T_s} \tag{3.17}$$

$$f_i = \frac{\arctan[\frac{Im(z_i)}{Re(z_i)}]}{2\pi T_s} \tag{3.18}$$

$$A_i = |\beta_i| \tag{3.19}$$

$$\theta_i = \arctan[\frac{Im(\beta_i)}{Re(\beta_i)}] \tag{3.20}$$

When analysing complex signals, meaning signals requiring a large number of modes to properly approximate the signal, sorting of the characteristic equation is advised. For example, when the analysis is required to show dominant modes, these eigenvalues of the system should be sorted on energy. Whilst analysing undamped modes, it is suggested to sort on damping factor. In the implementation this can be done by appropriately indexing both matrices $\mathbf{U}$ and vector $\beta$.

The algorithm will give complex eigenvalues with their conjugates and one set will result in in intrinsic frequency mode (IMF) as described in [37]. For simplicity lets assume that the complex eigenvalue $z_{i+1}$ and $\beta_{i+1}$ are the complex conjugates of $z_i$ and $\beta_i$. Constructing the IMF's from the matrix $\mathbf{U}$ and vector $\beta$ becomes:

$$\beta_i u_i + \beta_i^* u_i^* = \beta_i \begin{bmatrix} z_i^1 \\ z_i^2 \\ \cdots \\ z_i^k \\ \cdots \\ z_i^N \end{bmatrix} + \beta_i^* \begin{bmatrix} (z_i^*)^1 \\ (z_i^*)^2 \\ \cdots \\ (z_i^*)^k \\ \cdots \\ (z_i^*)^N \end{bmatrix} \tag{3.21}$$

where, $\beta_i$ and $z_i$ are defined as follows:

$$z_i = e^{\lambda_i T} = e^{(\alpha_i + j\omega_{di})T} \qquad \beta_i = \frac{A_i}{2} e^{j\theta_i}, \qquad i = 1, 2, \ldots, n \tag{3.22}$$

By rewriting equation 3.15 with equation 3.22 results in:

$$\beta_i u_i + \beta_i^* u_i^* = \begin{bmatrix} A_i e^{j\alpha_i T} \cos(\omega_{di} T + \phi_i) \\ A_i e^{j\alpha_i (2T)} \cos(\omega_{di} (2T) + \phi_i) \\ \vdots \\ A_i e^{j\alpha_i (kT)} \cos(\omega_{di} (kT) + \phi_i) \\ \vdots \\ A_i e^{j\alpha_i (NT)} \cos(\omega_{di} (T) + \phi_i) \end{bmatrix}, \qquad i = 1, 2, \ldots, n \tag{3.23}$$

Equation 3.23 shows that for each mode $(i)$ a contains a sinusoidal function. Compared to Fourier this decomposition is not limited by a base frequency and also includes damping for a single mode. These sinusoids are often referred to as Intrinsic mode frequency or IMF. The investigation of a signal can be focused by selecting a subset of modes or IMFs. For example, based on only the biggest partitioning mode, then the signal should be ordered on energy. When looking for unstable signals it should be ordered in descending damping ratio. Some of the modes in a signal do not have complex eigenvalues which means that there is no complex conjugate. To calculate the IMFs the following expression is made:

$$IMF_i(t = kT) = \beta) i u_i(k) + c_i \beta_i^* u_i^*(k), \qquad i = 1, 2, \ldots, n \tag{3.24}$$

The parameter $c_i$ is a logic value when the mode has a complex part $c_i = 1$ and when it only consists of a real number $c_i = 0$.

## 3.3. NODE CONTRIBUTION FACTOR

The algorithm from section 3.2 describes the basic implementation for prony analysis. Data-driven analysis is used to identify relations between signals or find certain frequencies within a signal. It is required to obtain a sense of participation between certain signals to use prony analysis as a root cause tool. In [37] an augmented prony analysis is proposed in which a note contribution factor (NCF) is calculated. This factor represents the contribution of a mode of a signal compared to another signal mode for each mode within that signal. For example, when an unstable mode is observed, this NCF can be used to find which signal has the largest contribution to that mode. It may result in determining which parameter should be altered to improve damping.
The amplitude of the NCF value does not give insight in itself. The NCF is purely used as an indication to determine which signal has the largest contribution. Thus when large variations of NCF are seen for a certain mode one could state that the largest NCF factor has the biggest contribution to that mode and thus may be controlled differently such that its performance increases.

The NCF is formulated as follows [37]:

$$NCF_{s,i} = E_{s,i} cos(\phi_{s,i}) \tag{3.25}$$

where, $NCF_{s,i}$ is used as the contribution of signal $s$ in mode $i$. The energy $E_{s,i}$ of the obtained signal $IMF_i$ is defined as [37]:

$$E_{s,i} = \sum_{i=1}^{n} IMF_{s,i}^2(t = kT) \tag{3.26}$$

The energy of each mode within a signal is calculated by equation 3.26. Equation 3.25 $\phi_{s,i}$ is the avarage relative phase of $IMF_{s,i}$ that is relative to the selected mode e.g. $IMFs, 1$. A few assumpations are made here. First off when analysing different signals it is assumed that the mode $i$ of signal $s$ and signal $s+1, s+2, \ldots, s+n$ are similar. If the signal frequency of mode $i$ is not found in signal $s$ than that signal does not contribute to that oscillatory mode. The relative phase $\phi s, i$ is calculated as follows [37]:

$$\phi_{s,i} = \frac{1}{N} \sum_{t=1}^{n} \theta_{s,i}(t) - \theta_{s,1}(t) \tag{3.27}$$

[37] explains that to calculate the $\phi_{s,i}$ a phase angle is to be assigned to each data point of $IMF_{s,i}$ for each point. The first IMF from the extracted measured signal of the network is assigned with an initial phase angle, the reference phase ($\theta_{s,1}(t) = 0$). It describes that for a specific IMF, the phase angle of maximum, minimum, positive zero-crossing and the negative zero-crossing points are assigned to $\pi/2, 3\pi/2, 0 and \pi$ respectively. This raises questions, what happens with the intermediate phases, why only these points and what is the meaning of a specific IMF?

The paper [37] remarks that the execution of prony given by equations (3.24) - (3.27) allows direct calculations of the IMF's and thus avoids mode mixing, empirical mode decomposition, end effect and Gibbs phenomena. This because it bypasses the problems of nonlinear and the iterative methods of Hilbert-Huang transform for IMF calculations.

Within the algorithm the total number of modes $N$ is assumed to be known. However in many applications this is not the case and should be determined. The paper [37] gives an approximation system order equation which gives the smalles index m that satifies the following inequality:

$$\frac{\sum_{i=1}^{m} IMF_{s,i}^2}{\sum_{i=1}^{n} IMF_{s,i}^2} \geq \tau \tag{3.28}$$

the treshold value $\tau$ is close to 1 and $n$ is the initial value of the system order. The formula shows that the fraction of initial energy of the signal is compared to the energy of the approximated signal. Since the original signal is known and the energy points of each IMF can be determined this formula is expanded:

$$\sum_{t=1}^{M}\sum_{i=1}^{N}(IMF_{s,i}(t)^2 - y_s(t)^2) \geq \tau \tag{3.29}$$

The difference between each data point is calculated and the total error of the signal is compared to $\tau$.

## 3.4. METHOD VALIDATION

Prony analysis is self-validating since the goal is to reproduce the original signal. The error between the original signal and the reproduced signal gives the accuracy of the algorithm. To validate the method two models are used. First, a simple signal consisting of multiple damped sinusoids with known damping, frequency, amplitude and phase is used. Secondly, a well-known power oscillation problem is used to analyse the system. The two-area problem from Kundur is used to check whether the same dominant oscillations can be obtained with this prony algorithm.

### 3.4.1. SIMPLE SIGNAL

First a simple signal is constructed consisting of four sinusoids. Each sinesoid consists of a complex pair of conjugate eigenvalues. In this case the damping $\alpha_i$, frequency $f_i$, amplitude $A_i$ and phase $theta_i$ is known and with equation 3.23 the four modes can be constructed. This results in the following equation for each mode:

$$y(t) = \sum_{i=1}^{4} y_i(t) = \sum_{i=1}^{4} A_i e^{\alpha_i T} cos(2\pi f_i t + \phi_i) \tag{3.30}$$

The allocated parameters for the signal are as follows:

Table 3.1: Simple signal parameters

| $y_i$ | A | $\phi$ | $\alpha$ | f |
|---|---|---|---|---|
| 1 | 4 | 0 | -0.8 | 0.2 |
| 2 | 2 | $\pi/5$ | -0.5 | 0.7 |
| 3 | -0.8 | $\pi/6$ | -0.7 | 0.8 |
| 4 | 0.2 | $\pi/2$ | -1 | 1 |

The parameters of table 3.1 are filled in equation 3.30 to form a signal. The period ($T$)which is analysed is 20 seconds with a sampling time ($T_s$) of $10ms$. The validation are testing the following functions:

1. Validate accuracy of the approximated signal
2. Validate automatic order approximation from 3.29
3. Validate the ordering on basis of undamped to damped signals from 3.16
4. Investigate the effect of the selected inital modes from 3.29

The produced signal with the parameters from table 3.1 is shown in figure 3.2. The dataset is analysed by the prony function with an initial order of $N = 40$. The signal consists of 8 eigenvalues of which 4 are complex conjugates. The function works correctly if the selected modes equal the 8 eigenvalues from the original signal. The results are shown in figure 3.3, the lift part depicts the approximated signal and the right part the error between the original and the approximation. It is evident that the signal is approximated correctly and the error is negligible. However, for the complete set $N = 40$ modes the error is growing meaning that there is an undamped signal in the set of $N = 40$ modes. Due to the long time period, this undamped signal grows and will eventually lead to an incorrect approximation. Here lies the danger in the tool of prony for an incorrect number of initial modes may lead to incorrect conclusions.

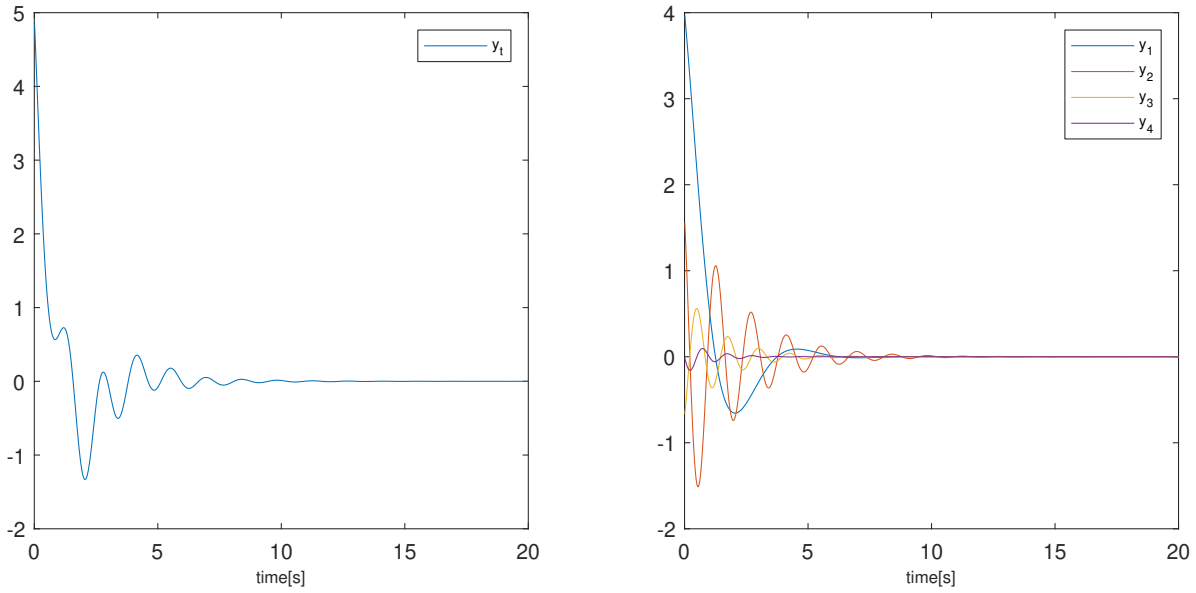


Figure 3.2: Original Signal according left the total signal, right the modes 3.30

The solution is already implemented by sorting the columns of equation 3.16, from there the error is calculated for each signal and the selected modes according to equation 3.29 is selected, in this case, 8. Figure 3.4 shows the modes of the original signal compared to the approximated signal in ascending order from top to bottom. It shows that mode 1 and mode 2 are interchanged this is due to the sorting of the eigenvalues based on their real part. This allows calculating the modes based on descending damping order. This way the prominent undamped signals occur first. Since there is an analytical equation for each IMF in the form of 3.30 we can compare the calculated parameters. The parameters of the modes are shown in table 3.2. It shows that the damping and frequency are calculated correctly and a minor error is observed with the amplitude and phase. Mode 3 shows that the amplitude is missing a negative sign. This is compensated by the phase shift of $\pi$ since $cos(A) = -cos(A+\pi)$).

Table 3.2: Results of prony analysis with a subset of $N = 8$ modes from the total 40 calculated modes

| Mode | Amplitude | | Phase | | Damping | | Frequency | |
|---|---|---|---|---|---|---|---|---|
| Original/Prony | Original | Prony | Original | Prony | Original | Prony | Original | Prony |
| 1/2 | 4 | 3.97 | 0 | 0.013 | -0.8 | -0.8 | 0.2 | 0.2 |
| 2/1 | 2 | 1.99 | $\pi/5$ | $0.672 \approx \pi/4.69$ | -0.5 | -0.5 | 0.7 | 0.7 |
| 3/3 | -0.8 | 0.79 | $\pi/6$ | $-2.567 \approx \pi/5.46$ | -0.7 | -0.7 | 0.8 | 0.8 |
| 4/4 | 0.2 | 0.20 | $\pi/2$ | $1.634 \approx \pi/1.92$ | -1 | -1 | 1 | 1 |

It shows that the method is validated and a single synthetic signal can be analyzed with high accuracy. The automatic approximation function can determine the minimum amount of modes correctly, it can determine that the signal has 8 dominant eigenvalues. The ordering however is not working correctly. According to [37], the ordering should give the more dominant modes which are true. However, the statement that it orders based on damping is not correct. The ordering does not take the complex eigenvalues into account which in this case result in a shift in the ordering.

The importance of the initial modes is also important. There are three situations:

1. underdetermined system $m < N$
2. exact fit $m = N$
3. overdetermined system $m > N$

$m$ is here the number of actual modes in the signal and $N$ is the approximated order. For an underdetermined system, the solution is highly inaccurate and the inequality of equation 3.29 may be unsolvable. It results in

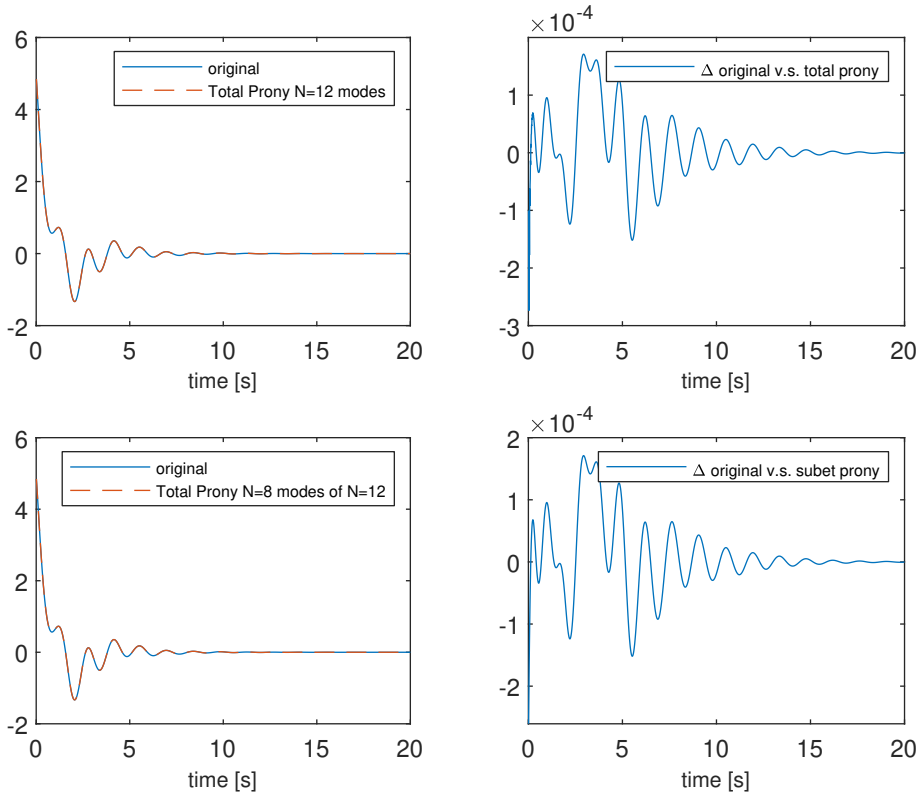


Figure 3.3: Original signal and approximated signal, Left columns: Approximation; Right columns: Error of the approximation

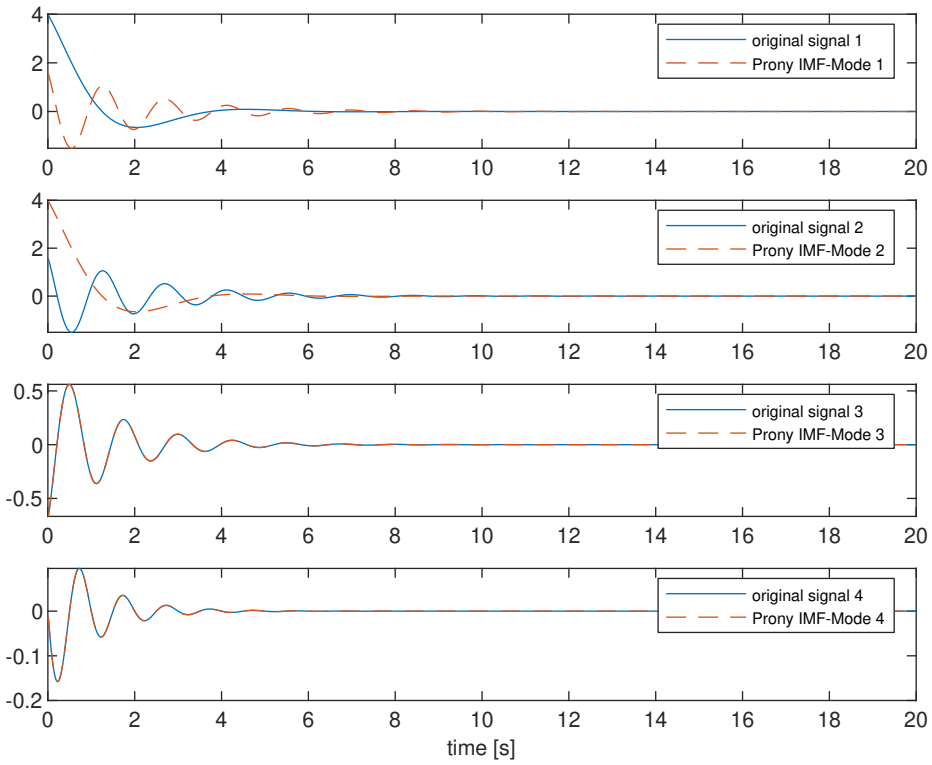


Figure 3.4: Modes of original signal compared to the approximated signal

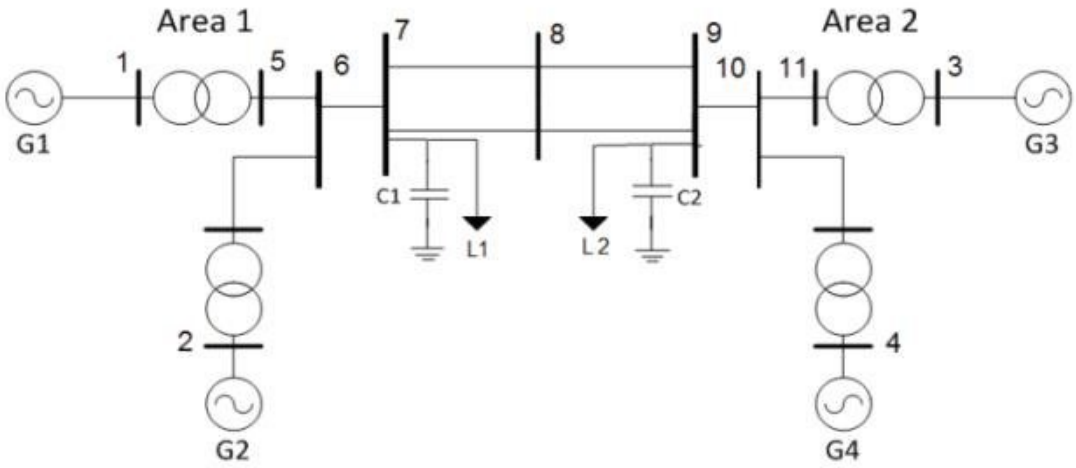


Figure 3.5: Overview of Kundur two area problem

missing modes of the signal therefore a poor approximation of the signal. An exact is also not advisable because noise may pollute the solution. It is better to overdetermine the number of modes of the signal and order them on the energy. Those of high energy benefit most to the signal and will give the best approximation. With empirical tests on multiple signals, it can be concluded that an overdetermined system results in the highest accuracy.

### 3.4.2. KUNDUR TWO AREA MODEL

The Four-Machine Two-Area test system by Kundur is used to validate the method using multiple signals in parallel. The model used is the example model (*power_PSS*) from Matlab-Simulink version 2020a. An overview of this problem is given in figure 3.5 it depicts two areas within both areas 2 generators. This test case is used to validate the functionality and use of the analysis tool. The following functions are tested:

1. Approximation of a signal with a DC-offset
2. IMF conjugate function allowing DC and AC signals
3. The use of phase from IMFs to identify inter-area oscillations
4. The use of phase from IMFs to identify local-area oscillations
5. Frequency of IMFs and comparability
6. Calculation of NCF value and its value

The analysed data consists of both a DC offset as AC components. The conjugate function in the code will identify them and is validated with this test. The augmented prony from [37] is implemented to calculate the NCFs. The result of dominant damped and undamped signals are compared with the results given from the example of Matlab-Simulink. The main goal is to test whether the same unstable oscillatory modes are obtained from the prony analysis as to that of the Matlab-Simulink model.

Small-signal analysis of the system is performed in which the open-loop responses to a 5%-magnitude pulse at the voltage reference of G1 is initiated. The modal analysis of the acceleration powers of the four machines are analysed and from Matlab-Simulink the following three modes are dominant:

1. An interarea-mode ($fn = 0.64Hz$) involving area 1 against area 2
2. A local mode of area 1 ($fn = 1.12Hz$) involving machines G1 and G2 against each other
3. A local mode of area 2 ($fn = 1.16Hz$) involving machine G3 against machine G4

Table 3.3: Frequencies from figure 3.6

| Mode | f Gen 1 | f Gen 2 | f Gen 3 | f Gen 4 |
|---|---|---|---|---|
| 2 | 0.6393 | 0.6391 | 0.6393 | 0.6394 |
| 3 | 1.2803 | 1.2766 | 1.2760 | 1.2862 |
| 4 | 1.1180 | 1.1187 | 1.9063 | 1.1326 |
| 5 | 1.7718 | 1.7532 | 1.1027 | 1.9122 |

Table 3.4: Phase from figure 3.6

| Mode | $\phi$ Gen 1 | $\phi$ Gen 2 | $\phi$ Gen 3 | $\phi$ Gen 4 |
|---|---|---|---|---|
| 2 | -27.88 | -44.72 | 134.53 | 137.50 |
| 3 | 94.40 | 78.48 | 76.73 | -33.60 |
| 4 | 29.20 | -154.61 | -124.51 | -113.14 |
| 5 | 45.81 | -100.10 | 1.98 | 175.42 |

The results of the prony analysis are depicted in figure 3.6. The first row shows the original signal of the response of the generator power and the prony approximation of that signal. The initial number of mode influence the accuracy of the approximation. In this case, the initial amount of modes is $N = 140$. The script determines the number of modes required to approximate the signal fulfilling the inequality in 3.29. This may result in different modes for each signal which fulfils this requirement. In this case the inequality parameter $\tau = 0.01$.

The columns in figure 3.6 are the generators and the rows are the IMF modes. The modes start from the second mode and end at the fifth. The first mode is the DC offset from the signal, it is clear from the first row that the DC offset is calculated correctly since the approximated signal is a good fit.

The number of modes $N$ is important to determine. It may result in a cluttered signal decomposition in which minor frequency shifts obscure the ability to analyse the signal. In this case, the amount of initial modes has been determined by trial and error. A script could work, however, for large signals this may result in computational restrictions.

First, a check of the calculated frequencies is required to validate whether a row consists of the same frequencies, table 3.3 shows the results. It is evident that modes 2 and 3 are similar in frequency and 4 and 5 are not. The initial modes influences this result it may occur that the frequencies do not align like this. This because smaller modes are cluttering the results.

It seems that the prony analysis can both analyse the frequency and the type of oscillatory mode. From the example an interarea-mode of $f_n = 0.64Hz$ is observed, from table 3.3 the frequency of 0.6393 is observed. Moreover, figure 3.6 shows that the modes of generator 1 and 2 oscillate in antiresonance. This means that area 1 oscillates against area 2, thus an interarea mode. This can also be concluded by looking at the phase of the signals from the approximated signals in table 3.4. It shows that area 1 and area 2 are oscillating in antiresonance, the phase angle difference is around 180°

The local mode of area 1 and 2 are observed. Mode 4 shows that generator 1 and 2 are oscillating in antiresonance with a frequency similar to the Matlab-Simulink results. However, the local area mode of area 2 is missing, mode 5 looks promising however the frequencies of the modes differ and cannot be compared. The suggested sorting from paper [37] may come a bit short here. Either the criteria on which the sub-modes are selected or the sorting of the residues is insufficient.

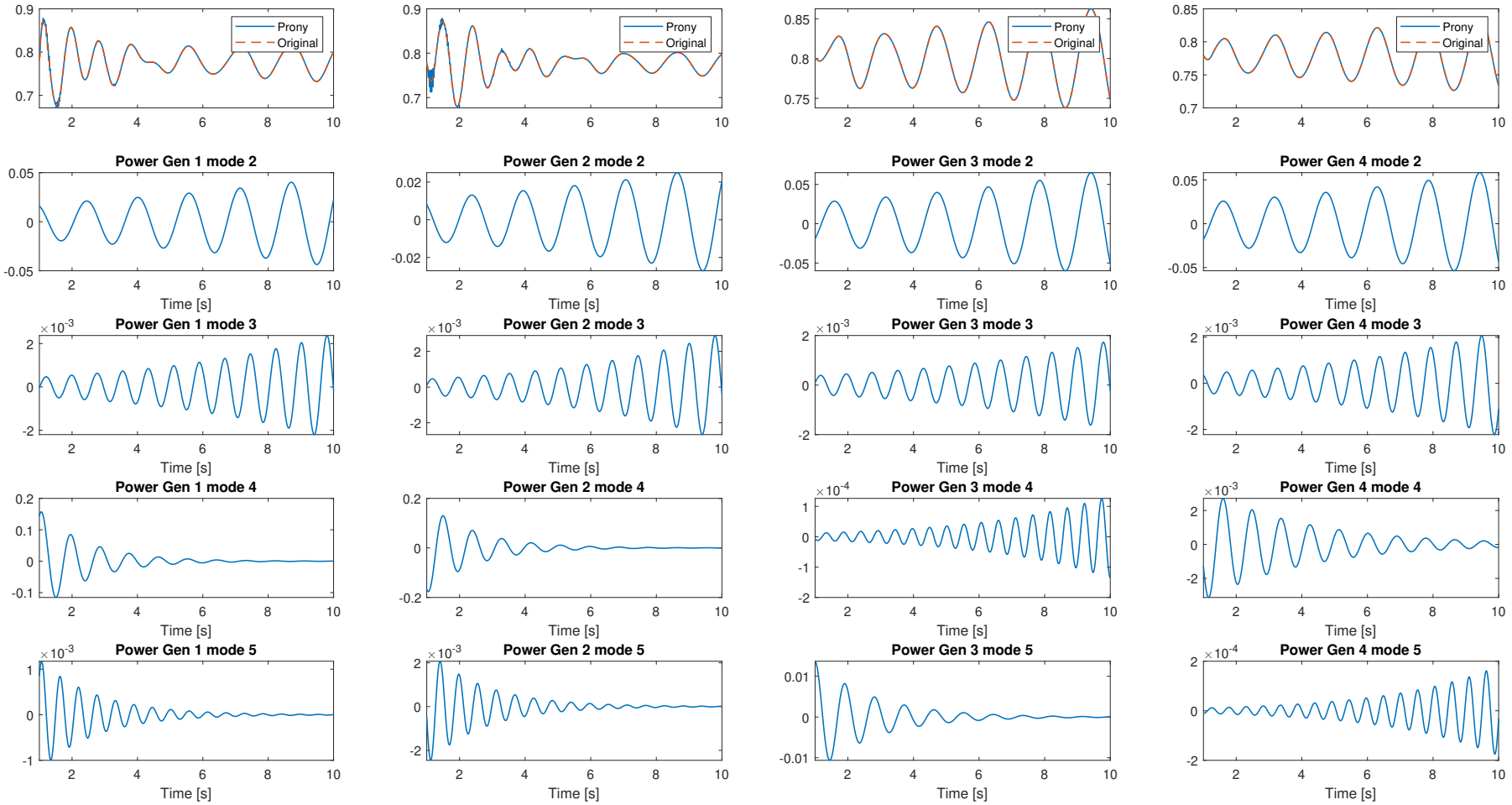


Figure 3.6: obtained first 4 modes from the prony analysis

Table 3.5: NCF from figure 3.6

| Mode | Gen 1 | Gen 2 | Gen 3 | Gen 4 |
|---|---|---|---|---|
| 1 | 327.8871 | 327.8402 | 345.9560 | 327.9282 |
| 2 | 0.2521 | 0.0980 | 0.5623 | 0.4501 |
| 3 | 0.0005 | 0.0006 | - | - |
| 4 | 0.6520 | 0.8089 | 0.0000 | - |
| 5 | 0.0000 | 0.002 | - | 0.0000 |

The importance of similar frequencies becomes clear when looking at the NCFs. When comparing these values the frequencies have to be the same. The following frequencies are similar:

1. Mode 2 all generators
2. Mode 3 all generators
3. Mode 4 generator 1 and 2
4. Mode 5 generator 1 and 2
5. mode 4 generator 4 and mode 5 generator 5

The NCF factors are calculated and depicted in table 3.5. Only the values with similar frequencies are filled in the table. The green values indicate the last similarity of mode 4 generators 4 and mode 5 generator 5. it shows that for modes 1, 2 and 5 generator 3 has the largest contribution. Generator 2 is mostly contributing in mode 3 and 4. Mode 1 is the DC offset and is not of interest here however, mode 2,3 and 5 are undamped especially mode 2. The analysis shows that the power control of generator 3 will have the largest influence on the instability. Altering the controls of this generator will have the largest effect on stability.

This section showed that the prony analysis is capable of reconstructing a sufficiently similar signal. It can do this with DC-offsets in the signal and can do it for multiple signals. It shows that the frequency, phase, amplitude and damping of the signals can be calculated accurately. The information of these parameters from the IMFs gives a good indication of unstable behaviour in a power system. Furthermore, it allows identification of the contribution of a mode by a source through the NCFs value. Local and inter-area oscillations are identified however, the frequencies of the modes need to be similar. This is a drawback of this method, the initial modes influence the accuracy of the model and may result in cluttering of modes with low energy values. The tool can identify all modes but it is recommended to expand the tool such that low energy modes are filtered out from the solution. It should also implement a check to see whether frequencies of the same mode are available.

## 3.5. CONCLUSIONS

In this chapter a prony analysis tool has been proposed. The performance of the tool has been tested on a synthetic signal and can approximate the modes accurately. The performance of multiple signals in the example of the two-area Kundur model is accurate. It showcased some of the difficulties in determining the initial order of the modes. The tool shows that can identify different oscillatory modes similar to the example from Kundur.

The results of this chapter contribute to answering the research question represented in chapter 1 by proposing an analysis tool able to identify the IMFs. This allows us to use the tool on the model under study proposed in chapter 2. The case study which implements the tool and the model is described in chapter 4.

# 4

# CASE STUDIES

This chapter combines the results of the previous two chapters. In chapter 2 the model under study has been proposed and validated. To analyse the behaviour of the power system and to be able to analyse the voltage stability in more detail an analysis tool has been developed in chapter 3. This chapter contributes to answering the research questions. It helps by determining critical scenarios where standard control methods may be ineffective. It helps to show unstable operation points and categorize these. It also gives insight into how this analysis compares to the conventionally used method.

Two case studies are performed. The first described in section 4.1 is to test the performance of the prony analysis by analyzing a data set received from a vessel. The data retrieved consists of a sudden power oscillation on the vessel. The tool is used to find the oscillatory modes of the oscillation.

The second test described in section 4.2 is to combine both the Matlab-Simulink simulation of the DC-PPS with the analysis tool. All the parameters of the simulation are given in appendix A. A set of tests is performed in the DC-PPS to test the performance of the analysis tool and the ability to see the differences between simulations. The goal of these tests is to check whether the prony tool can be used to allocate problems and lead to the same solution. It tests whether the tool can act as a fast prototyping design tool for the control system of the power system. The AVR, governor and other possible systems may be parameterized by this tool and be fine-tuned on-board during commissioning.

## 4.1. REAL DATA CASE

As mentioned before real application data is often sent to the vessel supplier to help find and solve onboard problems. The current procedure is to analyse this by hand. The figures are replotted from the data and from there the figures are analysed.

The analysis tool may be beneficial to use when analysing data from the field. The data is acquired from the AVR onboard the vessel. The sampling time of the AVR is $0.1ms$. The problem under investigation is the shut-down of several components after voltage oscillations. The vessel has a similar power layout as the AC dredger given in figure 1.1. In this case, two busses portside (PS) and starboard (SB) are used and are fed by two generators, one on each board. Figure 4.1 shows relevant parameters for the voltage control of the AVR from top to bottom: reactive power, average voltage, AVR output and field voltage respectively. It shows that around $t = 525s$ the voltage suddenly drops. After the initial drop, the voltage oscillates heavily. After about 50 seconds the oscillation stops possibly due to a switch-off of a component. The results of the power, frequency and average current on the port side are also measured and shown in figure 4.2. The switch-off is visible in the frequency at $t = 570s$, where the frequency increases to $51Hz$. The power slowly decreases and at $t = 650s$ the coupler is probably opened due to the unequal frequencies, however, this part is not under investigation. The oscillations seem to be in phase.

The oscillation between $t = 530s$ and $t = 570s$ has been selected to use in this case study specifically the power measurement. Pre-processing is important when using this data, minor oscillations of high frequen-

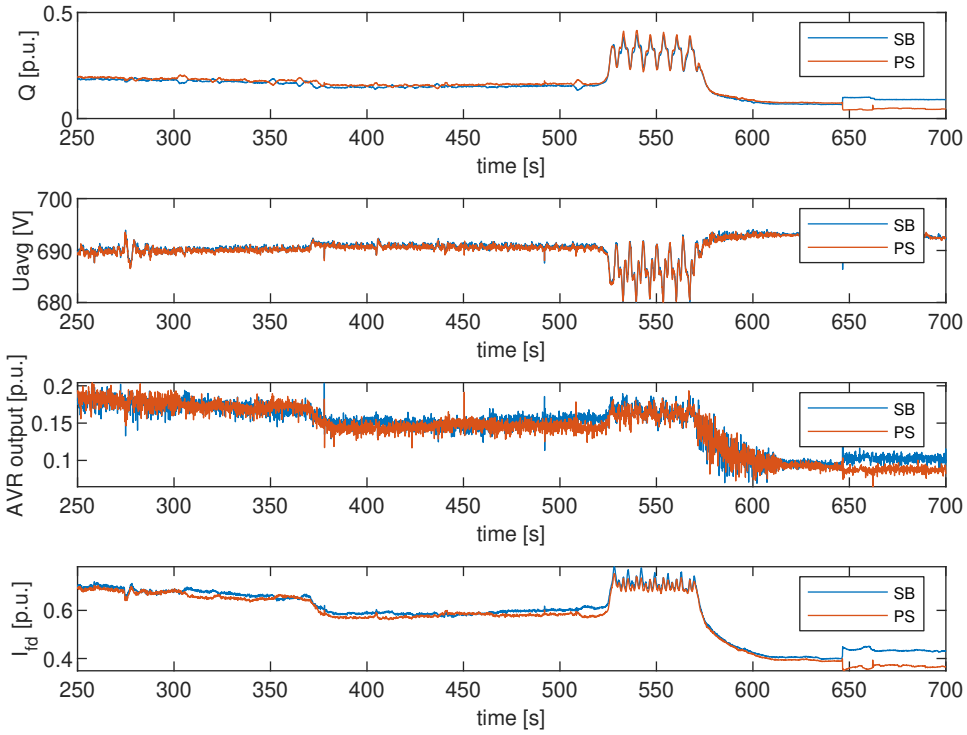


Figure 4.1: Data received from vessel under study related to the voltage control

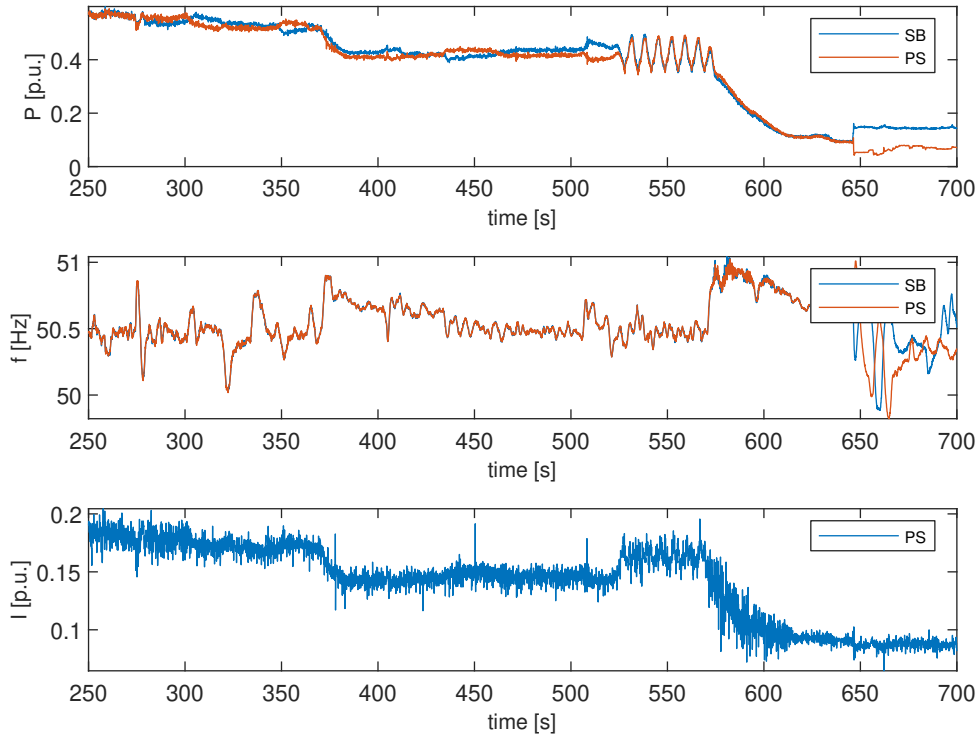


Figure 4.2: Data received from vessel under study related to the power control

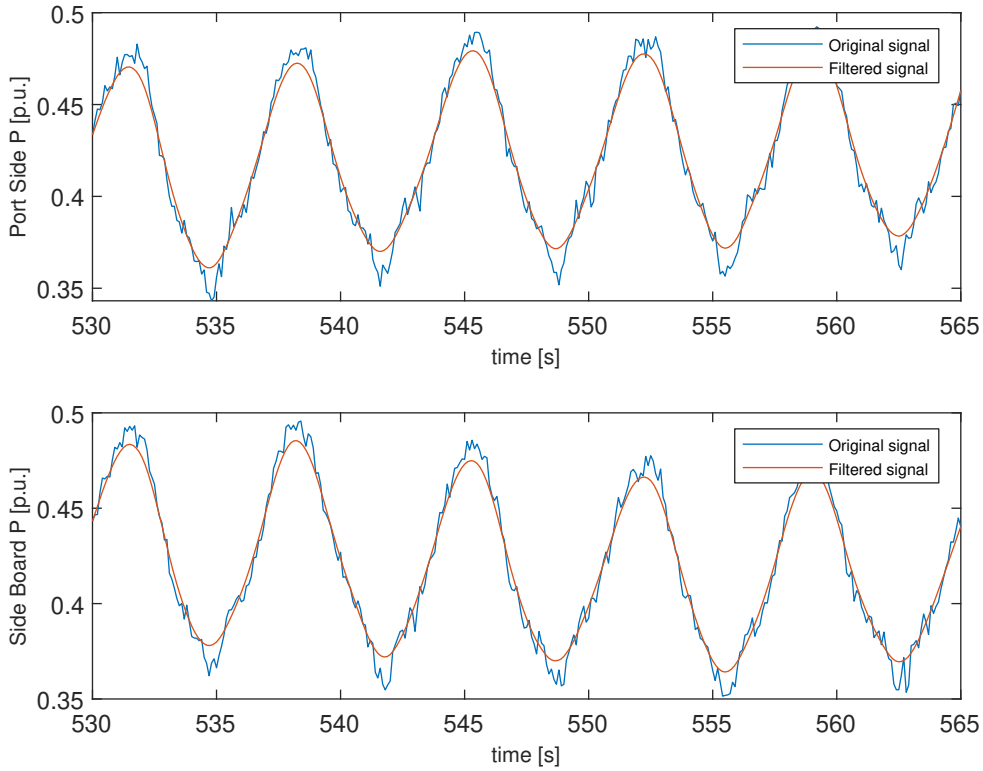


Figure 4.3: Results of preprocessing the input data to filter out high frequencies.

cies distort the signal. This noise decreases the accuracy of the analysis tool significantly. Figure 4.3 shows the preprocessing of the data and the gained results. The high frequencies have been filtered out while maintaining an accurate representation of the data.

The data is analysed with the analysis tool in which the selected initial modes are $N = 35$ and the first 5 most dominant modes are used to reconstruct the signal. With these 5 dominant modes, the approximation is accurate enough and is not cluttered by low energy modes. This results in a clear analysis of modes that contribute to the signal. The result of this analysis is given in figure 4.4. The corresponding amplitude, phase, frequency, damping and NCF is depicted in table 4.1. The results show that the frequency of the modes from the two different signals is similar thus the results can be compared. It can be concluded that the analysis tool can accurately approximate the signal and give information about the dominant modes.

Analysing the data results in the following observations:

- Dominant frequencies are low oscillatory modes
- All oscillatory modes are in phase with minor deviations
- Mode 2 contributes largely to the signals oscillation (highest energy)
- Mode 2 is poorly damped

The data and the modes from the signal show no particular problems, except mode 2. The frequency of this mode is low $0.14Hz$ and both modes from both generators are in phase. This excludes the possible source of local-area oscillations. Both generators contribute equally to this oscillation which is shown by the NCF values. Unfortunately, this result does not allow to couple the oscillation to any of the measurements. However, it can exclude the option of local-area oscillations.

The first indication of the problem was ought to be the generator controls when this data was received from the vessel. However, the analysis tool points out that this is not the case. There are no local-mode oscillations, the oscillations are in phase and there is no distinct difference in amplitude or damping. From this,

Table 4.1: Frequency and phase from prony analysis from figure 4.4

| Mode | Frequency $Hz$ | | Phase ° | | Damping | | Amplitude | | NCF | |
|---|---|---|---|---|---|---|---|---|---|---|
| - | PS | SB | PS | SB | PS | SB | PS | SB | PS | SB |
| 1 | 0 | 0 | 0 | 0 | 0.0011 | 0.0011 | 0.8269 | 0.8573 | 49.9765 | 49.6732 |
| 2 | 0.1438 | 0.1443 | 65.97 | 69.30 | -0.0007 | -0.0031 | 0.0529 | 0.0530 | 0.3760 | 0.3483 |
| 3 | 0.2907 | 0.2952 | -173.00 | -164.93 | -0.0309 | -0.0867 | 0.0046 | 0.0062 | 0.0012 | 0.0009 |
| 4 | 0.4360 | 0.4256 | -126.32 | 167.93 | -0.0634 | -0.0672 | 0.0020 | 0.0017 | 0.0001 | 0.0001 |
| 5 | 0.5839 | 0.5832 | 118.17 | 103.68 | -0.0529 | -0.0609 | 0.0012 | 0.0010 | 0.0000 | 0.0000 |

it can be concluded that the controller, in this case, is not the source of the problem but that the source lies within the network. Therefore, introducing more damping or a PSS, in this case, is not a viable option. For it may introduce more damping but the problem may still be there. The source of the problem was later found to be a saturation of one of the transformers.

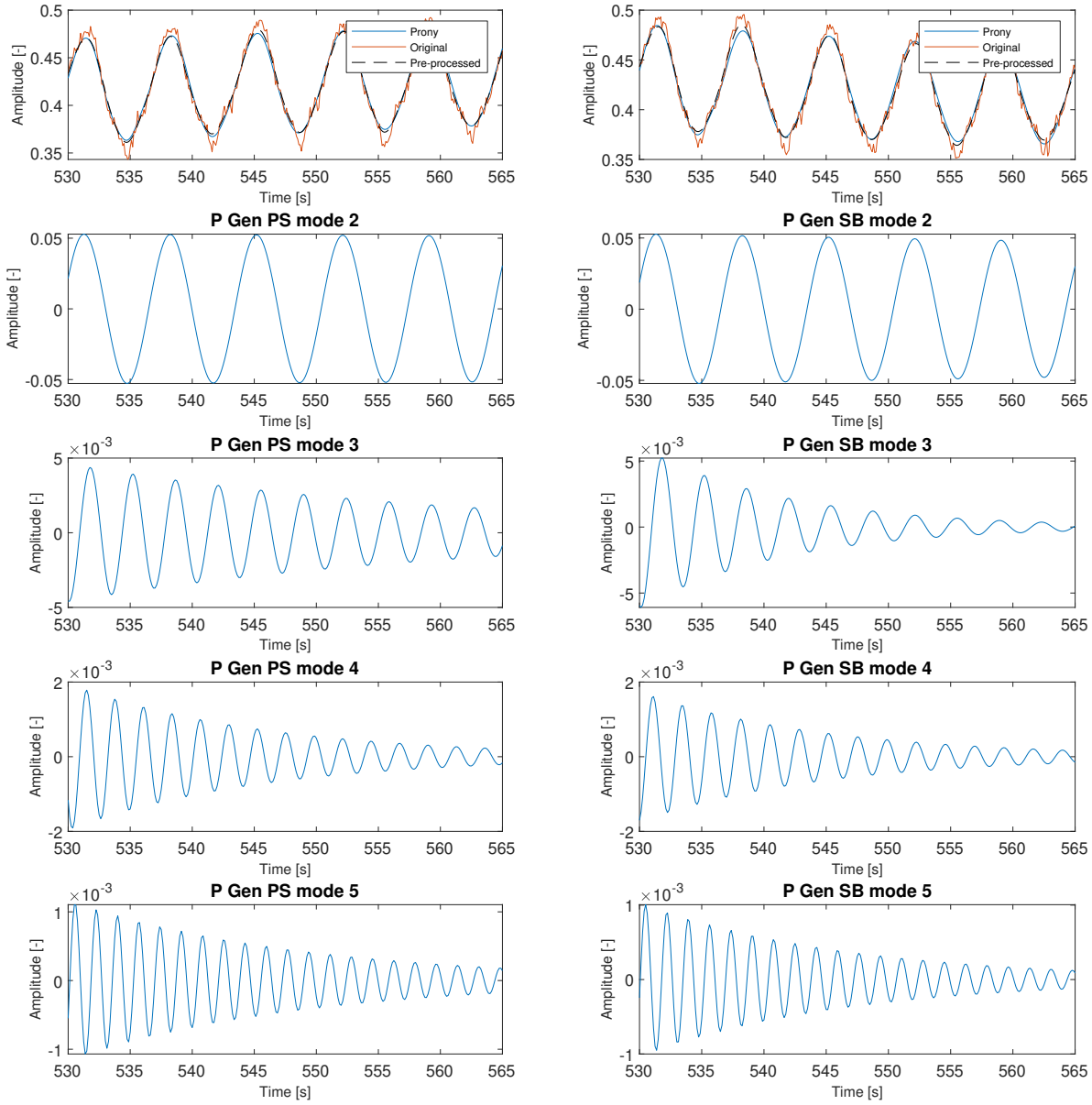


Figure 4.4: Prony analysis of the real data with $2_{nd} \ldots 5_{th}$ modes

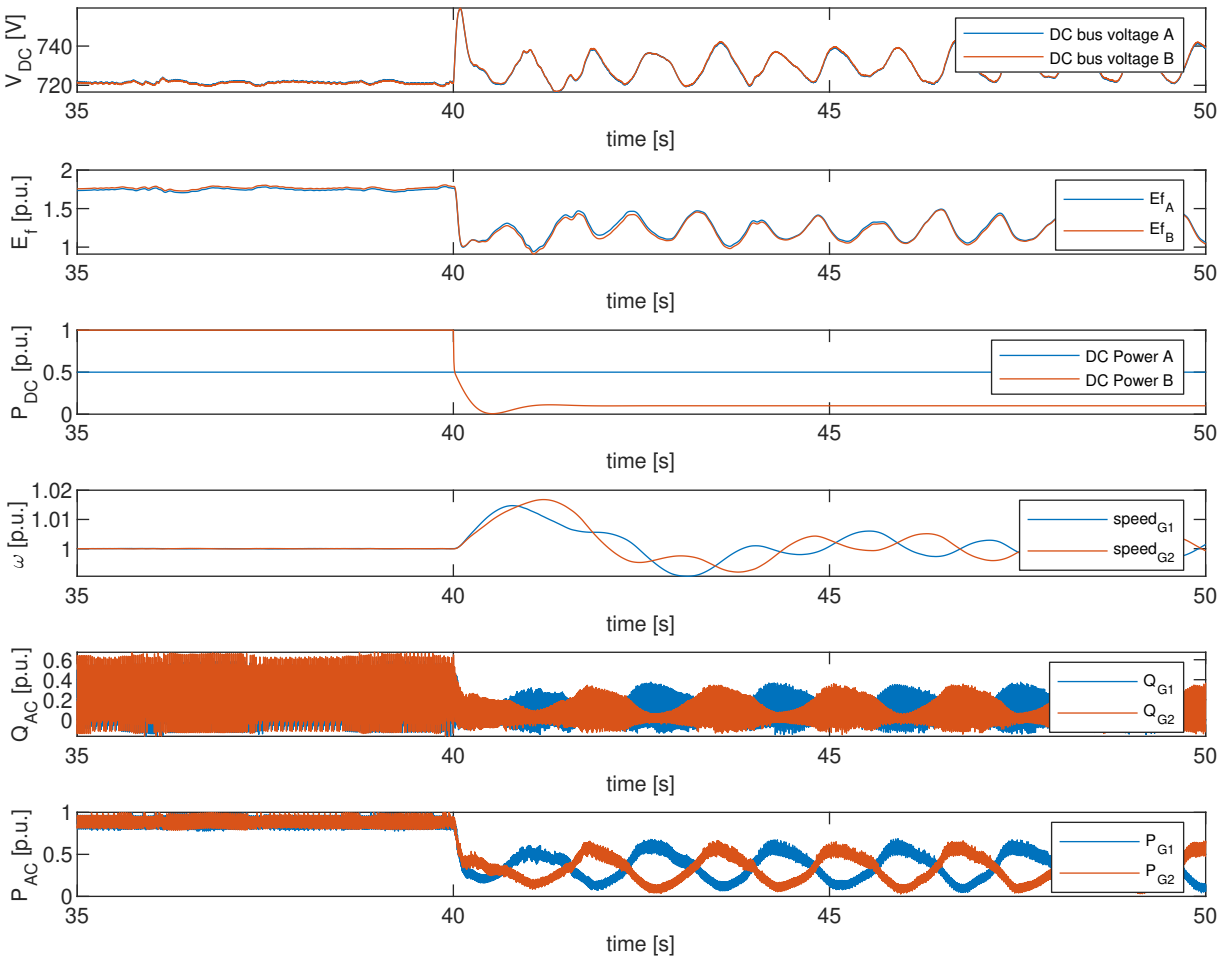


Figure 4.5: results of pulsed power

## 4.2. SIMULATION CASE

Subsection 2.4.5 showcased the system under study with the parameters of the proposed model given in appendix A. During the test, noticeable oscillations occurred during the low load operation. As suggested, the analysis tool could be beneficial for further analysis. The tool is tested to see if it can deliver insight into the oscillation and its source. The data from the test of subsection 2.4.5 are analysed with the tool. Figure 4.5 shows the results of the test between $t = 35s$ and $t = 50s$ which is used for the analysis.

The model is subjected to a pulsating load from area B whereas area A keeps a stable $0.5p.u.$ load. Due to the load drop of area B the voltage will increase, the current of the CPL in area A will decrease due to the larger voltage on the DC bus. This introduces a fast change in the impedance of the system which the AVR and governor of both generator sets need to compensate. This test investigates the ability of the system to maintain a stable voltage when objected to a large load step.

The goal of this case is to test the usability of the stability analysis tool on simulated data from a Matlab-Simulink model. The execution of the analysis also gives insight into the method which is required to determine the stability of a DC-PPS. The usability of the tool is determined by the ability of the tool to find unstable oscillations within the system. Furthermore, the analysis tool may indicate a source of the oscillation with the help of the NCF or finding similar frequencies across different signals. This means that multiple signals, measured in the simulation, need to be analysed and linked to see whether they are related. During the analysis, limitations of the tool are found as well as general observations. First, these limitations will be described followed by the results of this simulation case the last part consists of a mitigation action to further improve stability.

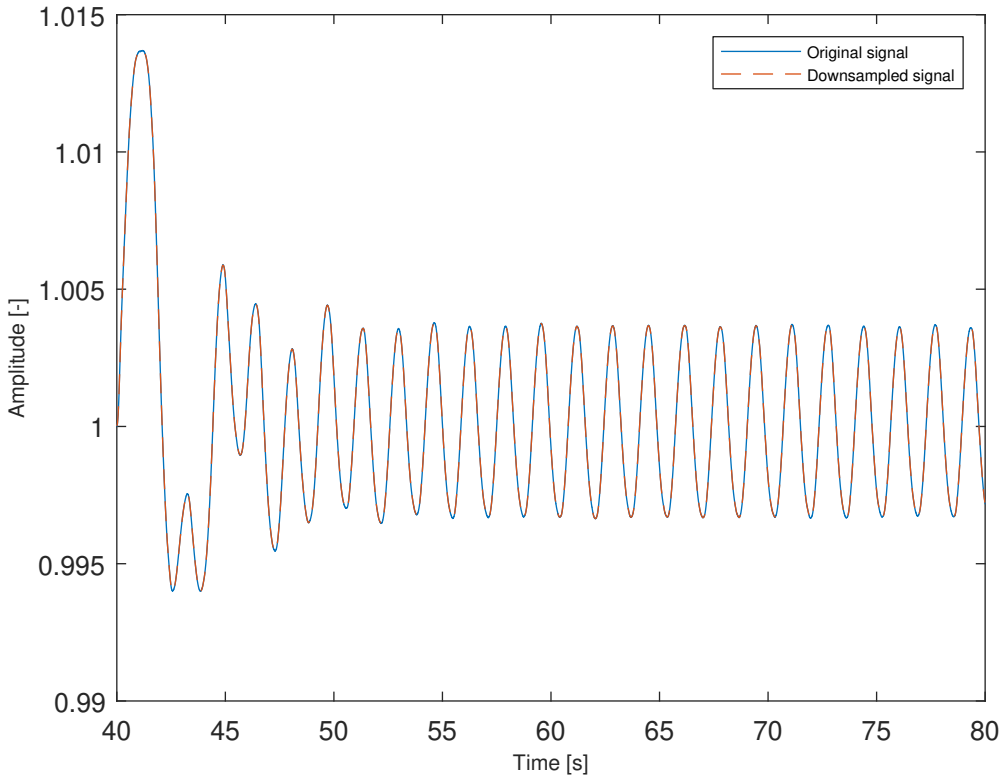


Figure 4.6: Comparison of original signal to the downsampled signal

### ANALYSIS TOOL PERFORMANCE OBSERVATIONS

The data received from the simulation has a high sample rate and requires to be preprocessed. The simulation data has a sample time of $0.5ms$, this results in an array of $160k$ samples. The data is downsampled with a factor of 60 reducing the $160k$ samples to 2666 samples. An example of the downsampled and the original dataset is depicted in figure 4.6 and shows enough similarity with the original signal.

The simulation allows the analysis of all computed variables within the simulation, therefore a selection of the measurements need to be made for the analysis. As shown in figure 4.5 the oscillation is visible in the speed, power and voltage. The goal is to couple the oscillation to a source, in this simulation this could be the load or the generator. The load shows a stable current and does not introduce the oscillation. The generator speed is oscillating where the generator in area A is oscillating against the speed of area B. The question is, is this phenomenon due to the governor or the diesel controller? To analyse this the following parameters are used in the prony analysis:

1. Mechanical torque of the diesel and field voltage of area A and B
2. Field voltage on the generator and DC voltage of area A and B
3. Rotational speed and mechanical torque of the generator of area A and B

The first test investigates if there is a relation between the governor output and the AVR output. It investigates which controller is accountable for the oscillation. The second and third tests investigate if the oscillation of the output e.g. speed and voltage is only influenced by its input the torque and field voltage respectively.

One of the limitations of the tool becomes visible when trying to analyse test 1. The tool can process multiple signals which allows comparison between signals. However, if signals differ too much this causes

Table 4.2: overview of approximation parameters of figure 4.5

| Parameter | Initial Modes [$N_i$] | Max Allowed Error | Required Modes [$N_r$] |
|---|---|---|---|
| Bus Voltage $V_A$, $V_B$ | 234 | 38 | 10 |
| Field Voltage $Ef_A$, $Ef_B$ | 198 | 0.03 | 9 |
| Engine Torque $T_A$,$T_B$ | 62 | 0.01 | 5 |
| Engine Speed $\omega_A$, $\omega_B$ | 90 | 0.00001 | 5 |

Table 4.3: Results of Field voltage and Torque in analysis tool

| | Frequency $Hz$ | | | | Phase ° | | | |
|---|---|---|---|---|---|---|---|---|
| | Torque | | Field Voltage | | Torque | | Field Voltage | |
| Mode | Area A | Area B | Area A | Area B | Area A | Area B | Area A | Area B |
| 1 | 0 | 0 | 0 | 0 | 0 | 0 | 0 | 0 |
| 2 | 0.62 | 0.62 | 0.61 | 0.62 | -93.64 | 92.29 | -93.95 | -99.73 |
| 3 | 0.23 | 0.22 | 0.42 | 0.41 | 176.88 | -169.63 | -26.34 | -35.04 |
| 4 | 1.25 | 1.27 | 0.23 | 0.22 | -145.99 | 19.98 | 26.82 | 12.78 |
| 5 | 1.87 | 1.87 | 0.74 | 0.78 | -148.44 | -25.92 | 32.90 | 96.97 |

problems for a large difference in required modes for an accurate approximation may occur. For example, assume two hypothetical signals of which signal A requires 5 modes and signal B need 50 modes. Signal A will be overdetermined to have a good approximation of signal B. Signal B will be underdetermined if we want an accurate approximation of signal A. An overdetermined approximation will allow poorly damped signals to increase the error of the approximation.

Table 4.2 shows the required number of modes which give a good approximation. The allowed error for the Bus Voltage is larger for the values of the voltage have not been normalized. The engine shows that it requires fewer initial modes, this is because the voltage and the field voltage consists of higher frequency noise. The noise comes from the passive rectifier and the faster control loop of the AVR. Using both bus voltage and field voltage in the analysis is possibly similar to engine torque and speed because of the small difference in initial modes. However, analysing the field voltage and mechanical torque is not possible in one go, due to the large difference in required modes. They have to be computed by the tool separately and the results need to be compared by hand.

The limitation of running multiple signals occurs due to the implementation of the code. The data is stored in large matrices consisting of the solutions of the different modes. This means that all signals analysed must comply with the dimensions of the matrix. The dimension of the matrix is determined by the initial order of modes. This could be improved by restructuring the code and having the output be a certain amount of submodes which make the best approximation for example 5. The number of initial modes can differ within the loop and the output only gives the 5 most dominant modes.

### RESULTS OF CASE SIMULATION

The first test compares the 5 dominant modes of the torque of the diesel engine with those of the field voltage of area A and B. For the first test, we are interested in the frequencies and the phases of the signal. The result is shown in table 4.3. It shows that the field voltage and torque have some similar frequencies such as mode 2. The main difference is that the torque input differs in phase for area A and B with approximately 180°. This is also visible in the speed in figure 4.5. From this, it can be concluded that the oscillation in both voltage and speed is most likely from the governor control. Area A and area B are in a local oscillation. Appendix D shows the time domain approximations. Figure D.1 gives the approximation of the Torque value and figure D.2 depicts the approximation of the field voltage.

The next test is that of the Field Voltage and the DC bus Voltage. This test investigates the relation of the AVR to the DC voltage. Table 4.4 show the results of the analysis and appendix D gives the time domain result in figure D.3. Mode 2 shows similar frequencies but the voltage does not show a large phase shift. The

Table 4.4: Results of Field voltage and DC Voltage in analysis tool

| | Frequency $Hz$ | | | | Phase ° | | | |
|---|---|---|---|---|---|---|---|---|
| | Field Voltage | | DC Voltage | | Field Voltage | | DC Voltage | |
| Mode | Area A | Area B | Area A | Area B | Area A | Area B | Area A | Area B |
| 1 | 0 | 0 | 0 | 0 | 0 | 0 | 0 | 0 |
| 2 | 0.61 | 0.61 | 0.61 | 0.61 | -107.11 | -112.00 | 28.29 | 6.12 |
| 3 | 0.37 | 0.37 | 0.79 | 0.79 | -108.05 | -125.76 | -111.89 | -99.62 |
| 4 | 0.22 | 0.21 | 0.40 | 1.03 | 15.34 | 5.91 | 43.86 | 128.29 |
| 5 | 0.78 | 0.79 | 1.03 | 0.49 | 121.03 | 136.90 | 112.54 | -124.00 |

Table 4.5: Results of Torque and speed in analysis tool

| | Frequency $Hz$ | | | | Phase ° | | | |
|---|---|---|---|---|---|---|---|---|
| | Torque | | $\omega$ | | Torque | | $\omega$ | |
| Mode | Area A | Area B | Area A | Area B | Area A | Area B | Area A | Area B |
| 1 | 0 | 0 | 0 | 0 | 0 | 0 | 0 | 0 |
| 2 | 0.62 | 0.62 | 0.62 | 0.62 | -85.20 | 94.29 | 67.99 | -112.84 |
| 3 | 0.22 | 0.22 | 0.23 | 0.22 | 176.04 | -165.26 | -73.20 | -64.52 |
| 4 | 1.25 | 1.27 | 1.24 | 1.27 | -47.40 | 22.44 | 122-24 | -176.25 |
| 5 | 1.13 | 1.1 | 1.03 | 1.04 | -35.22 | 155.00 | 90.49 | -62.47 |

other modes cannot be compared since the frequencies differ from the field voltage and the DC voltage. This means that there are different oscillatory modes within the DC voltage signal, not caused by the Field voltage. A possible explanation for this is the effect of the passive rectifier which introduces non-linear behaviour.

The last test is to investigate the Torque setpoint of the diesel and the speed of the diesel engine. The speed of the diesel engine is similar to that of the synchronous machine. Table 4.5 depict the resulting frequency and phase of the signals of torque and speed. Appendix D depicts the time domain result of the analysis tool in figure D.4 The first observation is the better fit of the frequencies compared to the test of field voltage and DC voltage. It shows that introducing non-linear behaviour decreases the accuracy of the analysis. Mode 2 and 5 show a clear phase difference of 180° between the areas in both speed and torque.

From the previous three tests, we can conclude the following: The local area oscillation is caused by the governor control and is visible in the speed of the machine. Furthermore, the frequency is also observable in the DC voltage. This shows that there is a relation between the speed of the generator and the voltage on the DC bus. The AVR tries to compensate for this which is also visible in the analysis. Since no phase shift is noticeable on the AVR it can be excluded as a source of the oscillation.

### MITIGATION ACTION TO IMPROVE STABILITY

The instability is caused by poorly damped oscillating frequencies in the governor controller. Low-frequency oscillations are known to be damped by a Power System Stabilizer. To determine the parameters of the PSS the frequencies of the poorly damped modes can be used. The NCF value could indicate which generator is most dominant in the oscillation, since the simulation consists of two identical pairs this value should be the same. Table 4.6 gives all the information of the oscillation of speed. The following observations are made from analysing table 4.6:

- Mode 2 and 4 are an inter-area oscillations $\Delta\phi = 180°$
- Mode 2 is poorly damped
- Damping of mode 5 differs between the generators

A common procedure of increasing the damping of a power system for a low-frequency band (0.1 to 1 Hz) is by introducing a PSS. This control circuit tries to enhance the damping of power system oscillations through excitation control, thus reactive power. A PSS1A is used from [33] and is parameterized to damp the frequency of mode 2 based on the frequencies given in 4.6. The parameters of the PSS are found in appendix

Table 4.6: Result of the prony tool with the input of the diesel speed from 4.5

| Mode | Frequency $Hz$ | | Phase ° | | Damping | | Amplitude | | NCF | |
|---|---|---|---|---|---|---|---|---|---|---|
| - | Area A | Area B | Area A | Area B | Area A | Area B | Area A | Area B | Area A | Area B |
| 1 | 0 | 0 | 0 | 0 | 0 | 0 | 1.0001 | 0.9999 | 1334.1 | 1333.9 |
| 2 | 0.61 | 0.61 | -35.67 | 143.42 | -0.0017 | -0.0028 | 0.0036 | 0.0028 | 0.0082 | 0.0080 |
| 3 | 0.22 | 0.22 | 88.48 | 93.615 | -0.3699 | -0.3965 | 0.0204 | 0.0238 | 0.0089 | 0.0106 |
| 4 | 0.69 | 0.69 | -177.4727 | -3.51 | -0.2339 | -0.3216 | 0.0018 | 0.0024 | 0.0001 | 0.0002 |
| 5 | 1.22 | 1.21 | -64.14 | -62.65 | -0.0118 | -0.0376 | 0.0002 | 0.0002 | 0.0000 | 0.0000 |

A.

The same test is performed and the result is shown in figure 4.7. As stated the PSS tries to dampen power system oscillations by adjusting the AVR. This is visible in the field voltage. The speed and voltage oscillations are damped and a constant speed and voltage are observed. A downside of the PSS is the voltage peak which occurs at $40s$, this has increased to $800VDC$. This can be solved by altering the gain of the AVR controller. It shows that the parameterisation of the power systems controller is not advisable to do on the fly during commissioning. It shows that by altering one value another problem may arise which may be even more dangerous. Fine-tuning can be done on-board but should be done with caution.

## 4.3. CONCLUSIONS

In this chapter two case studies are performed. The goal of the first case study is to test the performance of the stability analysis tool and to see if it is of added value when searching for the cause of oscillations. The goal of the second case is to test the performance of the stability analysis tool when it is used as a parameterisation tool for the controllers in a DC-PPS.

The first case study showed that the stability analysis tool was able to approximate the signals, including noise, adequately. Pre-processing was required to enhance the performance to get an accurate approximation without losing the oscillatory modes which were under study. It showed that the tool can exclude some of the possible sources of the source of the oscillation. From the data, there was no evident link to the controller of the generators, AVR or Governor, of being the cause of the sudden oscillation. In a later stage of the thesis, it became apparent that indeed the source was something else.

The second case study showed that the stability analysis tool is of added value in the parameterisation of the system. It showed that it was able to extract the dominant oscillation modes and could identify the type of the dominant oscillation modes. It can find the source of the oscillation. The solution to add stability within the grid was a PSS and with that controller, the oscillatory modes were damped sufficiently. The case study showed that conventional control in a DC-PPS requires thorough analysis. Inter-area oscillation modes may be undamped which results in power and voltage fluctuations.

There are some limitations to the analysis tool, such as large differences between the initial modes between signals. If signals are analysed at the same time in the analysis tool this might cause problems. If the surplus of required modes exceeds becomes too large the accuracy of the approximation decreases. This results in the requirement of analysing the signals seperatly.

The results of this chapter contribute to answering the research questions represented in chapter 1 by testing the proposed model and analysis tool. It showcased the performance and the possible added value of both products. The stability analysis tool can determine the IMF's for both a simulation and real data out of the field. With the help of the analysis tool some of the possible error sources can be excluded which is an added value for Royal IHC. These case studies contribute to answering the research questions described in chapter 5.

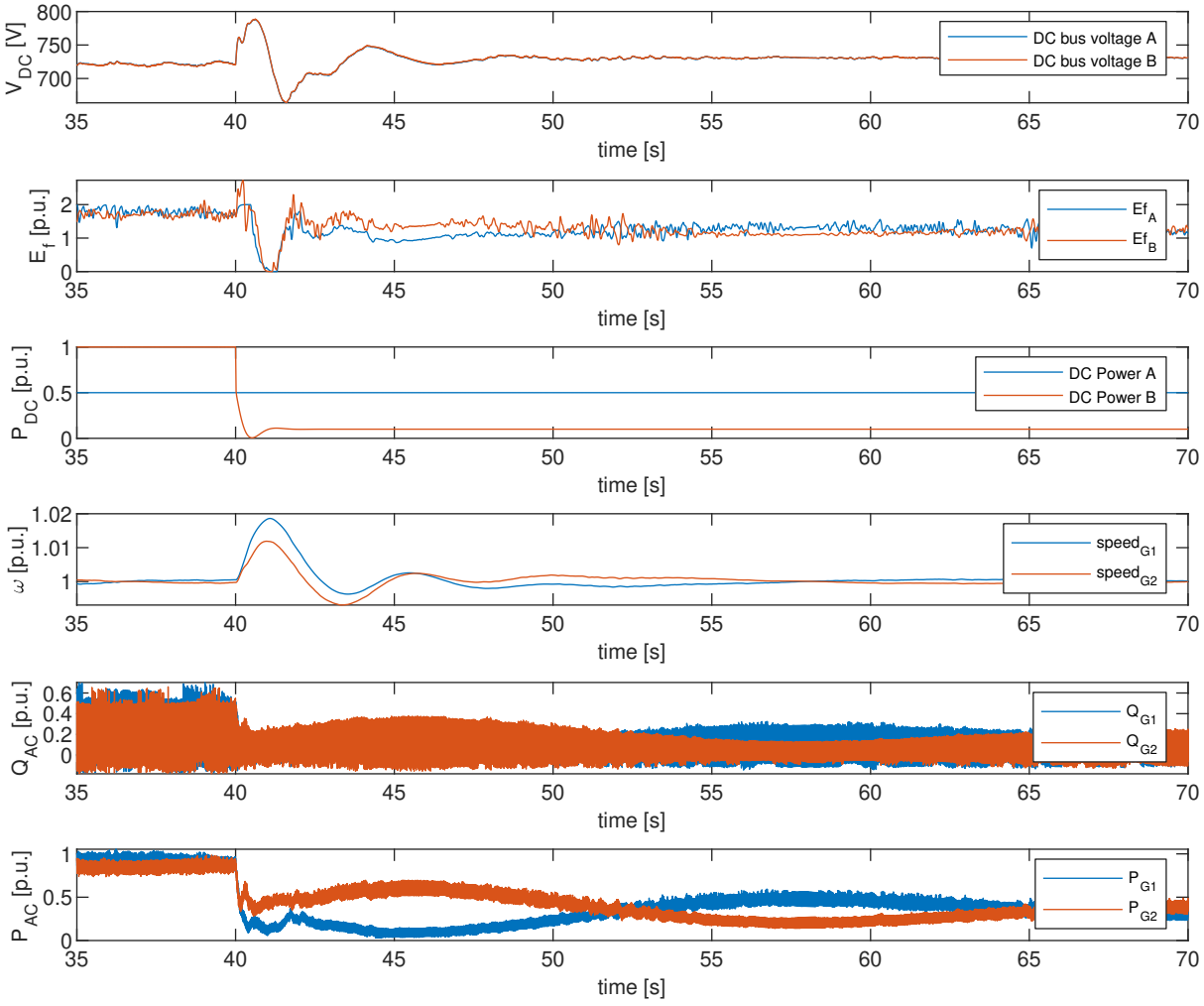


Figure 4.7: DC-PPS with PSS

# 5

# CONCLUSION AND RECOMMENDATIONS

This chapter describes the conclusions of this thesis by answering the research questions stated in 5.1. First, the sub-questions are answered and finally the main research question. The recommendations are given in section 5.2. The recommendations describe how to continue on this work.

## 5.1. CONCLUSIONS

The research question given in section 1.3 is as follows:
*"How to ensure robust dynamic voltage performance of a DC shipboard power system whilst using passive rectification of the DC voltage?"*

The thesis project has been split into two separate products namely, a DC-PPS simulation model and a stability analysis tool. For both products, research questions have been described which contribute to answering the above-stated research question.

### WHAT IS THE NECESSARY DETAIL OF THE DC-PPS MODEL FOR VOLTAGE STABILITY ANALYSIS?

In essence, a simulation model its sole function is to simulate the behaviour which is to be analysed. This means that the detail of the model is determined by the aspects of the model which influence this behaviour in any way or form. Assumptions can be made whether some effects are so small that they may be neglected. The goal was to simulate a DC-PPS which consists of two parallel sets of a diesel-synchronous machine combination connected to a common DC bus via a passive rectifier. It is to investigate the voltage stability of the DC bus. The range of simulation time is between $40s$ to $120s$ and the phenomenon of interest are those of low frequency. Therefore some assumptions on the detail of the model are made.

The detail of the model is determined by three parts. First, the components which influence voltage stability have to be determined. Second, the critical scenarios in which voltage stability could be under stress need to be determined and the last part is the control of the DC-PPS. What kind of control is required to enhance the voltage stability.

### WHICH COMPONENTS OR PARAMETERS INFLUENCE THE VOLTAGE STABILITY?

During the modelling and the initialisation of the model parameters which influence the voltage, stability became noticeable. Every part of the model influences stability in a way. The thesis focuses on the parameters and components affecting voltage stability. A prerequisite is that of the usage of a passive rectifier. The components which influence the voltage stability are determined during the initialisation of the DC-PPS and tests cases. The following components have an observed influence on the voltage stability of a DC-PPS:

1. Generator AVR
2. Prime mover and governor
3. DC bus impedance
4. Load

The passive rectifier cannot compensate voltage deviations of the DC bus or AC supply voltage, thus the generator is in full control of the power and voltage quality. The AVR is therefore one of the main controllers which determine voltage stability. The input for the AVR is critical for a stable DC voltage. Results showed that the DC voltage input is required to maintain a stable DC voltage on the DC bus. Using the DC voltage increases the risk of overexcitation, requiring limiters such as over-excitation protection to prevent damage. The parameters of the controller of the AVR influence the dynamic response of the generator and should be properly dimensioned before used in a test.

The prime mover and its controller supply the mechanical power for the synchronous generator. Operating multiple machines in parallel generates local-area oscillations. These were observed in tests of the case study. These low oscillatory modes need to be damped to lower stress on components. The governor and the type of prime mover determine the speed at which the load can be changed. The engine delay, therefore, limits the rate of change of power.

The DC-bus impedance tends to be a critical parameter in the simulation. The DC-bus parameters such as its resistance and inductance limit the rate of change between areas. The model of the DC bus has been kept simple in this thesis but it is advised to investigate this in more detail. It has been observed that a low impedance results in fast power fluctuations between the two areas.

The load influences the stability as well. Fast-acting loads will increase the instability and the requirements of power generation. The load determines the speed at which power fluctuates in the system and thus the dynamic performance required of the system.

#### WHAT ARE CRITICAL SCENARIO'S IN WHICH A STANDARD CONTROL METHOD MAY BE INEFFECTIVE?

A literature study showed that the driving force behind voltage instability is usually the load. The response of the controllers after a disturbance may result in a voltage drop, voltage oscillations or progressive collapse of the grid. Disturbances in the power grid are represented by load changes. To cope with this the generator controller have to support the grid by supporting the voltage. However, these may be limited by the field or armature current they can provide. Therefore the model of the synchronous machine has to be detailed.

The proposed model allows testing the system under different loading conditions. It shows that both AVR and Governor influence over and undervoltage cases. It showed that the conventional input for the AVR, namely the AC line voltage, was insufficient to maintain the voltage constant on the DC bus. Voltage dips were observed when large load steps were initiated, this suggested that the input for the AVR should be the DC voltage after the rectifier. This voltage allows the AVR to make the line to line voltage variable such that it can cope with the fluctuations on the DC side. It should be noted that the AC voltage fluctuations should be within the voltage limitations of the generator.

The system is parameterized by opening the DC common bus making two separate systems. Load steps and voltage steps are initiated to test the performance of the governor and AVR respectively. When closing the common-bus inter-area oscillations were observed when the system perturbed with a load step. It showed that a second step is required in initializing and parameterizing the generators when using them in parallel and maintaining a decentralized control topology.

#### WHAT KIND OF CONTROL IS REQUIRED TO ENHANCE THE STABILITY OF THE DC-PPS?

The requirements of the controller are influenced by the components and parameters. When a vessel is expected to experience large and fast load fluctuations the controller needs to be fast as well. This work investigated different topologies of control on a literature basis. It showed that to investigate the possibilities and the performance of such novel control strategies, a model is required. In this thesis, a conventional control strategy has been adapted which is a decentralized control. The controllers are a PID based AVR and a governor these are analysed and parameterized.

Decentralized control has limited knowledge and only observes the values they directly control. The system showed inter-area oscillations which were not observed in the controller input as such. Therefore this oscillation was unnoticed and therefore undamped. The stability analysis tool implementing prony analysis showed undamped inter-area oscillations. It gives information regarding its frequency, phase, amplitude and

damping. With this information, a PSS has been implemented. The PSS changes the field voltage to dampen oscillations of the input variable, in this case, the speed. The PSS can maintain a stable voltage on the DC-PPS with a pulsed load.

Enhancing the stability, in this case, is done by the inclusion of a PSS. It is advised to investigate centralized and distributed control strategies and include these strategies in the simulation. Another method could be a different control strategy which has been investigated in a literature study. For example, model predictive controllers. The model of the DC-PPS allows testing of newer types of controllers.

### WHAT METHOD CAN BE USED TO ANALYSE THE STABILITY OF A DC-PPS?

Voltage stability has been defined as the ability to maintain steady voltages in all busses in the system after being subjected to a disturbance. Thus an analysis tool that is to investigate the stability of a certain signal needs to find poorly damped or undamped signals out of the data. These undamped signals are directly related to instability or large fluctuations. Therefore giving information about how they should be solved.

There are multiple methods available to analyse oscillatory modes within a signal three have been analysed during this thesis which is Fourier, Koopmans and prony. Eventually, prony has been selected as the method to be used for the stability analysis. Prony is mathematically less complex than Koopmans and has a similar performance according to the reviewed literature. Prony doesn't require a base frequency and can calculate damping and phases of each frequency, compared to Fourier.

The tool requires the following two functions, first, it needs to be able to identify unstable operation points (or modes) and secondly it needs to be able to categorize them preferably linking them to a source.

### HOW CAN UNSTABLE OPERATIONS POINTS OF A DC-PPS BE IDENTIFIED?

The Prony Analysis method allows the acquisition of the IMFs of a data set. These IMF's give insight into the frequency, phase, amplitude and damping. An undamped signal may indicate an unstable operation point or a poorly damped one. In addition to prony, an augmentation on the method has been implemented which allows to directly calculate the NCF of the signal. This allows us to see which signal contributes most to a certain mode. The tool is used in two situations, the first situation is from real data from a vessel and the second situation is for analysing simulation data.

The obtained data from a vessel is analysed using the analysis tool. In comparison to the synthetic signals, data from the field requires pre-processing. The noise within the signal significantly reduces the accuracy of the analysis tool. The signal requires to be filtered such that high frequencies, or a band of frequencies that are not of interest, are filtered out. By doing so the tool can approximate the signal accurately. The analysis can identify poorly damped modes.

The simulation model of the DC-PPS is also analysed with the analysis tool. In the load step test, a clear oscillation occurred on the DC bus voltage but also in the power and speed of the generators. It was clear by visual inspection that there was an inter-area oscillatory mode. With the use of the analysis tool, the data was easily analysed and the dominant modes were acquired. The data from the simulation was reproduced by the 5 most dominant modes and an accurate approximation was made. From the analysis, two modes appeared to be in anti-resonance. With the help of the tool, a PSS has been implemented which damped these modes. The result was an increase in voltage stability for load steps.

### HOW CAN UNSTABLE OPERATIONS POINTS CATEGORIZED OR LINKED TO A SOURCE?

The augmented prony analysis proposes the direct calculation of the NCF. This factor indicates the contribution of one mode from a signal. The value in itself does not have any meaning only the difference between the NCF values of the modes. This makes the direct relation of a source difficult. The NCF is a good way to give insight into which component has the largest benefit to the total signal if damping measures are undertaken. However, it does not mean that a large NCF value indicates that it is the source of said oscillation.

### HOW TO ENSURE ROBUST DYNAMIC VOLTAGE PERFORMANCE OF A DC-PPS INCORPORATING PASSIVE RECTIFICATION?

This thesis proposed a method to analyse the voltage stability of a DC-PPS incorporating passive rectification of the AC to DC voltage. The challenge was to build a verified model of a DC-PPS and a validated analysis tool that allows analysis of the voltage stability. Previous research has worked on single generator-rectifier-load setups. This thesis continued to investigate the relation between two parallel sets and look into predominantly long-term voltage stability.

The model has been verified by comparison with an RScad simulation. This verification showed that highly specialized hardware and software, in this case, RScad on a real-time operating system, had similar results compared to the Matlab-Simulink simulation. After the verification, the Matlab-Simulink model has been improved and further parameterized. The simulation showcased the required passive rectifier and CPLs. The simulation allows testing load changes and system splits.

An analysis tool has been developed which allows the analysis of unstable oscillatory modes. The analysis method is prony with an augmented component which allows the direct calculation of the NCF. The tool is validated through a synthetic signal and by using a well-known example from Kundur. It showed that it was able to accurately approximate the signal and that it was able to determine the undamped modes. The Case studies showed that the tool can work with different types of data and showed that some pre-processing is required. It showed that the tool gives insight into the data and may indicate a probable solution.

Ensuring a stable power grid requires models, tests and proper parameterisation of the different controllers. The dynamic behaviour of vessels is changing due to the increase in power electronic loads and new energy sources such as hydrogen and liquified natural gas. The following procedure is proposed to ensure a stable power system of a DC-PPS:

1. Adjust model parameters such that it reflects the real situation as close as possible
2. Determine the load cases of the vessel
3. Run multiple load cases in different situations (layout may change of the vessel)
4. Analyse results with the stability analysis tool
5. Enhance voltage stability by changing control parameters accordingly
6. Return to step 2 until all different situations have been tested

From this thesis, it became clear that models of the complete power system are required for Royal IHC to guarantee the power stability of its vessels. Especially with the shift in power sources and the increasing demand for sustainability. Newer control topologies are low hanging fruit in terms of sustainability but require simulation testing. The stability of vessels can be increased by implementing newer control strategies or implementing additional controllers such as a PSS.

The model of the DC-PPS is run from a script. The code to run the simulation is provided in appendix B and the code for the analysis tool is provided in appendix C.

## 5.2. RECOMMENDATIONS

This thesis delivered two main products namely a model of a DC-PPS and a stability analysis tool implementing the prony analysis. The model build can be used as a building platform and the model can be expanded in many ways to incorporate different aspects. These aspects are given as recommendations. The recommendations regarding the model of the DC-PPS described in chapter 2 are:

- The main recommendation is to keep building and extending the simulation. Different aspects such as energy storage systems, hydrogen power generation, liquified nitrogen generators and different control strategies can be investigated. Furthermore, a similar analysis but on an AC-PPS is useful to allow direct comparison between the systems.
- Different control strategies such as centralized control can be investigated with the help of this model. It is recommended to investigate the possibility of centralised control and optimizing for example the fuel consumption of the diesel generators.
- The controllers used by Royal IHC should be modelled and stored in a library such that the functionality of the controller is implemented in the simulation. For now, the DC-PPS consists of standardized controllers of the AVR and Governor. It is recommended to expand this towards the used AVR and governor such that the model is comparable to the implementation.
- The DC bus of the model should be investigated in more detail. The size of the DC bus and its cables may differ per ship. The model should be extended with a building block of the DC bus where the length and size of the bus can be used as input.

The second product is the stability analysis tool. This tool allows analysing of different oscillatory modes within a signal. The method proves to be interesting but also shows some challenges regarding noisy signals. The recommendations regarding the stability analysis tool described in chapter 3 are:

- The initial order of modes of the prony analysis is selected by hand and looped until the approximation is below a certain error value. It is recommended to expand this such that an algorithm selects the best possible fit with the least amount of initial modes. This would increase the accuracy of the approximation and reduce the number of modes with very minor frequency deviations.
- The stability tool proves to be useful in both designing and data analysis for Royal IHC. The tool should be made into a tool with a good user interface such that different departments can work with it.

# A

# SIMULATION PARAMETERS

This appendix give the parameters of the final simulation of the DC-PPS. The generator model parameters are given in table A.1

Table A.1: Parameters of the generator used in the DC-PPS under study

| Parameter description | Symbol | Value | Unit |
|---|---|---|---|
| Rated apparent power | $P_n$ | 2.467 | MVA |
| Rated line-to-line voltage | $V_{LL}$ | 550 | V |
| Rated frequency | $f_n$ | 60 | Hz |
| d-axis open circuit transient time constant | $T'_{d0}$ | 4.4849 | s |
| d-axis open circuit sub-transient time constant | $T_{d0}$" | 0.0681 | s |
| q-axis open circuit sub-transient time constant | $T_{d0}$" | 0.1 | s |
| d-axis reactance | $X_d$ | 1.37 | p.u. |
| d-axis transient reactance | $X'_d$ | 0.17 | p.u. |
| d-axis sub-transient reactance | $X''_d$ | 0.11 | p.u. |
| q-axis reactance | $X_q$ | 1.34 | p.u. |
| q-axis sub-transient reactance | $X_q$" | 0.14 | p.u. |
| Leakage reactance | $X_l$ | 0.05 | p.u. |
| Stator Resistance | $R_s$ | 0.0378 | p.u. |
| Inertia Coefficient | $H$ | 9.2 | s |

The AVR model parameters are given in table A.2

Table A.2: Parameters of the AVR used in the DC-PPS under study

| Parameter description | Symbol | Value | Unit |
|---|---|---|---|
| Low-pass filter time constant | $T_r$ | $\frac{1}{360}$ | s |
| Regulator gain | $K_a$ | 40 | - |
| Regulator time constant | $T_a$ | 0.1 | s |
| Exciter gain | $K_e$ | 1 | - |
| Exciter time constant | $T_e$ | 0.05 | s |
| Transient gain reduction time constant | $T_b$ | 0.5 | s |
| Transient gain reduction time constant | $T_c$ | 2 | s |
| Damping filter gain | $K_f$ | 0.01 | - |
| Damping filter time constant | $T_f$ | 0.1 | s |
| Regulator maximum output limit | $E_{fmax}$ | 4 | p.u. |
| Regulator minimum output limit | $E_{fmin}$ | 0 | p.u. |

The Governor model parameters are given in table A.3

Table A.3: Paramters of the Governor used in the DC-PPS under study

| Parameter description | Symbol | Value | Unit |
|---|---|---|---|
| Regulator Gain | $K$ | 40 | - |
| Regulator time constant | $T_1$ | 0.01 | s |
| Regulator time constant | $T_2$ | 0.02 | s |
| Regulator time constant | $T_3$ | 0.2 | s |
| Actuator time constant | $T_4$ | 0.25 | s |
| Actuator time constant | $T_5$ | 0.009 | s |
| Actuator time constant | $T_6$ | 0.0384 | s |
| Torque minimum limit | $T_{min}$ | 0 | p.u. |
| Torque maximum limit | $T_{max}$ | 1.4 | p.u. |
| Droop constant* $D$ | 0.03- | | |
| Engine time delay | $T_d$ | 0.024 | s |

* the droop constant is only used during the validation test in which the values of the RScad simulation are compared to the Matlab-Simulink simulation.

The PSS model parameters are given in table A.4

Table A.4: Paramters of the PSS used in the DC-PPS under study

| Parameter Description | Symbol | Value | Unit |
|---|---|---|---|
| PSS gain | $K_S$ | 3.15 | - |
| Lead compensating time constant | $T_1$ | 0.76 | s |
| Lag compensating time constant | $T_2$ | 0.1 | s |
| Lead compensating time constant | $T_3$ | 0.76 | s |
| Lag compensating time constant | $T_4$ | 0.01 | s |
| Washout time constant | $T_5$ | 5 | s |
| Transducer time constant | $T_6$ | 0 | s |
| Max output | $V_{STmax}$ | 0.09 | p.u. |
| Min output | $V_{STmin}$ | -0.09 | p.u. |

# B

# MATLAB SCRIPT TO RUN SIMULATION

## CONTENTS



```
clc
clear
% this code simulates the Voltage response test
```

## INITIALIZE

```
PnomT=2850e3;   %Nominal power thruster
Pnomw=186e3;    %Nominal power towing winch
T=80;
TaPS=[0.0 1.0 15 40 80];   %Azimuth thruster port side time array in seconds
PaPSA=[0 0.5 0.5 0.5 0.5];
PaPSB=[0 0.1 1.0 0.1 0.4];


Link=1; %DC link 0=open 1=closed;
PSSA=1;  %0=disabled 1=enabled
PSSB=1;  %0=disabled 1=enabled
```

## AVR SETTINGS

```
Tr=1/360;
Ka=40;
Ta=0.1;
Ke=1; %afblijven
Te=0.05;%afblijven
Tb=0.5;
Tc=2;
Kf=0.01;
Tf=0.1;
K=40;
c1=1; %0= AC measurement 1= DC measurement
k=1; %figure counter
```

### PSS SETTINGS

```
K_S=3.15;       %
T_1=0.76;       %
T_2=0.1;        %
T_3=0.76;       %
T_4=0.01;       %
T_5=5;          %Washout time constant 10 seconds or less is recomended to
%quickly remove low frequencies
T_6=0;          %low pass filter time constant
```

### RUN SIMULATION

```
%The simulation is runned from script and the data from the to-workspace
%bloack is loaded. the for loop allows to run mulitple simulations with
%different values.
for i=1:1:1
    A=sim('DC_PPS_improved_parralel_Case');
    output(:,:,i)=A.get('Voltage_step');
    t(:,i)=output(:,1,i);
    P_A(:,i)=output(:,2,i);
    P_B(:,i)=output(:,3,i);
    w_A(:,i)=output(:,4,i);
    w_B(:,i)=output(:,5,i);
    Pgen_A(:,i)=output(:,6,i);
    Pgen_B(:,i)=output(:,7,i);
    Qgen_A(:,i)=output(:,8,i);
    Qgen_B(:,i)=output(:,9,i);
    Ef_A(:,i)=output(:,10,i);
    Ef_B(:,i)=output(:,11,i);
    V_A(:,i)=output(:,12,i);
    V_B(:,i)=output(:,13,i);

end
```

### PLOT

```
%zoom paramters
x1=find(t(:,1)==35); %start time of interest
x2=find(t(:,1)==70); %end time of interest

figure(k)
subplot(6,1,1)
plot(t(x1:x2),V_A(x1:x2,:),t(x1:x2),V_B(x1:x2,:))
legend({'DC bus voltage A','DC bus voltage B'},'FontSize',6)
xlabel('time [s]','FontSize',8);
ylabel('V_{DC} [V]','FontSize',8);
subplot(6,1,2)
plot(t(x1:x2),Ef_A(x1:x2,:),t(x1:x2),Ef_B(x1:x2,:))
legend({'Ef_A','Ef_B'},'FontSize',6)
xlabel('time [s]','FontSize',8);
ylabel('E_f [p.u.]','FontSize',8);
subplot(6,1,3)
plot(t(x1:x2),P_A(x1:x2,:),t(x1:x2),P_B(x1:x2,:))
legend({'DC Power A','DC Power B'},'FontSize',6)
xlabel('time [s]','FontSize',8);
ylabel('P_{DC} [p.u.]','FontSize',8);
subplot(6,1,4)
plot(t(x1:x2),w_A(x1:x2,:),t(x1:x2),w_B(x1:x2,:))
```

```
legend('speed_{G1}','speed_{G2}','FontSize',6)
xlabel('time [s]','FontSize',8);
ylabel('\omega [p.u.]','FontSize',8);
subplot(6,1,5)
plot(t(x1:x2),Qgen_A(x1:x2,:),t(x1:x2),Qgen_B(x1:x2,:))
legend('Q_{G1}','Q_{G2}','FontSize',6)
xlabel('time [s]','FontSize',8);
ylabel('Q_{AC} [p.u.]','FontSize',8);
subplot(6,1,6)
plot(t(x1:x2),Pgen_A(x1:x2,:),t(x1:x2),Pgen_B(x1:x2,:))
legend('P_{G1}','P_{G2}','FontSize',6)
xlabel('time [s]','FontSize',8);
ylabel('P_{AC} [p.u.]','FontSize',8);
k=k+1;
```

### SAVE REQUIRED DATA

here the data can be saved which is to be analysed for the Prony analysis, this could be in one script.

```
% save('DC_PPS_2_PSS','t','w_A','w_B')
```

### EXPORT FUNCTION

figure export function which allows transparant borderless figures

```
export_fig figuur1 case_matlab_pss.eps -transparent

% downsample
```

# C

# Analysis Tool Script

## Contents

- Form toeplitz matrix of data H for order N (modes)
- Solve linear least square error
- Solve the polynomial characteristic equation achieved from step 2
- Solve LSE problem using z values in step 3
- IMF based on augmented prony
- Determine ammount of modes
- figures
- construct ci from paper
- IMF's of the signals
- Construct real IMF's
- data voor de tabel eruit friemelen
- NCF calculation
- export function

```
% this code uses one input column of data and tries to approximate it with
% N modes. It selects a certain amount of submodes in which the error does
% not exceed the crit value.
% The script will increase the modes if the error criteria is not achieved.
% it plots the resulting signal with total amount of modes and the
% required amount of modes to keep inside the criteria value crit for
% maximum error per data point.

clc
clear
close all
% Construct to be tested signal

% load('DC_PPS_1')
load('Output'); %t,Pa,Pb,wa,wb,PgenA,PgenB,QgenA,QgenB,EfA,EfB,VA,VB,TA,TB,Vlink,Ilink
t=output(:,1);
pA=output(:,2);
pB=output(:,3);
wA=output(:,4);
wB=output(:,5);
PgenA=output(:,6);
PgenB=output(:,7);
QgenA=output(:,8);
QgenB=output(:,9);
EfA=output(:,10);
```

```
EfB=output(:,11);
VA=output(:,12);
VB=output(:,13);
TA=output(:,14);
TB=output(:,15);
Vlink=output(:,16);
Ilink=output(:,17);

% load('DC_PPS_2_PSS')
x1=find(t(:,1)==40);
x2=find(t(:,1)==80);
test_time1=t(x1:x2);
dfactor=200;

Y2(:,:)=[TA(x1:x2),TB(x1:x2),wA(x1:x2),wB(x1:x2)]; %T and E;
Y1(:,:)=downsample(Y2,dfactor);
N=10; %no pss TA,wA 120
crit=0.00005; %no pss TA,wA 0.01
k=1;
Y(:,:)=Y1;
test_time=downsample(test_time1,dfactor);

figure(k)
plot(t(x1:x2),TA(x1:x2),test_time,Y(:,1),'--')
legend('Original signal','Downsampled signal','Fontsize',6)
xlabel('Time [s]','Fontsize',8)
ylabel('Amplitude [-]','Fontsize',8)

k=k+1;

A=1;

while A==1
rzsorted=zeros(N,size(Y,2));
Bsorted=zeros(N,size(Y,2));
for q=1:1:size(Y,2)

Yt=Y(:,q);
% t=test_t_increment;
Ts=test_time(2)-test_time(1);
time=test_time;
```

### FORM TOEPLITZ MATRIX OF DATA H FOR ORDER N (MODES)

Augmented prony paper step 1

```
% h is data set
% N=the order of modes
% the code has been taken out of the matlab function prony by open prony


h=Yt;
K = length(h) - 1;

if K <= max(N)      % zero-pad input if necessary
    K = max(N)+1;
    h(K+1) = 0;
```

```
end
c = h(1);
if c==0    % avoid divide by zero
    c=1;
end
Hin = toeplitz(h/c,[1 zeros(1,K)]);
% K+1 by N+1
if (K > N)
    H = Hin(:,1:N+1);
%     H(:,(N+2):(K+1)) = [];
else
    H = Hin;
end
h1 = H((N+2):(K+1),1); % K-M by 1
H2 = H((N+2):(K+1),2:(N+1)); % K-M by N
%According to augmented prony paper, H=D, d=h and a has to be calculated
```

### SOLVE LINEAR LEAST SQUARE ERROR

Augmented prony step 2

```
%using total least squares
a=-H2\h1; %from this the polynomial equation pc can be obtained

pc=[1; a];
```

### SOLVE THE POLYNOMIAL CHARACTERISTIC EQUATION ACHIEVED FROM STEP 2

Augmented prony step 3 the roots wil give information about the frequency and the damping

```
rz=roots(pc); % the roots of the polynomial equation z-domain
zpoles=rz; %z-domain poles
eigval=log(zpoles)/Ts; %eigenvalues
```

### SOLVE LSE PROBLEM USING Z VALUES IN STEP 3

Augmented prony step 4 First construct the complex z value matrix formula 3 out of augmetned prony U=Z-matrix out of bioinformatics B=h

```
U=zeros(length(h),N);
for i=1:length(rz)
    U(:,i)=transpose(rz(i).^(0:length(h)-1));
end

B=tls(U,h); %beta vector simmilar as a_list out of prony
```

### IMF BASED ON AUGMENTED PRONY

```
%stap voor stap de IMF uitrekenen volgens augmented prony paper

%first sort the columns of the complex matrix U on their real part

[rzsort,index]=sort(rz,1,'descend','ComparisonMethod','real'); %sort on real part


for i=1:length(rz)
    Usorted(:,i)=transpose(rzsort(i).^(0:length(h)-1));
end
rzsorted(:,q)=rzsort;
```

```
Bsorted(:,q)=B(index);
```

### DETERMINE AMMOUNT OF MODES

sorted on amp,freq,damp or phase versus sorted on real(rz)

```
for ii=1:1:length(Bsorted)

SUB_N=ii;

for i=1:1:SUB_N %just on the sorted rz value.
    IMF_out(:,i)=real(Bsorted(i,q)*Usorted(:,i));
end
IMF_o(:,q)=sum(IMF_out,2);
e_o(ii)=sum((Yt-IMF_o(:,q)).^2,1);
[~, min_o]=find(e_o < crit);
end

A=isempty(min_o);

end
N=N+1
end

for q=1:1:size(Y,2)

min_o1(q)=min_o(1);

for i=1:1:min_o1(q) %
    IMF_out1(:,i,q)=real(Bsorted(i,q)*Usorted(:,i));
end
IMF_o1(:,q)=sum(IMF_out1(:,:,q),2);
```

### FIGURES

```
figure(k)
subplot(2,1,1)
plot(time,Yt,time,IMF_o(:,q),'--')
title('Signal reconstruction using total amount of modes')
text1=sprintf('Total Prony N=%d modes',N);
legend('original signal', text1)
subplot(2,1,2)
plot(time,Yt,time,IMF_o1(:,q),'--')
title('Signal reconstruction using a subset of modes')
text2=sprintf('Total Prony N=%d modes of N=%d',min_o1(q),N);
legend('original signal', text2)
k=k+1;
figure(k)
subplot(2,2,1)
plot(time,Yt,time,IMF_o(:,q))
legend('original',text1)
subplot(2,2,2)
plot(time,(Yt-IMF_o(:,q)))
legend('\Delta original v.s. total prony')
subplot(2,2,3)
plot(time,Yt,time,IMF_o1(:,q))
legend('original',text2)
subplot(2,2,4)
```

```
plot(time,(Yt-IMF_o1(:,q)))
legend('\Delta original v.s. subset prony')
k=k+1;

end



\subsection*{construct ci from paper}

\begin{verbatim}
min_o2=max(min_o1);
for q=1:size(Y,2)
    rzsorted1(:,q)=rzsorted(1:min_o2,q);
    Bsorted1(:,q)=Bsorted(1:min_o2,q);
end
con_table(:,:,size(Y,2))=zeros(length(rzsorted1),length(rzsorted1));
con_tableb(:,:,size(Y,2))=zeros(length(rzsorted1),length(rzsorted1));
for q=1:size(Y,2)
    for a=1:1:length(rzsorted1)
        for b=1:1:length(rzsorted1)
            if (imag(rzsorted1(a,q))~=0)
                if rzsorted1(a,q)==conj(rzsorted1(b,q))
                    con_table(a,b,q)=2;
                    con_tableb(a,b,q)=1;
                end
            end
        end
    end
end
% find non conjugate signals

for q=1:size(Y,2)
    row(:,:,q)=sum(con_table(:,:,q),1);
    non_con=find(~row(:,:,q));
    % add a 1 in the con_table on the position a=b position according to
    % non_con
        for i=non_con
        con_table(i,i,q)=1;
        con_tableb(i,i,q)=1;
        end
end



%zero out duplicates
for q=1:size(Y,2)
    for a=1:1:size(con_table,1)
        for b=1:1:size(con_table,1)
            if con_table(a,b,q) == 2 && con_table(b,a,q) ==2
                con_table(a,b,q)=0;
                con_tableb(a,b,q)=0;
            end
        end
    end
end
```

```
for q=1:size(Y,2)
    rz_int(:,q)=con_table(:,:,q)*rzsorted1(:,q);
    B_int(:,q)=con_tableb(:,:,q)*Bsorted1(:,q);
    zero_length(q,1)=size(find(real(rz_int(:,q))),1);
    rowb(:,:,q)=sum(con_table(:,:,q)',1);
end
max_length=max(zero_length);
index1=zeros(max_length,size(Y,2));
rz_real=zeros(max_length,size(Y,2));
B_real=zeros(max_length,size(Y,2));

for q=1:size(Y,2)
    ind_real=find(real(rz_int(:,q))); %values kept in B_matrix
    ind_nonzero=nonzeros(rz_int(:,q));
    B_nonzero=nonzeros(B_int(:,q));
    for i=1:length(ind_real)
       index1(i,q)=ind_real(i);
    end
end

% find first zero location
zero_i(:,1:4)=length(index1);
for i=1:size(index1,2)
    a=nonzeros(~index1(:,i));
    if a==1
        zero_a(:,i)=find(~index1(:,i), 1 )-1;
        if zero_a(:,i)==0
            zero_i(:,i)=zero_i(:,i);
        else
            zero_i(:,i)=zero_a(:,i);
        end
    end
end
m_n=min(zero_i);
```

## IMF'S OF THE SIGNALS

```
%Construct U matrix for each signal
%Dit valideert dat de vector rzsorted en Ux nog steeds hetzelfde signaal
%opbouwen, ofwel uit deze set kan de damping gehaald worden.
for s=1:1:size(Bsorted1,2)
    for i=1:length(rzsorted1)
        Ux(:,i,s)=transpose(rzsorted1(i,s).^(0:length(h)-1));
    end
    for i=1:1:min_o1(1)
        IMF_outx(:,i,s)=real(Bsorted1(i,s)*Ux(:,i,s));
    end
    for i=1:1:length(Bsorted1)
        IMF_out_t(:,i,s)=real(Bsorted1(i,s)*Ux(:,i,s));
    end

    IMF_outr(:,:,s)=IMF_out_t(:,index1((1:m_n),s),s).*rowb(1,index1((1:m_n),s),s);
end
```

### CONSTRUCT REAL IMF'S

```
figure(k)
for i=1:1:size(Y,2)
   subplot(size(Y,2),1,i)
   plot(test_time,sum(IMF_outx(:,:,i),2),test_time,Y1(:,i),'--')
end
k=k+1;

figure(k)
for i=1:1:size(Y,2)
   subplot(size(Y,2),1,i)
   plot(test_time,sum(IMF_outr(:,:,i),2),test_time,Y1(:,i),'--')
end
k=k+1;

% first 4 IMF's for each signal
figure(k)
for a=1:1:4
subplot(5,size(Y,2),a)
plot(test_time,sum(IMF_outr(:,1:5,a),2),test_time,Y1(:,a),'--','LineWidth',1.5)
text1=sprintf('Torque Generator %d',a);
text2=sprintf('\\omega Generator %d',a-2);
if a<=2
title(text1)
else
    title(text2)
end
legend('Prony First 5 modes', 'Original signal','Fontsize',6)
xlabel('Time [s]','Fontsize',8)
ylabel('Amplitude [p.u.]                              .','Fontsize',8)
xlim([42 60]);
end
a=a+1;
for i=2:1:5
    for ii=1:1:size(Y,2)
        subplot(5,size(Y,2),a)
        plot(test_time,IMF_outr(:,i,ii),'LineWidth',1.5)
        text1=sprintf('Torque Generator %d mode %d',ii,i);
        tex2t=sprintf('\\omega Generator %d mode %d',ii,i);
            if ii<=2
            title(text1)
            else
            title(text2)
            end
        xlabel('Time [s]','Fontsize',8)
        ylabel('Amplitude [-]','Fontsize',8)
        xlim([42 60]);
        a=a+1;
    end
end
k=k+1;
```

### DATA VOOR DE TABEL ERUIT FRIEMELEN

```
Btable=zeros(5,size(Y,2));
rztable=zeros(5,size(Y,2));
for i=1:size(Y,2)
```

```
    Btable(:,i)=Bsorted1(index1(1:5,i),i);
    rztable(:,i)=rzsorted1(index1(1:5,i),i);
end

alfa(:,:)=log(abs(rztable))/Ts; %damping factor of the modes
freq(:,:)=atan2(imag(rztable),real(rztable))/(2*pi*Ts); %frequency of the modes
Amp(:,:)=abs(Btable);
phi(:,:)=atan2(imag(Btable),real(Btable)).*180/pi;
```

### NCF CALCULATION

```
for s=1:1:size(Y,2)
     for i=1:1:5
        Es(i,s)=sum(IMF_outr(:,i,s).^2,1);
     end
end
ni=1; %the mode under investigation
for s=1:1:size(Y,2)
[phis(:,s), phase, Esr(:,s), NCFs(:,s)]=relativephase(test_time,IMF_outr(:,1:5,s),ni);
end
```

### EXPORT FUNCTION

```
figure(12)
export_fig Tw.eps -transparent
% figure(8)
% export_fig figuur1 case_prony_base.svg -transparent
```

# D

# Results of Analysis Tool on Matlab Simulink Model

This appendix shows the results of the tests performed in subsection 4.2.

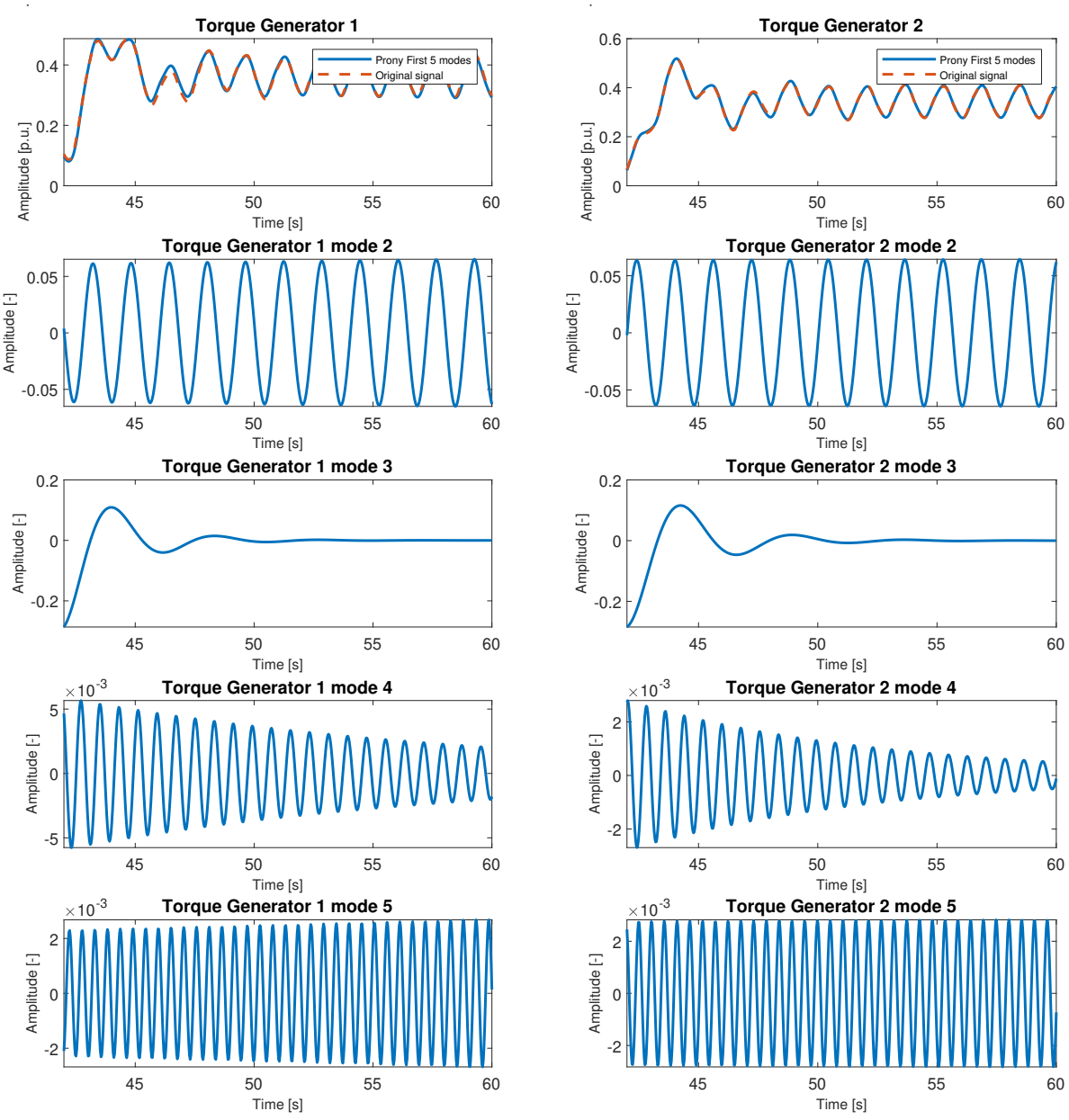


Figure D.1: Result of Torque in Analysis tool

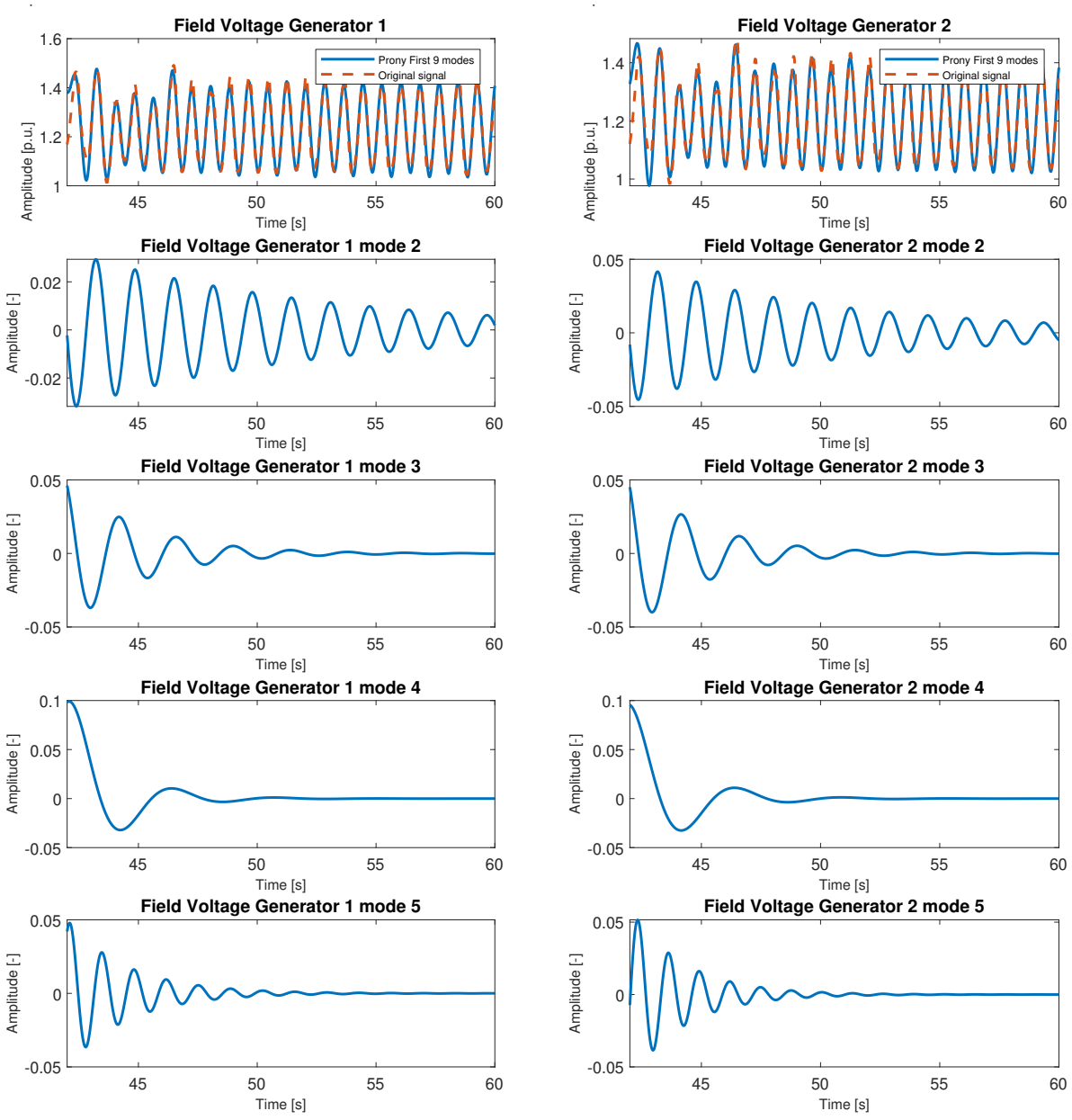


Figure D.2: Result of Field Voltage in Analysis tool

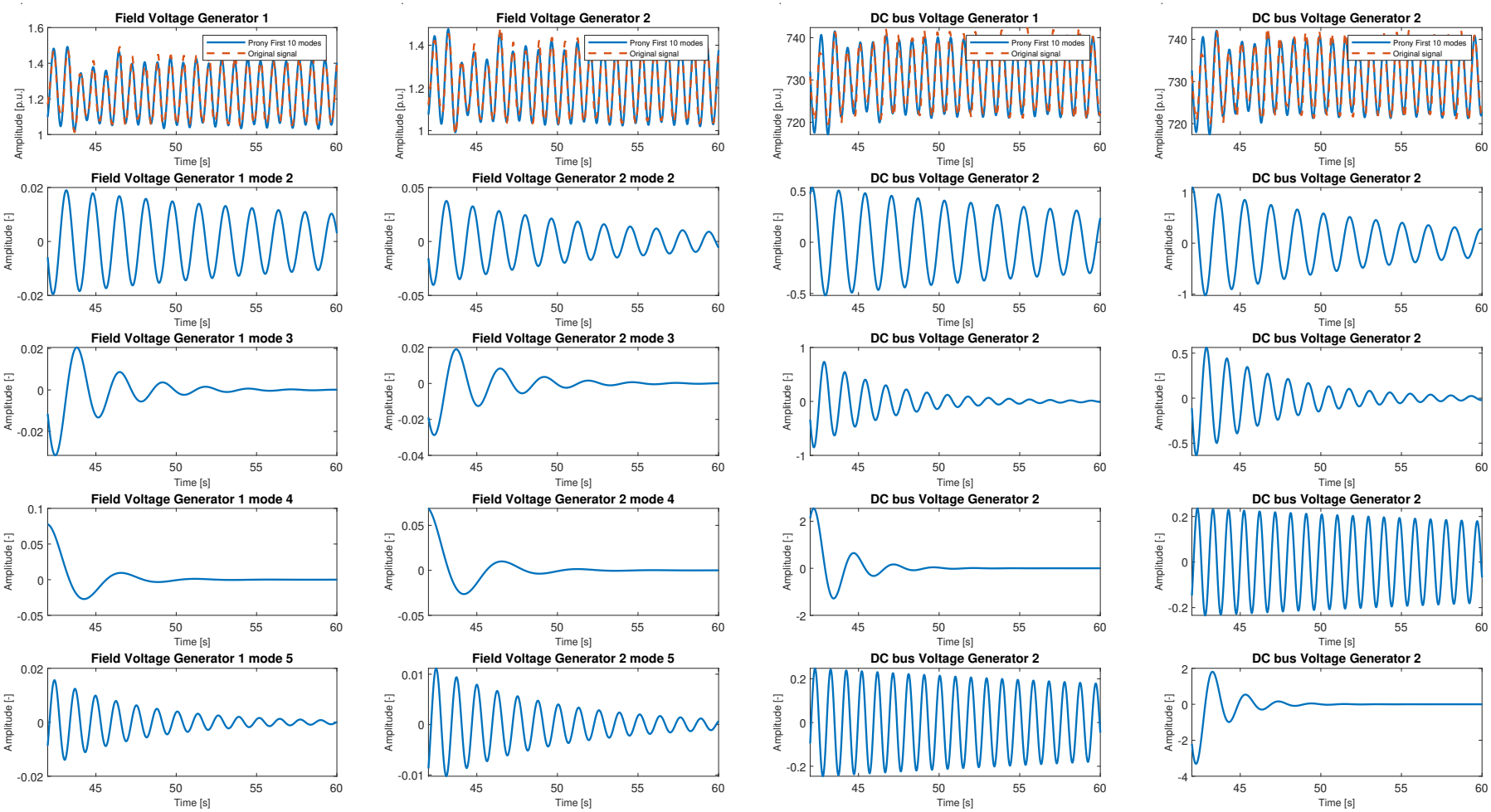


Figure D.3: Result of Field Voltage and DC bus Voltage in Analysis tool

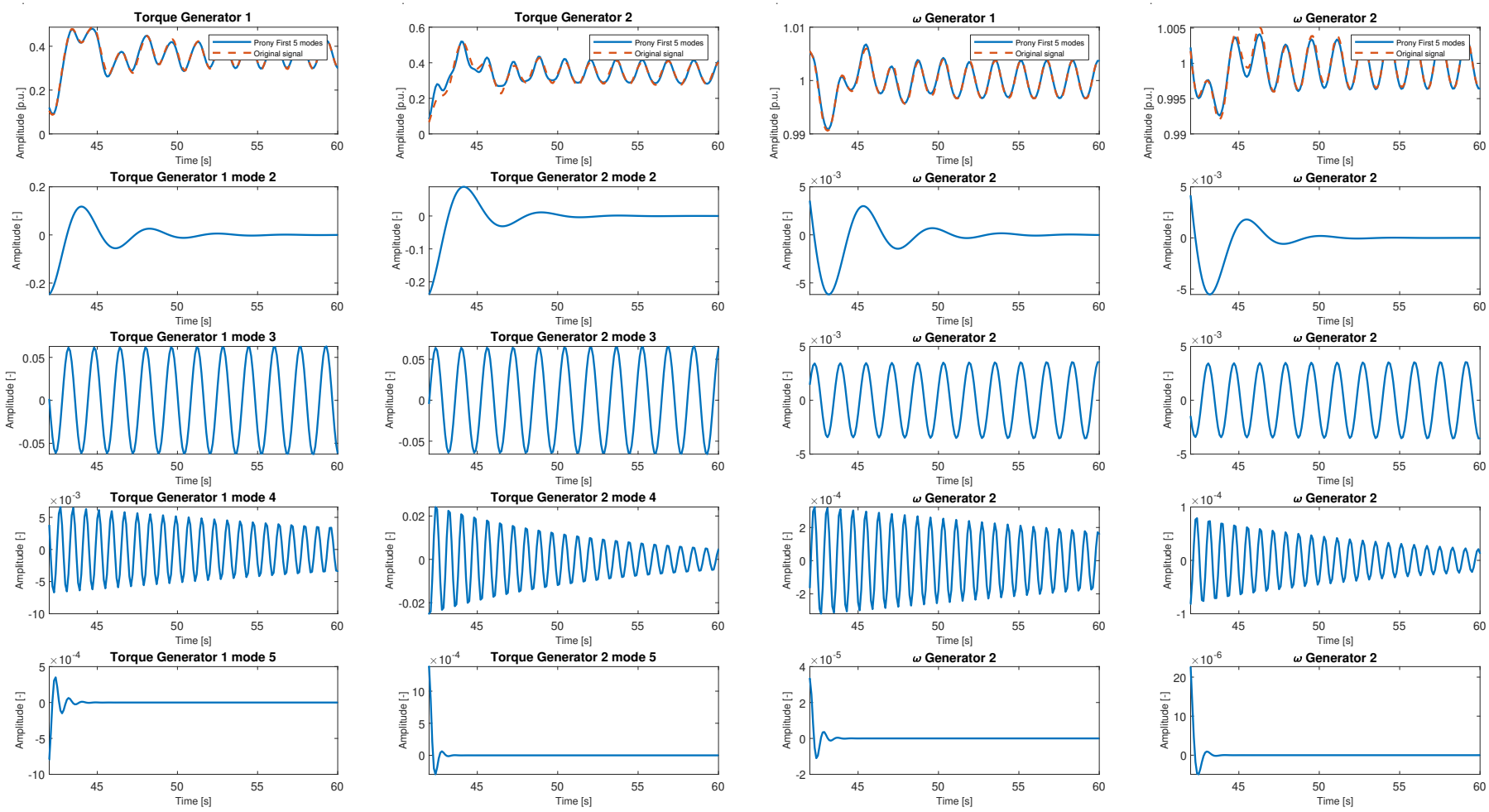


Figure D.4: Result of Torque and speed analysis in Analysis tool

# BIBLIOGRAPHY


[1] A. Shekhar, L. Ramirez-Elizondo, and P. Bauer, *DC microgrid islands on ships,* in *2017 IEEE Second International Conference on DC Microgrids (ICDCM)* (IEEE, 2017).

[2] K. Kim, K. Park, G. Roh, and K. Chun, *DC-grid system for ships: a study of benefits and technical considerations,* Journal of International Maritime Safety, Environmental Affairs, and Shipping (2018), 10.1080/25725084.2018.1490239, https://doi.org/10.1080/25725084.2018.1490239 .

[3] Z. Jin, G. Sulligoi, R. Cuzner, L. Meng, J. C. Vasquez, and J. M. Guerrero, *Next-Generation Shipboard DC Power System: Introduction Smart Grid and dc Microgrid Technologies into Maritime Electrical Netowrks,* IEEE Electrification Magazine **4**, 45 (2016).

[4] R. Nilsen and I. Sorfonn, *Hybrid Power Generation Systems,* in *2009 13th European Conference on Power Electronics and Applications* (Wärtsilä Ship Power Technology, 2009).

[5] *Definition and classification of power system stability IEEE/CIGRE joint task force on stability terms and definitions,* IEEE Transactions on Power Systems **19**, 1387 (2004).

[6] N. Hatziargyriou, J. V. Milanovic, C. Rahmann, V. Ajjarapu, C. Canizares, I. Erlich, D. Hill, I. Hiskens, I. Kamwa, B. Pal, P. Pourbeik, J. J. Sanchez-Gasca, A. M. Stankovic, T. V. Cutsem, V. Vittal, and C. Vournas, *Definition and classification of power system stability revisited & extended,* IEEE Transactions on Power Systems , 1 (2020).

[7] A. Kwasinski and C. N. Onwuchekwa, *Dynamic Behavior and Stabilization of DC Microgrids With Instantaneous Constant-Power Loads,* IEEE Transactions on Power Electronics **26**, 822 (2011).

[8] Z. Jin, M. Savaghebi, J. C. Vasquez, L. Meng, and J. M. Guerrero, *Maritime DC microgrids - a combination of microgrid technologies and maritime onboard power system for future ships,* in *2016 IEEE 8th International Power Electronics and Motion Control Conference (IPEMC-ECCE Asia)* (IEEE, 2016).

[9] T. Dragicevic, X. Lu, J. Vasquez, and J. Guerrero, *DC Microgrids–Part I: A Review of Control Strategies and Stabilization Techniques,* IEEE Transactions on Power Electronics , 1 (2015).

[10] A. Emadi, A. Khaligh, C. Rivetta, and G. Williamson, *Constant Power Loads and Negative Impedance Instability in Automotive Systems: Definition, Modeling, Stability, and Control of Power Electronic Converters and Motor Drives,* Vehicular Technology, IEEE Transactions on **55**, 1112 (2006).

[11] J. Kumar, A. Agarwal, and V. Agarwal, *A review on overall control of DC microgrids,* Journal of Energy Storage **21**, 113 (2019).

[12] D. E. Olivares, A. Mehrizi-Sani, A. H. Etemadi, C. A. Canizares, R. Iravani, M. Kazerani, A. H. Hajimiragha, O. Gomis-Bellmunt, M. Saeedifard, R. Palma-Behnke, G. A. Jimenez-Estevez, and N. D. Hatziargyriou, *Trends in Microgrid Control,* IEEE Transactions on Smart Grid **5**, 1905 (2014).

[13] M. Belkhayat, R. Cooley, and A. Witulski, *Large signal stability criteria for distributed systems with constant power loads,* in *Proceedings of PESC '95 - Power Electronics Specialist Conference* (IEEE, 1995).

[14] Y. Han, X. Ning, P. Yang, and L. Xu, *Review of Power Sharing, Voltage Restoration and Stabilization Techniques in Hierarchical Controlled DC Microgrids,* IEEE Access **7**, 149202 (2019).

[15] I. Novickij and G. Joos, *Model Predictive Control Based Approach for Microgrid Energy Management,* in *2019 IEEE Canadian Conference of Electrical and Computer Engineering (CCECE)* (IEEE, 2019).

[16] T. V. Vu, S. Paran, F. Diaz, T. E. Meyzani, and C. S. Edrington, *Model predictive control for power control in islanded DC microgrids,* in *IECON 2015 - 41st Annual Conference of the IEEE Industrial Electronics Society* (IEEE, 2015).

[17] Y. Shen, W. Gao, D. W. Gao, and W. Yan, *Inverter controller design based on model predictive control in microgrid,* in *2017 IEEE International Conference on Electro Information Technology (EIT)* (IEEE, 2017).

[18] M. A. Morales-Caporal, J. de Jesus Rangel-Magdaleno, J. M. Ramirez-Cortes, E. Tlelo-Cuatle, and R. Morales-Caporal, *Control algorithm using trajectory-based MPC for MPPT application,* in *2015 IEEE International Autumn Meeting on Power, Electronics and Computing (ROPEC)* (IEEE, 2015).

[19] E. H. Abdou, A.-R. Youssef, S. Kamel, and M. M. Aly, *Sensorless Wind Speed Control of 1.5 MW DFIG Wind Turbines for MPPT,* in *2018 Twentieth International Middle East Power Systems Conference (MEPCON)* (IEEE, 2018).

[20] A. Haseltalab and R. R. Negenborn, *Model predictive maneuvering control and energy management for all-electric autonomous ships,* Applied Energy **251**, 113308 (2019).

[21] P. Ghimire, M. Zadeh, E. Pedersen, and J. Thorstensen, *Dynamic modeling, simulation, and testing of a marine DC hybrid power system,* IEEE Transactions on Transportation Electrification **7**, 905 (2021).

[22] D. Park and M. Zadeh, *Modeling and predictive control of shipboard hybrid DC power systems,* IEEE Transactions on Transportation Electrification **7**, 892 (2021).

[23] T. Sopapirm, K. Areerak, S. Bozhko, C. Hill, A. Suyapan, and K. Areerak, *Adaptive Stabilization of Uncontrolled Rectifier Based AC-DC Power Systems Feeding Constant Power Loads,* IEEE Transactions on Power Electronics **PP**, 1 (2017).

[24] T. H. Helland, *Stability analysis of diode bridge rectifier-loaded synchronous generators characterized with high values of reactances,* (2015).

[25] J. Kirkeluten, *Stability of synchronous generators - stability analysis of synchronous generators connected to rectifiers,* (2016).

[26] J. Hauer, C. Demeure, and L. Scharf, *Initial results in prony analysis of power system response signals,* IEEE Transactions on Power Systems **5**, 80 (1990).

[27] O. Chaari, P. Bastard, and M. Meunier, *Prony's method: an efficient tool for the analysis of earth fault currents in petersen-coil-protected networks,* IEEE Transactions on Power Delivery **10**, 1234 (1995).

[28] L. Qi, L. Qian, S. Woodruff, and D. Cartes, *Prony analysis for power system transient harmonics,* EURASIP Journal on Advances in Signal Processing **2007** (2007), 10.1155/2007/48406.

[29] M. A. H. Ortega and A. R. Messina, *An Observability-based Approach to Extract Spatiotemporal Patterns from Power System Koopman Mode Analysis,* Electric Power Components and Systems **45**, 355 (2017).

[30] RTDS Technologies Inc, *Manual set. rscad tutorial manual.* .

[31] P. Kundur, *Power System Stability and Control* (MCGRAW HILL BOOK CO, 1994).

[32] *IEEE Guide for Synchronous Generator Modeling Practices and Parameter Verification with Applications in Power System Stability Analyses,* IEEE Std 1110-2019 (Revision of IEEE Std 1110-2002) , 1 (2020).

[33] *IEEE Recommended Practice for Excitation System Models for Power System Stability Studies,* IEEE Std 421.5-2016 (Revision of IEEE Std 421.5-2005) , 1 (2016).

[34] J. Jatskevich, S. Pekarek, and A. Davoudi, *Parametric average-value model of synchronous machine-rectifier systems,* IEEE Transactions on Energy Conversion **21**, 9 (2006).

[35] M. K. Zadeh, B. Zahedi, M. Molinas, and L. E. Norum, *Centralized stabilizer for marine DC microgrid,* in *IECON 2013 - 39th Annual Conference of the IEEE Industrial Electronics Society* (IEEE, 2013).

[36] L. Herrera, W. Zhang, and J. Wang, *Stability analysis and controller design of DC microgrids with constant power loads,* IEEE Transactions on Smart Grid , 1 (2015).

[37] M. K. Arpanahi, M. Kordi, R. Torkzadeh, H. H. Alhelou, and P. Siano, *An Augmented Prony Method for Power System Oscillation Analysis Using Synchrophasor Data,* Energies **12**, 1267 (2019).

[38] D. Trudnowski, J. Johnson, and J. Hauer, *Making prony analysis more accurate using multiple signals,* IEEE Transactions on Power Systems **14**, 226 (1999).

[39] A. F. Rodríguez, L. de Santiago Rodrigo, E. L. Guillén, J. M. R. Ascariz, J. M. M. Jiménez, and L. Boquete, *Coding prony's method in MATLAB and applying it to biomedical signal filtering,* BMC Bioinformatics **19** (2018), 10.1186/s12859-018-2473-y.

[40] Satnam Singh (2021). Prony Toolbox (https://www.mathworks.com/matlabcentral/fileexchange/3955-prony-toolbox), MATLAB Central File Exchange. Retrieved March 13, 2021., .

[41] T. W. Parks, *Digital filter design* (Wiley, New York, 1987).